

---

# Chemical Investigation of Hassium (Hs, Z=108)

---

Inauguraldissertation der  
philosophisch-naturwissenschaftlichen  
Fakultät der Universität Bern

vorgelegt von

**Christoph Emanuel Düllmann**

von Ferenbalm (BE)

Leiter der Arbeit:  
Prof. Dr. H.W. Gäggeler  
Departement für Chemie und Biochemie  
der Universität Bern



---

# Chemical Investigation of Hassium (Hs, Z=108)

---

Inauguraldissertation der  
philosophisch-naturwissenschaftlichen  
Fakultät der Universität Bern

vorgelegt von

**Christoph Emanuel Düllmann**

von Ferenbalm (BE)

Leiter der Arbeit:  
Prof. Dr. H.W. Gäggeler  
Departement für Chemie und Biochemie  
der Universität Bern

Von der philosophisch-naturwissenschaftlichen Fakultät angenommen

Bern 24.06.2002

Der Dekan:  
Prof. P. Bochsler



*Für Salomé*

"Ordnung ist das erste Gesetz des Himmels."

Alexander Pope (1688 - 1744), englischer Dichter



# Table of Contents

Summary.....	I
Zusammenfassung .....	III
<b>1. Introduction.....</b>	<b>1</b>
1.1 Stability of the heaviest nuclei .....	2
1.1.1 Spherical nuclei.....	2
1.1.2 The influence of deformation .....	3
1.2 Production of transactinides .....	4
1.3 Chemistry of the transactinides .....	5
1.4 Chemical properties of transition elements.....	8
1.4.1 The group 8 elements .....	9
1.5 Experimental techniques used for chemical investigation of transactinides in the gas phase .....	11
1.6 Hassium.....	13
1.6.1 Identification using physical separation systems .....	13
1.6.2 Long-lived $\alpha$ -decaying isotopes.....	14
1.6.2.1 $^{269}\text{Hs}$ .....	15
1.6.2.2 $^{270}\text{Hs}$ .....	16
1.6.3 Past attempts to chemically identify hassium.....	18
1.6.4 Proposed set-ups for the chemical investigation of hassium.....	20
1.7 Conditions for the chemical identification of single atoms .....	21
1.8 Outline of the thesis .....	24
<b>2. Development of the IVO-COLD system .....</b>	<b>35</b>
2.1 Experiments using a carbon aerosol gas-jet .....	35
2.2 Optimization of a Ar/Pb aerosol.....	37
2.3 Publication "IVO, a device for <u>I</u> n situ <u>V</u> olatilization and <u>O</u> n-line detection of products from heavy ion reactions" .....	39
2.3.1 Introduction .....	40
2.3.2 IVO, a device for in situ volatilization and on-line detection .....	42
2.3.2.1 <i>Technical description of IVO</i> .....	43
2.3.3 First experiments with volatile osmium tetroxide ( $\text{OsO}_4$ ) to model a chemistry with Hs (element 108).....	46
2.3.3.1 <i>Experimental</i> .....	46
2.3.3.2 <i>Results and discussion</i> .....	48
2.3.4 First experiments with mercury (Hg) to model a chemistry with elements 112 and 114 .....	52
2.3.5 Conclusions .....	55
2.4 The <u>C</u> ryo <u>O</u> n- <u>L</u> ine <u>D</u> etector COLD .....	58
2.5 Test experiments with COLD .....	61
2.5.1 Short-lived $\alpha$ -decaying Os isotopes.....	61
2.5.2 Detection of fission fragments of $^{252}\text{Cf}$ .....	63

<b>3. The experimental identification of hassium.....</b>	<b>65</b>
3.1 The IVO-COLD set-up.....	65
3.1.1 Calibration of COLD.....	65
3.1.2 Operation of the IVO-COLD system.....	66
3.1.3 Data acquisition.....	66
3.2 Analysis of the data and identification of Hs isotopes.....	67
3.2.1 Alpha spectra.....	67
3.2.2 Fission fragments.....	69
3.3 Publication "Decay properties of $^{269}\text{Hs}$ and evidence for the new nuclide $^{270}\text{Hs}$ ".....	71
3.4 Evaluation of the enthalpy of adsorption of $\text{HsO}_4$ on the detector surface material ( $\text{Si}_3\text{N}_4$ ).....	82
3.4.1 Monte Carlo simulation.....	83
3.4.2 Model of mobile adsorption.....	89
3.5 Publication "Chemical investigation of hassium (element 108)".....	91
<b>4. Publication "On the stability and volatility of group 8 tetroxides, <math>\text{MO}_4</math> (<math>\text{M}=\text{ruthenium, osmium, and hassium (Z=108)}</math>)" ...</b>	<b>105</b>
4.1 Introduction.....	107
4.2 Extrapolation of chemical properties from $\text{RuO}_4$ and $\text{OsO}_4$ to $\text{HsO}_4$ .....	108
4.2.1 Stability and volatility of oxides.....	109
4.2.2 Relation between sublimation enthalpy and adsorption enthalpy.....	113
4.3 A model for the physisorption of volatile molecules on dielectric surfaces.....	113
4.3.1 Adsorption of polarizable molecules.....	114
4.3.2 Calculation of the adsorption distances of noble gases.....	116
4.3.3 Application of the model to $\text{OsO}_4$ .....	117
4.3.4 Extrapolation of the adsorption enthalpies for $\text{RuO}_4$ and $\text{HsO}_4$ .....	118
4.4 Conclusions.....	119
<b>5. Outlook and closing remarks.....</b>	<b>125</b>
Acknowledgments.....	133
Appendix - Pictures of the experiment.....	137
Curriculum vitae.....	139

## Summary

The present work describes experiments which led to the first chemical investigation of hassium (Hs,  $Z=108$ ) and its classification into the periodic table. Based on the systematics of the periodic table it was assumed that hassium is a member of group 8 and is therefore expected to behave similarly to ruthenium (Ru) and osmium (Os). Both these elements form volatile tetroxides  $MO_4$  ( $M=Ru, Os$ ) in the reaction with oxygen.

The properties of  $HsO_4$  were evaluated on the basis of two different models. From the extrapolation of the trend established by  $RuO_4$  and  $OsO_4$ , formation of a stable  $HsO_4$  is to be expected. The interaction of  $HsO_4$  with dielectric surfaces is expected to be similar to the one of  $OsO_4$  and a value for the adsorption enthalpy on quartz of  $\Delta H_{ads}(HsO_4)=(-46\pm 15)$  kJ/mol was extrapolated.

In a different approach, the adsorption of gaseous tetroxides was treated as a physisorption process similar to that of noble gases on surfaces. The enthalpy of adsorption on the surface material was calculated using only molecular properties and agreed with the experimental value for  $OsO_4$  on quartz. The respective value of  $HsO_4$  was calculated using published calculated molecular properties to  $\Delta H_{ads}(HsO_4)=(-47\pm 11)$  kJ/mol.

A new device was developed called "In situ Volatilization and On-line detection apparatus" (IVO) allowing for the transport of volatile species, e.g.  $HsO_4$ , with a carrier gas from the place of their production to the detection system. IVO was tested in experiments with short-lived Os isotopes ( $T_{1/2} < 1$  min) produced in heavy-ion induced fusion reactions on the PHILIPS cyclotron at the Paul Scherrer Institut (PSI) which were oxidized to  $OsO_4$ . These experiments yielded important information for an experiment with Hs. The high volatility of the tetroxides is of advantage allowing for a good separation of interfering species formed as by-products in the nuclear production reaction. Using isothermal gas adsorption chromatography, the enthalpy of adsorption of  $OsO_4$  on a quartz surface was determined as  $(-38.0\pm 1.5)$  kJ/mol. It was

## II

shown that the transport of OsO<sub>4</sub> on this material is in the form of a mobile adsorption (i.e. without any chemical reaction during adsorption and desorption).

A new detection device based on the method of thermochromatography was recently developed at the Lawrence Berkeley National Laboratory. It allows the detection of  $\alpha$ -active and spontaneously fissioning nuclides with high efficiency, and at the same time yields chemical information on the investigated species, namely the deposition temperature on the column surface material. An improved version called "Cryo On-Line Detector" (COLD) was built and coupled to IVO. This system allowed for the separation and detection of single atoms of Hs in their tetroxide form and the measurement of the deposition temperature of each single molecule on silicon nitride. The maximum of the distribution of OsO<sub>4</sub> was measured at a temperature of (-82±7) °C. From the deposition distribution, the adsorption enthalpy was evaluated as (-39±1) kJ/mol, in close agreement with the enthalpy of adsorption on quartz. For physisorption processes on dielectric surfaces such as silicon oxides or nitrides, the influence of the surface material appears to be negligible.

In an experiment conducted at the Gesellschaft für Schwerionenforschung mbH (GSI) in Darmstadt, relatively long-lived Hs isotopes ( $T_{1/2} \sim 10$  s) were produced in the heavy-ion induced fusion reaction of <sup>26</sup>Mg and <sup>248</sup>Cm. The decay of seven Hs atoms was unambiguously registered using COLD and their deposition temperature on the silicon nitride detector surface measured. The maximum of the deposition distribution was observed at a temperature of (-44±6) °C. The weak interaction of the observed compound with the detector surface gives strong evidence that indeed very volatile HsO<sub>4</sub>, which is expected to be the most stable compound of Hs with oxygen, was formed. From the distribution of the molecules, the enthalpy of adsorption of HsO<sub>4</sub> on silicon nitride was evaluated as (-46±2) kJ/mol.

With the formation of a highly volatile compound with oxygen, presumably HsO<sub>4</sub>, Hs behaves similarly to Os and is a member of group 8 of the periodic table.

## Zusammenfassung

In der vorliegenden Arbeit werden Experimente, die zur erstmaligen chemischen Untersuchung von Hassium (Hs, Z=108) und seiner Einordnung ins Periodensystem der Elemente führten, beschrieben. Dabei wurde aufgrund der Systematik des Periodensystems angenommen, dass Hassium ein Mitglied der Gruppe 8 ist und sich somit ähnlich verhalten sollte wie Ruthenium (Ru) und Osmium (Os). Von diesen beiden Elementen ist die Bildung eines sehr flüchtigen Tetroxids  $MO_4$  (M=Ru, Os) in der Reaktion mit Sauerstoff bekannt.

Die Eigenschaften von  $HsO_4$  wurden mittels zweier verschiedener Modelle abgeschätzt. Die Extrapolation des Stabilitätstrends von  $RuO_4$  über  $OsO_4$  zu  $HsO_4$  liess die Bildung eines stabilen  $HsO_4$  erwarten. Die Wechselwirkung von  $HsO_4$  mit dielektrischen Oberflächen wurde ähnlich derjenigen von  $OsO_4$  erwartet und eine Adsorptionsenthalpie von  $HsO_4$  auf Quarz von  $\Delta H_{ads}(HsO_4)=(-46\pm 15)$  kJ/mol wurde extrapoliert.

In einem anderen Ansatz wurde die Sorption gasförmiger Tetroxide ähnlich der Physisorption von Edelgasen auf Oberflächen betrachtet. Die Adsorptionsenthalpie auf dem Oberflächenmaterial wurde allein aus Moleküleigenschaften berechnet und stimmte für  $OsO_4$  mit experimentell gefundenen Werten auf Quarz überein. Der entsprechende Wert für  $HsO_4$  wurde durch Verwendung publizierter, theoretisch ermittelter Eigenschaften dieses Moleküls als  $\Delta H_{ads}(HsO_4)=(-47\pm 11)$  kJ/mol berechnet.

Eine neue Apparatur, genannt "In situ Verflüchtigung und On-line Detektionsapparatur" (IVO), die den Transport flüchtiger Spezies, z.B.  $HsO_4$ , vom Ort seiner Produktion zum Detektionssystem mit einem Trägergas erlaubte, wurde entwickelt. IVO wurde in Experimenten mit kurzlebigen Os Isotopen ( $T_{1/2} < 1$  min), welche in schwerioneninduzierten Fusionsreaktionen am PHILIPS Zyklotron des Paul Scherrer Instituts (PSI) hergestellt und zu  $OsO_4$  oxidiert wurden, getestet. Diese Experimente lieferten wichtige Informationen im Hinblick auf ein Experiment mit Hs. Die hohe Flüchtigkeit der Tetroxide erwies sich als sehr vorteilhaft für eine gute Abtrennung von störenden

## IV

Spezies, die als Nebenprodukte in der nuklearen Produktionsreaktion anfallen. Durch die Methode der isothermen Gaschromatographie wurde die Adsorptionseenthalpie von  $\text{OsO}_4$  auf Quarz zu  $(-38.0 \pm 1.5)$  kJ/mol bestimmt. Es wurde gezeigt, dass der Transport von  $\text{OsO}_4$  auf diesem Material in der Form einer mobilen Adsorption (d.h. ohne überlagerte chemische Reaktion bei Adsorption und Desorption) stattfindet.

Im Lawrence Berkeley National Laboratory wurde kürzlich ein neuartiges Detektionssystem auf der Basis der Thermochromatographie entwickelt. Dieses erlaubt die Detektion  $\alpha$ -aktiver und spontan spaltender Nuklide mit hoher Effizienz und liefert gleichzeitig chemische Information über die untersuchte Spezies, nämlich die Depositionstemperatur auf der Kolonnenoberfläche. Durch den Bau einer verbesserten Version dieses Systems, genannt "Cryo On-Line Detektor" (COLD) und die Kopplung an IVO wurde es möglich, einzelne Atome von Elementen der Gruppe 8 in der Form des Tetroxids abzutrennen und nachzuweisen und die Depositionstemperatur auf Siliziumnitrid für jedes einzelne Molekül zu messen. Das Maximum der Verteilung von  $\text{OsO}_4$  wurde bei einer Temperatur von  $(-82 \pm 7)$  °C gemessen. Die aus der Verteilung ermittelte Adsorptionseenthalpie auf Siliziumnitrid von  $(-39 \pm 1)$  kJ/mol stimmt gut mit dem entsprechenden Wert von  $\text{OsO}_4$  auf Quarz überein. Bei Physisorptionsprozessen auf dielektrischen Oberflächen (wie Quarz oder Siliziumnitrid) scheint der Einfluss des Oberflächenmaterials klein zu sein.

In einem Experiment an der Gesellschaft für Schwerionenforschung mbH (GSI) in Darmstadt wurden relativ langlebige Hs Isotope ( $T_{1/2} \sim 10$  s) in der schwerioneninduzierten Fusionsreaktion von  $^{26}\text{Mg}$  und  $^{248}\text{Cm}$  hergestellt. Unter Verwendung von COLD konnte der Zerfall von sieben Hs Atomen eindeutig nachgewiesen werden. Die Depositionstemperatur der Hassium enthaltenden Moleküle auf der Siliziumnitrid-Detektoroberfläche wurde gemessen. Das Maximum der Verteilung wurde bei einer Temperatur von  $(-44 \pm 6)$  °C beobachtet. Die schwache Wechselwirkung der beobachteten Verbindung mit der Detektoroberfläche ist ein sehr starker Hinweis darauf, dass wie angenommen sehr flüchtiges  $\text{HsO}_4$ , das die stabilste

Sauerstoffverbindung von Hs sein sollte, gebildet wurde. Aus der Verteilung der deponierten Moleküle wurde die Adsorptionenthalpie von  $\text{HsO}_4$  auf Siliziumnitrid zu  $(-46 \pm 2)$  kJ/mol bestimmt.

Mit der Bildung einer sehr flüchtigen Verbindung mit Sauerstoff, höchstwahrscheinlich  $\text{HsO}_4$ , verhält sich Hs ähnlich wie Os und ist damit als Mitglied der Gruppe 8 des Periodensystems der Elemente zu betrachten.



---

## 1. Introduction

The experimental investigation of the heaviest elements is an important and exciting task from both the physical and the chemical point of view. To physicists on the one hand, nuclei of transactinide elements ( $Z > 103$ ) offer unique possibilities for an insight into the nature of nuclear structure at extremes of stability with respect to high  $Z$  values. Chemists on the other hand can test the influence of the high nuclear charge on chemical properties of the elements and thus the validity of the periodic table, which was introduced by Mendeleev more than 100 years ago. It still serves as the basic table for chemical elements and is the most important and useful tool in predicting their general chemical behavior. From the experimentalist's point of view, experiments with transactinides are always a challenge, since the number of available atoms is drastically limited to a few single atoms per hour or day (or even month [Oga00a]), and their lifetimes are seconds to minutes at most.

All elements heavier than U ( $Z=92$ ) do not occur in nature (except for trace amounts of Np and Pu in U ores, formed in interaction of neutrons with  $^{238}\text{U}$  [Sea58] and ultra trace amounts of  $^{244}\text{Pu}$  [Hoff71]) since their half-lives are short compared to the age of the earth and thus they have decayed. They are artificial elements. Elements heavier than Fm ( $Z=100$ ) can only be produced in "one-atom-at-a-time" quantities [Hoff99] in nuclear fusion reactions using particle accelerators. Since 1940, when the first transuranium element, neptunium (Np), was positively identified by McMillan and Abelson [McM40], the periodic table has been extended up to elements with atomic numbers as high as 116 [Oga00a]. Whereas the first transuranium elements were identified by chemical means, the discovery of new elements has completely shifted to the field of nuclear physics due to the very short lifetimes of the nuclei at the end of the nuclear chart.

## 1.1 Stability of the heaviest nuclei

### 1.1.1 Spherical nuclei

The heaviest stable nuclide, which has both a closed proton and a closed neutron shell and is therefore spherical, is  $^{208}\text{Pb}$  ( $Z=82$ ,  $N=126$ ). When in 1966 Myers and Swiatecki attempted to calculate the masses of nuclei from a combination of a liquid-drop part (macroscopic part) with superimposed quantal shell corrections (microscopic part), they mentioned that superheavy nuclei might exist in a region far beyond the upper end of the then known chart of nuclides which owe their existence only to shell effects [Mye66]. Soon thereafter, Meldner predicted the next proton shell after  $Z=82$  to be closed at  $Z=114$ , and the next neutron shell after  $N=126$  at  $N=184$  [Mel67]. Hence, the next heavier doubly-magic nucleus was expected to be  $^{298}114$  [Mel67] whose fission barrier should have a height of several MeV [Mye66].

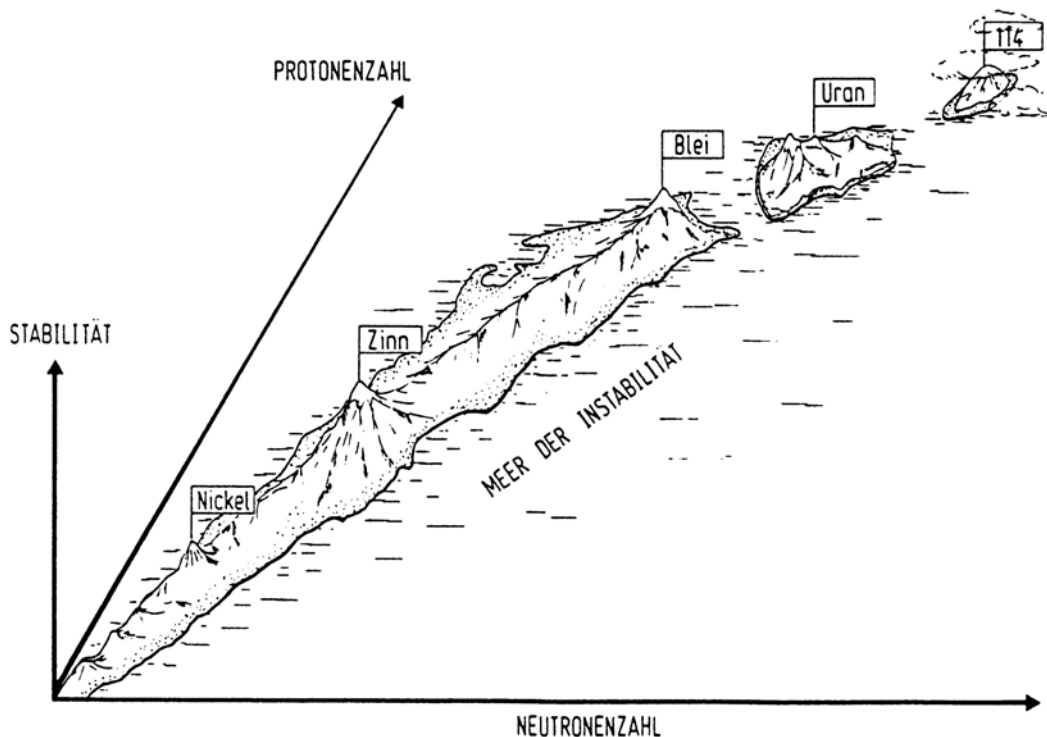


Fig. 1-1 The nuclear landscape. Indicated is the stability of the nuclides (i.e. the binding energy per nucleon) as function of proton and neutron number for nuclides with a half-life  $>1$  s. [Her88]

Since  $\alpha$ -decay half-lives are not so strongly influenced by shell stabilization as are fission half-lives, but decrease more smoothly with increasing atomic number, the longest-lived nucleus was predicted to be  $^{294}110$  [Nil69] with a calculated total half-life of about  $10^8$  y [Nil69]. Such calculations motivated the search for superheavy elements (SHE) in nature and a rush in quest of these "superheavies" began. The nuclear landscape had gained a so far unknown "island of stability" as shown in Figure 1-1.

In more recent calculations, there is no consensus among theorists on the exact location of the next heavier spherical shell closures [Cwi99] and the next shell closures are expected to be in the region of  $Z=114-126$  and  $N=172$  or  $N=184$ , respectively, depending on the model used (see e.g. [Möl94, Cwi96, Gup97, Rut97, Kru00]).

### 1.1.2 The influence of deformation

In 1989, Patyk et al. calculated nuclear masses in a large deformation space, i.e. the nuclei were allowed to minimize their ground-state energy by higher order deformations. From these calculations they predicted the nuclei around  $Z=108$  and  $N=162$  to be rather stable [Pat89, Pat91a], and  $^{270}\text{Hs}$  was predicted to be a relatively strongly bound, deformed doubly-magic nuclide. As the main decay mode, emission of  $\alpha$ -particles with a half-life of about 0.1 s was calculated. More recent calculations point to even longer half-lives. The classical spherical "superheavies" were no longer thought to form an island of stability separated by a swamp of unstable nuclei from the region around uranium, but to be connected via a so-called "rock of stability" around  $^{270}\text{Hs}$ , as is shown schematically in Figure 1-2.

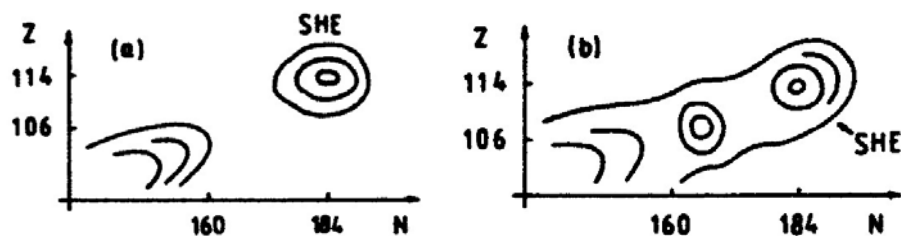


Fig. 1-2 Regions of relatively long-lived nuclei: As believed earlier (a), and presently (b) [Pat89].

A first indication of increased stability in this region of the nuclear chart was the relative stability of the isotopes  $^{265,266}\text{Sg}$  [Laz94, Tür98a] which was further confirmed by the discovery of  $^{267}\text{Bh}$  [Wil00], and  $^{269}\text{Hs}$  [Hof96, Hof00]. All of these isotopes have half-lives of seconds.

The discovery of the new region of shell nuclei, interconnecting the transuranium- and the superheavy elements, as well as the successful synthesis of spherical superheavies [Oga99a, Oga99b, Oga99c, Oga00a, Oga00b] created the basis of present transactinide research in physics and chemistry.

## 1.2 Production of transactinides

To generate heavy nuclei, accelerated particles (projectiles) are directed at target atoms at rest. When a projectile hits a target nucleus, often only a part of the constituents of both nuclei are exchanged (i.e. the target nucleus picks up a few nucleons from the projectile, or vice versa). Such reactions are referred to as transfer reactions. The complete fusion of two nuclei occurs only with a low probability. Important parameters and processes governing the production cross section of a heavy nuclide are the following (see e.g. [Zub02]):

(i) the capture of the projectile by the target with subsequent formation of a compound nucleus (CN) [Boh36]. A central collision is required since the high angular momentum induced by non-central collisions leads to immediate quasi-fission of the system (see e.g. [Gia00]).

(ii) the formed CN is usually excited. Depending on the excitation energy, one to several particles (in reactions used in heavy element investigations usually neutrons) evaporate, thus allowing the CN to cool down. Each evaporation step stands in strong competition with prompt fission, which is the much more probable process than particle evaporation [Boh98]. Only in few cases, a so-called evaporation residue (EVR), i.e. the interesting heavy nuclide in its ground (or sometimes metastable) state is formed.

---

The fusion probability depends on the projectile energy: a minimum energy is required to overcome the coulomb repulsion of both positively charged nuclei. At the point of contact, the projectile and target nucleus fuse, if the attractive nuclear force is stronger than the coulomb repulsion. This is always the case in light systems ( $Z_{\text{projectile}} \cdot Z_{\text{target}} < \sim 1600$ ). However, in very heavy systems, this process is hindered and an extra-energy of the projectile is required to bring both nuclei in closer contact (extra-push concept [Swi82]).

Fusion reactions are referred to as "cold" when the excitation energy of the CN at the so-called Bass barrier [Bas74] is very low (less than  $\sim 20$  MeV) and only few neutrons evaporate (usually one or two). Such reactions are e.g. the Pb based reactions that led to the discovery of elements 107-112 at GSI [Hof00]. In hot-fusion reactions, the CN has an excitation energy of about 30 to 50 MeV and about four to six neutrons are evaporated. Typical examples are actinide target based reactions which are usually used in chemistry experiments since more neutron rich nuclei can be created using this type of reaction. In general, a higher projectile energy increases the fusion cross section, but the higher excited CN has a lower chance of survival since more evaporation steps are necessary. In cold-fusion reactions, formation of a CN is less probable than in hot-fusion reactions but its survival is more probable in cold-fusion reactions than in hot-fusion reactions. The shell structure of both interacting nuclei, the CN and the EVR, their geometrical form as well as the fission barrier of the CN are other important parameters governing the magnitude of the production cross section of heaviest nuclei. The experimental and theoretical investigation of the different stages of the fusion process as well as the properties of the EVR's are topics of many recent projects in nuclear physics and chemistry.

### 1.3 Chemistry of the transactinides

The main interest in heavy element chemistry is in placing new elements in the periodic table, i.e. checking for chemical similarity to supposed homologues. In a very first approach one would instinctively continue the arrangement valid today which means that the elements Rf through 112 are placed in the d block below Hf through Hg. Elements 113 to 118 are then

---

expected to be p elements with element 118 being the next heavier noble gas. From quantum mechanical calculations it was concluded long ago that such simple assumptions may not be valid, since in this area of the periodic table, relativistic effects on the valence electron shells are so strong that some deviations from known trends in the chemical groups are expected [Fri75, Kel84, Pyy79, Per96]. Relativistic effects are caused by coulomb interactions between the positively charged nucleus and the negatively charged electrons, and are therefore present in all elements; they have to be taken into account even in highly precise calculations on  $H_2$  and  $H_2^+$  [Pyy88] and are known to be (at least partly) responsible for a number of well-known phenomena, e.g. the yellow colour of Au, the liquid standard state of Hg, the inert-pair effect or the lanthanide-contraction [Pyy88]. Since their influence increases with  $Z^2$ , the relativistic effects become especially large in the heaviest elements. The high nuclear charge leads to a relativistic spin-orbit splitting of the p-, d-, and f-orbitals and changes their geometrical shape. Electrons with a high density near the nucleus ( $s_{1/2}$  and  $p_{1/2}$  orbitals) are accelerated to relativistic velocities which increases their binding energies and leads to contraction of the respective orbitals. This is referred to as direct relativistic effect. As a consequence, the outer d and f electrons are more efficiently screened from the high nuclear charge, their orbitals are destabilized and more expanded (indirect relativistic effect).

The lightest transactinide, rutherfordium (Rf,  $Z=104$ ) was investigated for the first time in a gas chemistry experiment in the form of its tetrachloride in Dubna in 1966 by Zvara and co-workers [Zva66]. Many studies in different gas chemical systems (see e.g. [Zva70, Zva71, Zhu89, Tür92, Kad96, Tür98b, Syl00]) have been performed since then. The behavior of Rf in extraction experiments and on ion exchange resins (see e.g. [Sil70, Hul80, Cze94a, Cze94b, Kac96a, Kac96b, Schu98, Str00, Hab01, Omt02]) was investigated as well.

The next heavier elements dubnium (Db,  $Z=105$ ) and seaborgium (Sg,  $Z=106$ ) have also been studied both in gas phase (see e.g. [Zva76, Gäg92, Tür92, Tür96a] for Db and [Tim96, Yak96, Schä97a, Gäg98, Zva98, Tür99, Hüb01]



investigated so far. Thus, the question arises of the correct placement of elements with  $Z > 107$  in the periodic table. This question motivated the present work and the objective was the chemical investigation of the next heavier element, hassium, with  $Z = 108$ .

Hs is believed to belong to group 8 of the periodic table. It would then be homologous to iron (Fe), ruthenium (Ru) and osmium (Os), and belong to the transition elements.

## 1.4 Chemical properties of transition elements

When analyzing the trends valid in the d block of the periodic table, the following general rules are observed:

- Since the electron configuration of the transition metals differs only with respect to the second most outer shell, which has a less pronounced influence on the chemical behavior than the outermost shell, the properties of the transition elements within a period do not differ so much compared to those of the main group elements of a given period.
- The presence of a d shell, filled to a different degree and taking part in chemical bondings in the d elements, leads to a periodicity. However, the latter is less pronounced than in the main group elements.
- The highest oxidation state observed in at least the heavier members (5 d elements) corresponds to the group number for groups 4 through 8.
- The stability of the higher oxidation states increases within the groups with increasing atomic numbers.
- The stability of the lower oxidation states decreases within the groups with increasing atomic numbers.
- The volatility of the compounds in the highest possible oxidation state increases from the lighter to the heavier members of a group due to the faster stability increase of the solid state compared to that of the gaseous state.

-Within a period, the character of the oxides turns from basic, for the lighter members, to acidic for the heavier elements.

### 1.4.1 The group 8 elements

Fe, Ru and Os are known to exist in a large number of oxidation states: Fe is known in all states from -2 through +6, Ru in the states -2 through +8 (with the exception of +1 that has not been observed) and Os in all states from -2 through +8. This explains the large variety of their compounds. When going from left to right within a period, the metal atom radii are found to be minimal in group 8. These metals are the ones with the highest maximum valency within their periods. Ru and Os are the only elements which can form a state with an oxidation number as high as 8+ (with the exception of Xe, which is known to form tetrahedral XeO<sub>4</sub> [Gun70] while RnO<sub>4</sub> is unknown). Table 1-1 shows some binary inorganic compounds of Fe, Ru, and Os, respectively.

Tab. 1-1 Some binary inorganic compounds of group 8 elements.

Compounds	Fe	Ru	Os
Oxides	FeO, Fe <sub>2</sub> O <sub>3</sub> , Fe <sub>3</sub> O <sub>4</sub>	RuO <sub>2</sub> , RuO <sub>3</sub> <sup>a</sup> , RuO <sub>4</sub>	OsO <sub>2</sub> , OsO <sub>3</sub> <sup>a</sup> , OsO <sub>4</sub>
Sulfides	FeS, Fe <sub>2</sub> S <sub>3</sub> , FeS <sub>2</sub>	RuS <sub>2</sub>	OsS <sub>2</sub>
Fluorides	FeF <sub>2</sub> , FeF <sub>3</sub>	RuF <sub>3</sub> , RuF <sub>4</sub> , RuF <sub>5</sub> , RuF <sub>6</sub>	OsF <sub>4</sub> , OsF <sub>5</sub> , OsF <sub>6</sub> , OsF <sub>7</sub>
Chlorides	FeCl <sub>2</sub> , FeCl <sub>3</sub>	RuCl <sub>3</sub> , RuCl <sub>4</sub>	OsCl <sub>3</sub> , OsCl <sub>4</sub> , OsCl <sub>5</sub>
Bromides	FeBr <sub>2</sub> , FeBr <sub>3</sub>	RuBr <sub>3</sub>	OsBr <sub>3</sub> , OsBr <sub>4</sub>
Iodides	FeI <sub>2</sub> , FeI <sub>3</sub>	RuI <sub>3</sub>	OsI, OsI <sub>2</sub> , OsI <sub>3</sub>

<sup>a</sup> only known in the gas phase

However, in transactinide chemistry, only mononuclear compounds can be formed due to the minute production rates ("one atom at a time" chemistry [Hoff99]). Further important compounds in the Fe chemistry are the hydroxides and oxyhydroxides. One hydroxide compound is also known for Ru, whereas no hydroxides are reported for Os. All of the group 8 elements form a great variety of coordination complexes.

While the chemistry of Ru and Os is quite similar, Fe behaves differently. The reason is the existence of the lanthanide series which is inserted in the sixth period of the periodic table. Due to the lanthanide contraction, the atomic radius (half distance of two atoms in the metal) of Os (133.8 pm) is very similar to that of Ru (132.5 pm), whereas that of Fe (124.1 pm) is significantly

smaller. Similar arguments hold in groups 9 and 10 and although there are the usual vertical similarities (e.g. in Fe, Ru, Os), the horizontal ones (e.g. in Fe, Co and Ni) are particularly strong. Therefore, the three members of the fourth period (Fe, Co, Ni) are often distinguished from the six members of the fifth and sixth period of these three groups (Ru, Rh, Pd; Os, Ir and Pt), which are collectively known as the platinum metals. Because of the similarity of Ru and Os and the rather differing chemistry of Fe, extrapolations from trends within group 8 are preferentially performed only from Ru via Os to Hs. For a review of the chemistry of Ru and Os, Refs [Gri67, Rar85] (Ru) and [Gri67] (Os) are recommended. Figure 1-4 shows the energy levels for Ru, Os and Hs for the non-relativistic case (which is purely theoretical since relativity cannot be switched off) and the relativistic case. As can be seen, the influence of relativistic effects increases with increasing  $Z$ .

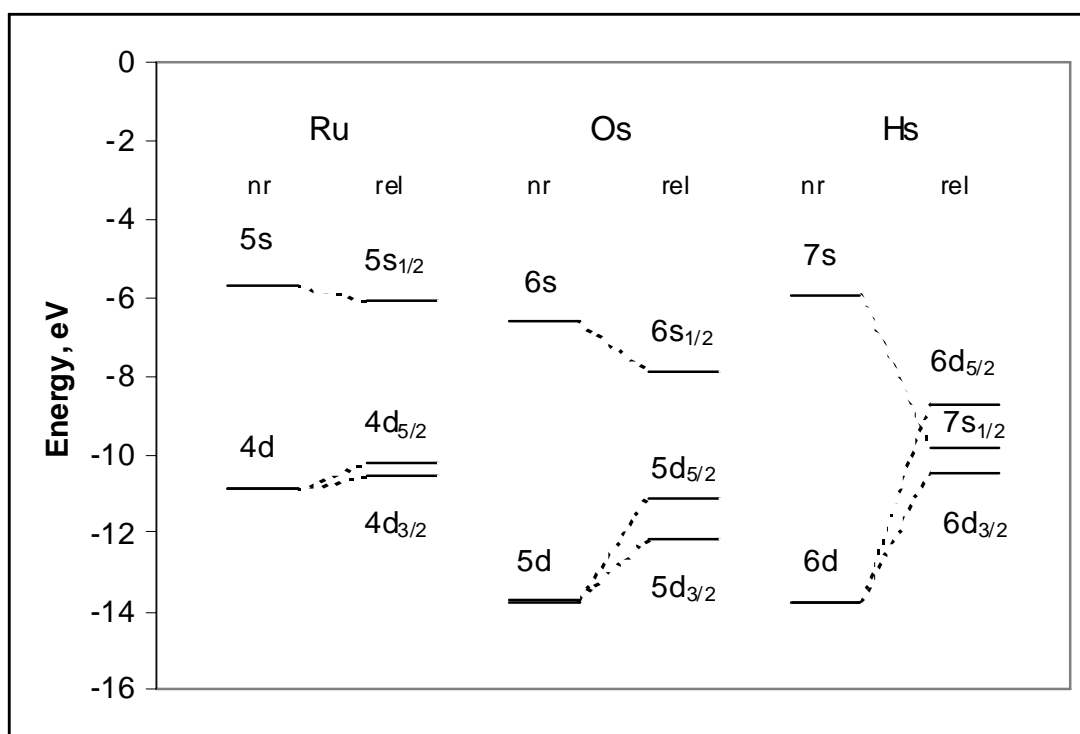


Fig. 1-4 Hartree-Fock (non-relativistic) and Dirac-Fock (relativistic) energy levels for group 8 elements Ru, Os and Hs (element 108). All values are from [Des73] except nr values for Hs which are from [Schw98]. (Figure courtesy by V. Pershina.)

---

Ru and Os are both known to form highly volatile tetroxides. The well-known "Gmelin Handbuch der anorganischen Chemie" introduces the section on the system Os-O as follows:

"The most important of these (oxides), and indeed the single most important compound of osmium is the tetroxide, OsO<sub>4</sub>." [Gri80]

Os metal forms OsO<sub>4</sub> with its characteristic smell in air at ambient temperature, which gave the element its name (greek: "osme" = smell). With respect to experiments where single atoms have to be separated from a huge background of unwanted products, the extraordinarily high volatility of the tetroxide is of special interest: its boiling point is as low as 130 °C [Opp98] and in experiments using carrier-free amounts it was volatile even at room temperature [Dom84a, Yak99, Yak00]. The same holds for RuO<sub>4</sub>. Since RuO<sub>4</sub> decomposes to RuO<sub>2</sub> + O<sub>2</sub> at 108 °C [Rar85], its boiling point had to be extrapolated. A value of (133±5) °C [Rar85] was calculated. While FeO<sub>4</sub> does not exist, the gas phase stability increases from RuO<sub>4</sub> ( $\Delta H_f^0(\text{RuO}_4)_{(g)} = (-193 \pm 4)$  kJ/mol) [Rar85] to OsO<sub>4</sub> ( $\Delta H_f^0(\text{OsO}_4)_{(g)} = (-336 \pm 8)$  kJ/mol) [Opp98, Hil92], in accordance with the rules given earlier. It seems therefore justified to assume that Hs also forms a highly volatile tetroxide, HsO<sub>4</sub>, which would be an ideal compound for the chemical investigation of this element as has already been mentioned by several authors, see e.g. [Dom84a, Dom84b, Fri75, Bäck71, Zud93]. This is in agreement with recent fully relativistic density functional theory (DFT) calculations on the group 8 tetroxides [Per01] that also predict the existence of HsO<sub>4</sub>, which is calculated to be more stable than OsO<sub>4</sub>.

## **1.5 Experimental techniques used for chemical investigation of transactinides in the gas phase**

Among the established experimental methods for the investigation of single atoms [Gäg97], investigations in the gas phase have proven to be fast and efficient enough to investigate nuclides which are formed with cross sections below 100 pb and have half-lives of less than half a minute. It is obvious to attempt to investigate group 8 elements in the gas phase since the high

volatility of their tetroxides seems to permit a very selective separation from unwanted by-products of the nuclear reaction. Two techniques have been used to evaluate thermochemical data of transactinide compounds in gas phase experiments. These are called thermochromatography (TC) [Mer61, Zva90] and isothermal gas chromatography (IC) [Gäg91, Tür96b] and are schematically shown in Figure 1-5.

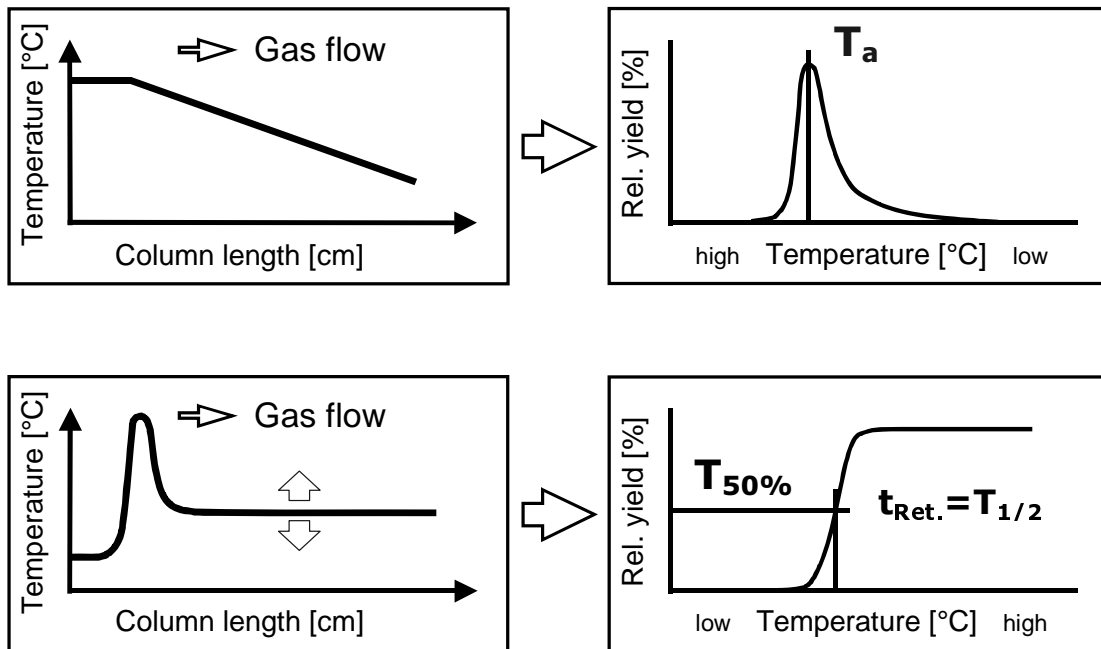


Fig. 1-5 TC (upper panels) and IC (lower panels) principle. For explanation see text.

In both techniques, the volatile species is injected into a chromatography column which is usually made from quartz. In TC, a longitudinal negative temperature gradient is established along the column length (upper left panel). The species is transported to lower temperatures by the carrier gas flow. According to the adsorption interaction of the species, deposition occurs at a characteristic temperature (upper right panel).

In IC (lower panels), the species is transported to a reaction zone kept at an elevated temperature, where formation of the volatile compound takes place. The latter is then injected into a chromatography column kept at an isothermal but variable temperature. At a high isothermal temperature the retention time is very short and almost 100% of the species reach the exit of the column. When the temperature is lowered, the retention time increases. At the

temperature  $T_{50\%}$  where the yield is 50% of the maximum yield, the retention time equals the nuclear half-life of the radionuclide contained in the species.

From the adsorption temperature  $T_a$  measured in TC experiments as well as from the temperature  $T_{50\%}$  determined in IC experiments (which are usually similar), the enthalpy of adsorption of the volatile species on the column material can be evaluated. The thermodynamic model of mobile adsorption [EiB82], and a Monte Carlo simulation procedure based on a microscopic model of the adsorption process [Zva85] have both been shown to yield similar results, on condition that a reversible adsorption process without superimposed chemical reaction (i.e. the transported species remain unchanged during adsorption and desorption) takes place within the column.

## 1.6 Hassium

### 1.6.1 Identification using physical separation systems

The identification of element 108 based on the observation of three atoms was reported in 1984 [Mün84] when the nuclide  $^{265}\text{Hs}$  ( $T_{1/2}=1.55$  ms) [Hof95] was produced in the heavy-ion induced fusion reaction of  $^{208}\text{Pb}+^{58}\text{Fe}$ . A much more long-lived isotope with mass 269 ( $T_{1/2}=11$  s) was discovered in the experiment that led to the first identification of element 112 [Hof96]. Presently known Hs nuclides are those with mass numbers 264 ( $T_{1/2}=0.45$  ms) [Mün86, Mün87], 265 ( $T_{1/2}=1.55$  ms) [Mün84, Mün87, Hof95], 266 ( $T_{1/2}=2.3$  ms) [Hof01], 267 ( $T_{1/2}=19$  ms) [Laz95], 269 ( $T_{1/2}=11$  s) [Hof96, Hof00], and 277 ( $T_{1/2}=11$  min) [Oga99c]. In addition, evidence has been obtained for the isotope  $^{263}\text{Hs}$  ( $T_{1/2}$  was not determined) [Ghi95a, Ghi95b].

<b>Hs</b>	<b>Hs 263 ?</b>	<b>Hs 264</b>	<b>Hs 265</b>	<b>Hs 266</b>	<b>Hs 267</b>	<b>Hs 269</b>	<b>Hs 277</b>
<b>108</b>	?	0,45 ms $\alpha$ 10,43; sf (50%)	870 $\mu$ s; 1,6 ms $\alpha$ 10,51-10,57 $\alpha$ 10,37	2,3 ms $\alpha$ 10,18	19 ms $\alpha$ 9,88; 9,83; 9,75	11,3 s $\alpha$ 9,14-9,23	11 min $\alpha$ 9,14-9,23

Fig. 1-6 Known Hs nuclides.  $\alpha$ -decaying nuclides are indicated in white, spontaneously fissioning nuclides in grey.

The half-lives of the isotopes  $^{264}\text{Hs}$  through  $^{267}\text{Hs}$  are too short for chemical experiments, nor is  $^{277}\text{Hs}$  suited for our purposes since it cannot be produced directly - it was the last member of a decay chain starting at  $^{289}114$  [Oga99c] -

and decays by spontaneous fission (SF), a mode that does not allow the unambiguous identification of the decaying nuclide. Hence,  $^{269}\text{Hs}$  is the most suitable nuclide for chemical investigations of Hs. More neutron-rich isotopes are predicted to be even more long-lived [Smo97]. The long lifetime of  $^{277}\text{Hs}$  [Oga99c] appears to confirm such predictions.

### 1.6.2 Long-lived $\alpha$ -decaying isotopes

A suitable reaction for the production of  $^{269}\text{Hs}$  is  $^{248}\text{Cm}(^{26}\text{Mg}, 5n)$ . The excitation function calculated with the HIVAP code [Rei92] is shown below.

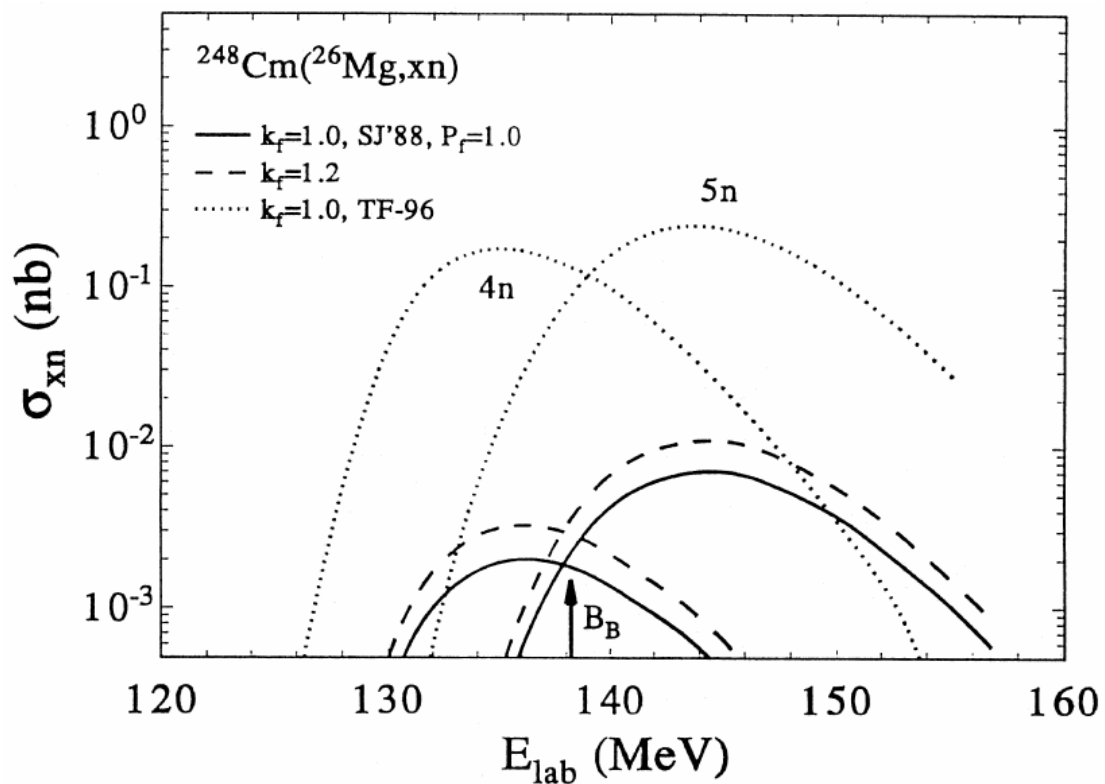


Fig. 1-7 HIVAP calculation [Rei92] for the reaction  $^{26}\text{Mg}+^{248}\text{Cm}$  using different values for the fission barrier ( $k_f$ ) and mass tables (SJ'88 form [Spa88, Aud95], TF-96 from [Mye96]). The arrow indicates the barrier according to the model of Bass [Bas74]. ([Sag99])

From these calculations it follows that the neighbouring nuclide  $^{270}\text{Hs}$  is produced in the same reaction in the 4n deexcitation channel with a comparable cross section.

From an analysis of hot-fusion systematics [Schä96b], production cross sections of a few picobarns are expected both for  $^{269}\text{Hs}$  and  $^{270}\text{Hs}$ .

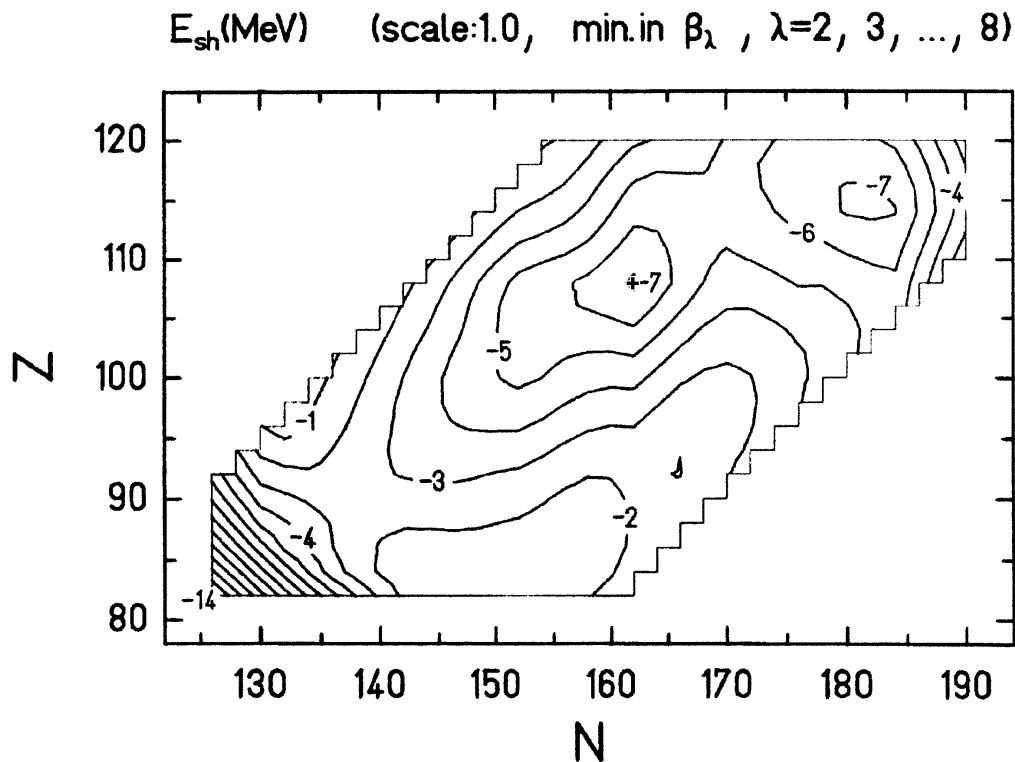


Fig. 1-8 Contour map of the ground-state shell correction energy,  $E_{\text{sh}}$  (in MeV). The position of  $^{270}\text{Hs}$  is marked by the cross (adapted from [Sob01]).

In Figure 1-8, the potential energy surface for the heaviest nuclei is shown where nuclear deformation has been taken into account [Sob01]. Three minima are visible. The deepest one (-14.3 MeV) is found for the well-known spherical doubly-magic nuclide  $^{208}\text{Pb}$ . For heavier elements, two almost identically deep minima are found for  $^{270}\text{Hs}$  (-7.2 MeV) and  $^{296}114$  (-7.2 MeV). While the latter is again predicted to be spherical, the minimum in the region of  $^{270}\text{Hs}$  appears only for deformed shapes. The strong shell stabilization leads to half-lives for nuclei in the vicinity of  $^{270}\text{Hs}$  that are long enough to make these isotopes suitable for chemical investigations.

#### 1.6.2.1 $^{269}\text{Hs}$

To date, the decay of three single  $^{269}\text{Hs}$  nuclei has been observed in experiments at the Separator for Heavy Ion reaction Products (SHIP) [Hof00]

---

in Darmstadt. Two of those were observed in the experiment where element 112 was identified for the first time [Hof96] and the third one in a confirmation experiment [Hof00] as granddaughters of  $^{277}112$ .  $^{269}\text{Hs}$  has not been produced directly so far. From the measured lifetimes, a half-life of  $11^{+15}_{-4}$  s has been derived. The margins of error were calculated according to [Schm84]. In all cases,  $\alpha$ -decay was observed with  $\alpha$ -particle energies of 9.17 to 9.23 MeV.

#### 1.6.2.2 $^{270}\text{Hs}$

As has already been mentioned,  $^{270}\text{Hs}$  is expected to be a deformed doubly magic nucleus [Pat89, Pat91a, Pat91b] and numerous theoretical papers deal with predicted properties of this nuclide. A more detailed investigation of the structure of both shell closures attributed the magicity of  $Z=108$  mainly to the influence of the quadrupole deformation  $\beta_2$  and the hexadecapole deformation  $\beta_4$ , whereas in the  $N=162$  shell also  $\beta_6$  contributed significantly to the shell correction energy [Pat91b]. Among the most important properties with respect to experimentalists is the half-life since chemistry experiments require much longer-lived isotopes ( $T_{1/2} > 1$  s, [Gäg97]) than experiments in which the nuclei are isolated physically ( $T_{1/2} > 1$   $\mu\text{s}$  [Hof00]). From nuclear structure calculations, often  $Q_\alpha$  values are derived from which the partial  $\alpha$ -half-life can be deduced. Several formula linking  $Q_\alpha$  and  $T_{1/2}(\alpha)$  can be found in the literature, among which the one from Ref. [Buc91] reproduces the half-lives of all known ground state to ground state  $\alpha$ -transitions in even-even nuclei having  $76 \leq Z \leq 100$  within a factor of approximately two. In other works, the properties of the fission barrier, which largely determines the partial SF-half-life, have been theoretically investigated. In Table 1-2, predictions concerning  $^{270}\text{Hs}$  are summarized. Where only the  $Q_\alpha$ -value was given in the original article, the corresponding half-life was deduced according to the formula given in Ref. [Buc91].

Tab. 1-2 Predictions of the decay properties of  $^{270}\text{Hs}$  in the literature.

$Q_\alpha$ [MeV]	$T_{1/2}(\alpha)$ [s]	$T_{1/2}(\text{SF})$ [s]	Ref
9.3	3.57 <sup>a</sup>		[Möl88a] (as cited in [Ren96])
8.8	121. <sup>a</sup>		[Möl88b] (as cited in [Ren96])
	0.1		[Pat91a]
9.44	0.76		[Pat91b]
	6.		[Smo95a, Smo96]
8.69	168.		[Iwa96]
9.0	28.5 <sup>a</sup>		[Ren96]
8.69	170.		[Möl97]
9.13	11.4 <sup>a</sup>		[Sob01]
8.88	9.1 <sup>b</sup>		[Roy02]
	28.8 <sup>c</sup>		[Roy02]
		$1.0 \cdot 10^8$ <sup>d</sup>	[Möl87]
		$8.2 \cdot 10^{-5}$ <sup>e</sup>	[Möl87]
		$9.5 \cdot 10^6$ <sup>d</sup>	[Möl89, Möl94]
		$7.2 \cdot 10^{-2}$ <sup>e</sup>	[Möl89, Möl94]
		$10^9$	[Pat89]
		$6.5 \cdot 10^3$	[Smo95b]

<sup>a</sup> Calculated from  $Q_\alpha$  using the formula of [Buc91]

<sup>b</sup> Generalized liquid drop model

<sup>c</sup> From  $\alpha$ -systematics derived in [Roy02]

<sup>d</sup> "Old path"

<sup>e</sup> "New path"

Möller et al. [Möl87, Möl89, Möl94] found a so-called "new path" in potential energy surfaces for nuclei with  $Z > 100$  which leads to compact shapes at the scission point. However, the observation of e.g.  $^{266}\text{Sg}$ , for which a partial SF half-life of  $\geq 11$  s is reported [Tür98a] is in contradiction to a half-life of less than 0.1 s which has been predicted for this nucleus in the "new path" [Möl89]. All other predicted SF half-lives are significantly longer than the  $\alpha$ -half-lives and hence,  $\alpha$ -decay is expected to be the dominant decay mode for  $^{270}\text{Hs}$ . A  $\alpha$ -particle energy of  $E_\alpha \sim 8.6$ -9.3 MeV can be expected. Its daughter will then be  $^{266}\text{Sg}$ , which decays with a half-life of  $(21^{+20}_{-12})$  s by emission of an  $\alpha$ -particle with an energy of 8.52 MeV (33%) or 8.77 MeV (66%) [Tür98a]. An upper limit of 82 % has been established for an SF branch in  $^{266}\text{Sg}$ . The daughter produced in the  $\alpha$ -decay is  $^{262}\text{Rf}$  which is known to fission symmetrically (an upper limit of 0.8 % for a possible  $\alpha$ -branch is reported [Lan96]) with a half-life of  $(2.1 \pm 0.2)$  s [Lan96].

Therefore, the signature expected in the decay of  $^{270}\text{Hs}$  is  $\alpha$ - $\alpha$ -SF or  $\alpha$ -SF with  $\alpha$ -particle energies above 8.0 MeV.

### 1.6.3 Past attempts to chemically identify hassium

In 1985 experiments searching for SF decaying isotopes of element 108 produced in the heavy-ion induced fusion reactions  $^{40}\text{Ar}+^{235}\text{U}$  (CN  $^{275}110$ ) were performed at Dubna [Zhu85a, Zhu85b]. In another experiment using the  $^{22}\text{Ne}+^{249}\text{Cf}$  reaction (CN  $^{271}\text{Hs}$ ) at 123 MeV,  $\alpha$ - or SF decaying  $^{267}\text{Hs}$  was searched for which was believed to have a half-life of the order of 1 s [Che85, Zhu85a]. The set-up used in this work is shown in Figure 1-9.

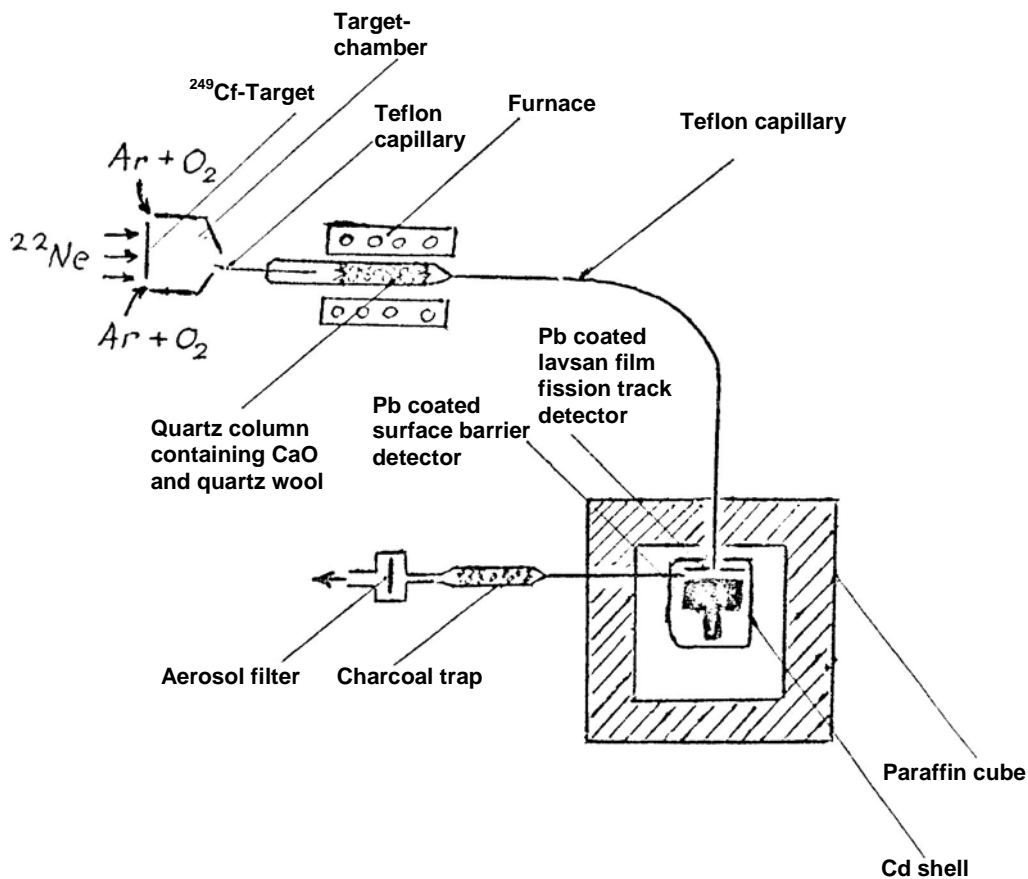


Fig. 1-9 Schematic of the set-up used for the search for Hs isotopes in Dubna (from [Zhu85a]).

Os recoil atoms were thermalized in a gas mixture of  $\text{Ar} + 2\% \text{O}_2$  (1.2 bar) and continuously swept out of the target chamber through a teflon capillary into a quartz column kept at 1000-1100 °C filled with  $\text{CaO}$  to separate non-volatile

transfer products as e.g. actinides, Ra, Fr, and Po. The volatile species were then transported through a teflon capillary and blown onto the surface of a Si detector covered with  $50 \mu\text{g}/\text{cm}^2$  of Pb. At the opposite side an annular lvsan track detector (also coated with  $50 \mu\text{g}/\text{cm}^2$  of Pb) was located for registering fission fragments. The whole counting device was placed inside a shielding of Cd and paraffin in order to decrease the background.

In model experiments with Os,  $\text{OsO}_4$  was efficiently absorbed on the lead surfaces, probably owing to reduction to non-volatile  $\text{OsO}_2$ . The decontamination from actinides was excellent (separation factor  $>10^6$ ) as well as that from Po ( $>10^3$ ). Nevertheless, no  $\alpha$ -particles in the energy range above 8.5 MeV and no SF events were registered and upper limits of 100 pb for the production cross sections of  $\alpha$ -decaying nuclides and 50 pb for SF decaying nuclides were established.

Another set-up called On-line Separation and Condensation AppaRatus (OSCAR) was installed at the 88-inch cyclotron in Berkeley [Dou87] and is shown in Figure 1-10.

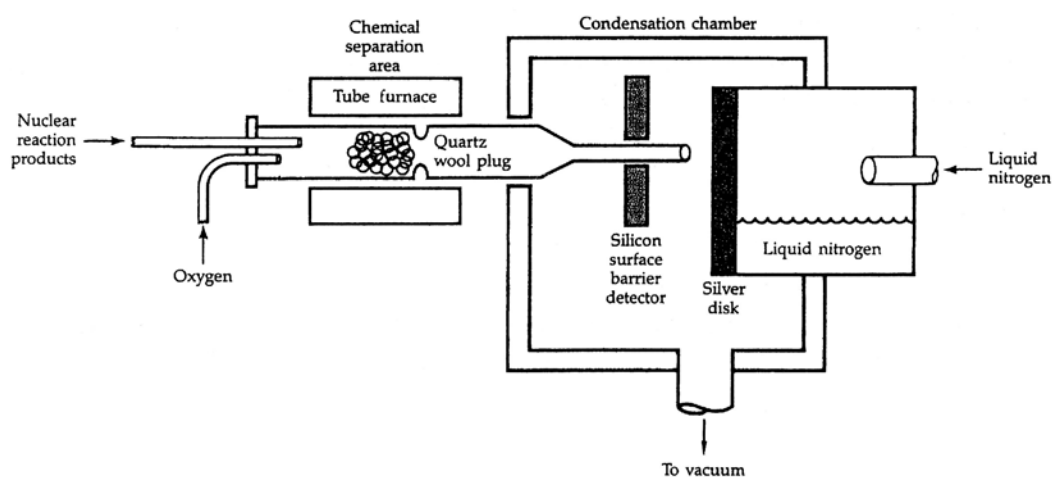


Fig. 1-10 Schematic drawing of OSCAR which was used to search for  $^{272}\text{Hs}$  [Dou87, Hul87].

Nuclear reaction products were attached to KCl aerosol particles in the recoil chamber. Via this so-called gas-jet they were subsequently transported to the chemical separation area where oxygen was fed into the system. The particles were caught on a quartz wool plug and destroyed and formation of

---

the tetroxide took place at a temperature of 650 °C. Non volatile transfer products remained quantitatively in the reaction area while the volatile oxides were swept out by the carrier gas flow into the condensation chamber at a low pressure (50 torr) where they were deposited on a silver disk which was cooled by liquid nitrogen (LN<sub>2</sub>) to temperatures  $\leq -155$  °C. Opposite of the metal disk, an annular Si surface barrier detector was mounted which registered  $\alpha$ - and SF decaying nuclides adsorbed on the disk. The carrier gas was He at a flow rate of 1.1-1.4 l/min; the oxygen flow rate was 30 ml/min. The efficiency for the separation and condensation of osmium was 36 %. Separation from the actinides was excellent:  $\leq 10^{-6}$  % of the actinide activity was detected on the cold silver disk.

OSCAR was used to search for  $\alpha$ -decaying <sup>272</sup>Hs which was expected to be the EC daughter product of <sup>272</sup>Mt (estimated T<sub>1/2</sub>: 25 min) produced in the <sup>254</sup>Es(<sup>22</sup>Ne, 4n) reaction at 117.5 MeV [Hul87]. However no  $\alpha$ -energy peak between 8.7 and 11 MeV was observed and an upper limit for the production cross section of 1 nb was obtained.

From a recent analysis of the cross sections in hot fusion reactions [Schä96b] as were used in these experiments it is obvious that the latter were not sufficiently sensitive.

#### **1.6.4 Proposed set-ups for the chemical investigation of hassium**

Different set-ups for the chemical separation of group 8 tetroxides have been proposed. In Mainz, v. Zweidorf et al. tested a detection system where OsO<sub>4</sub> was adsorbed on metallic Na [vZw01]. Deposition can be interpreted as acid-base reaction on a Na<sub>2</sub>O surface with formation of non-volatile osmates. In Dubna, Yakushev et al. reported on a system where OsO<sub>4</sub> was adsorbed on Pb aerosol particles which were deposited on a magnetic tape and subsequently subjected to  $\alpha$ -spectroscopy [Yak99, Yak00]. This system, too, is intended to be used for the investigation of Hs [Tsy02].

---

## 1.7 Conditions for the chemical identification of single atoms

The law of mass action which is used to describe a chemical system in its equilibrium can no longer simply be applied in the case of single atoms [Gui89]. Formulation of an equilibrium distribution between two phases is no longer possible since the species of interest is either in one phase or the other. However, Guillaumont et al. showed that partition methods can still be used to determine thermodynamic properties. The distribution coefficients are expressed in terms of probabilities to find a single species in one of the phases at a given time [Gui89], provided an experimental method is used where the species is exchanged sufficiently many times from one state into the other. This is fulfilled in the case of gas adsorption chromatography.

Prerequisites for the successful application of this method on the investigation of single atoms of transactinides with half-lives of a few seconds to a few minutes are:

a) Fast formation of a defined volatile species without kinetic hindrance.

From the literature it is known that at temperatures below 1200 °C the dominant gas phase species in the system Ru-O is RuO<sub>4</sub> [Nik65]. In a temperature range >1200 °C, formation of RuO<sub>3</sub> is favored. [Nik65]. In the system Os-O analogous molecular components are formed [Nik65, Opp98]. Decomposition of OsO<sub>4</sub> was observed only at temperatures above 700 °C [Opp98]. In on-line experiments with short-lived Os isotopes [Dom84a, Yak99, Yak00] formation of a very volatile oxide, presumably the tetroxide, was observed with high yield, indicating a fast formation process as can be assumed in the case of the rather simple OsO<sub>4</sub> molecule. In test experiments, which were part of the present work, short-lived Os isotopes were produced in heavy-ion reactions and the above mentioned observations were confirmed (see Chapters 2.3.3 and 2.5.1). Yields for the formation of OsO<sub>4</sub> and transport out of the recoil chamber of ~90 % were observed.

b) High separation factors with respect to (especially  $\alpha$ - and SF-decaying) species which severely interfere with the definite identification of the fusion product and its daughters.

Presumably the only way to definitely identify single atoms of transactinides is to register their characteristic decay sequences. The daughter nuclides are usually short-lived radionuclides as well, and hence a safe assignment of the separated nuclei is possible by establishing a genetic relationship of observed  $\alpha$ - and SF-decays. The expected decay sequences originating from the decay of  $^{269}\text{Hs}$  and  $^{270}\text{Hs}$  are shown in Figure 1-11.

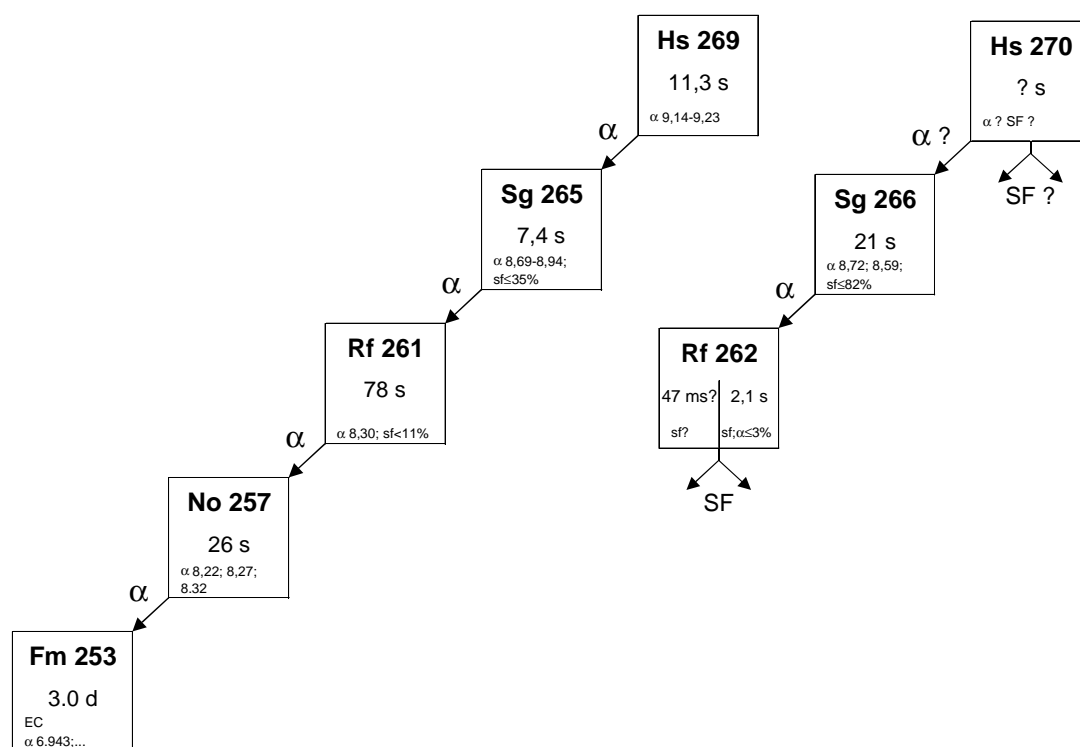


Fig. 1-11 Expected decay sequences originating from  $^{269}\text{Hs}$  and  $^{270}\text{Hs}$ .  $^{270}\text{Hs}$  has not yet been observed.

Any radionuclide that decays by emission of  $\alpha$ -particles in the energy range above 8.0 MeV, or by spontaneous fission, has to be prevented from entering the detection system. Known nuclides whose decay characteristics are similar to those shown in Figure 1-11 and can be present in a Hs experiment are:

-lighter transactinides that could be formed if the compound nucleus deexcites by emitting a  $\alpha$ -particle and several neutrons ( $\alpha xn$ -reactions) [Dre99].

However, none of the lighter transactinides are expected to form volatile oxides.

-heavier and lighter actinides, especially  $^{256}\text{Fm}$  (SF>90 %), formed in transfer reactions. Again, no volatile oxides of the actinides are known.

-Several nuclides of Pb, Bi, and Po:  $^{212}\text{Bi}$  ( $E_{\beta\alpha}=10.55$  MeV),  $^{212\text{m}}\text{Bi}$  ( $E_{\beta\alpha}=10.22$  MeV),  $^{211\text{m}}\text{Po}$  ( $E_{\alpha}=8.883$  MeV),  $^{212}\text{Po}$  ( $E_{\alpha}=8.785$  MeV),  $^{212\text{m}2}\text{Po}$  ( $E_{\alpha}=11.65$  MeV), and  $^{213}\text{Po}$  ( $E_{\alpha}=8.376$  MeV) are often formed in transfer reactions with Pb impurities in the target material. In the case of the very short-lived  $^{212}\text{Po}$  ( $T_{1/2}=0.3$   $\mu\text{s}$ ) an additional problem is the time-resolution of the electronics which is usually not high enough to resolve the preceding  $\beta$ -particle emitted by  $^{212}\text{Bi}$  and the  $^{212}\text{Po}$ - $\alpha$ -particle. Hence a sum signal of the two particles is registered in the energy range between 9 and 11 MeV ( $\alpha$ - $\beta$ -pile-up).

The long-lived precursors of the above mentioned nuclides,  $^{212,213}\text{Pb}$  and  $^{211,212,213}\text{Bi}$  have to be separated as well.  $^{212}\text{Pb}$  and  $^{212}\text{Bi}$  are members of the natural  $^{232}\text{Th}$  decay chain and can enter the detection system via their volatile and chemically inert precursor  $^{220}\text{Rn}$  ( $T_{1/2}=55.6$  s).

Since the difference in volatility governs the separation factors in gas chromatographic separations, the high volatility of the tetroxides makes this class of compounds very suitable. In the earlier experiments in Dubna [Che85, Zhu85a, Zhu85b] and Berkeley [Dou87, Hul87] high separation factors ( $>10^6$  for actinides) were indeed reported.

c) Fast transport of the volatile molecules to the detection system and efficient registration of time-correlated decay-chains ( $\alpha$ - $\alpha$ - $\alpha$  or  $\alpha$ -SF).

For the gas-chemical investigations of the four lightest transactinides Rf, Db, Sg, and Bh, the well-known On-Line-Gaschromatography-Apparatus (OLGA) technique [Gäg91] was applied, a device working in the isothermal regime. After chemical separation, the species was adsorbed to aerosol particles and transported using the gas-jet technique [Wol75, Nai89] to the Rotating wheel Multidetector Apparatus (ROMA) [Süm84] where the aerosol particles were impacted on thin polyethylene foils ( $30$   $\mu\text{g}/\text{cm}^2$ ) and subjected to  $4\pi$ - $\alpha$ -

---

spectrometry by step-wise transport of the samples along a series of up to 12 pairs of PIPS detectors. However, the counting time was limited to about 12 half-lives (the step time is usually set to one half-life of the mother nuclide), and decays that occurred during the step were missed. In addition, rather complicated decay paths [EiR00b] had to be followed, taking into account the possible recoil of the daughter from the catcher foil into the detector facing the sample.

Even with the prerequisites fulfilled in the Bh experiment, in a beamtime of one month's duration, a total of only five correlated  $\alpha$ - $\alpha$  and one  $\alpha$ - $\alpha$ - $\alpha$  decay chains was detected. The production cross section of  $^{267}\text{Bh}$  in the reaction  $^{249}\text{Bk}(^{22}\text{Ne}, 4n)$  is about 60 pb [EiR00a]. The beam intensity cannot be substantially increased due to the thermal load of the target, the target thickness is limited due to energy loss of the particles and the width of the excitation function, the cross section of the chosen reaction is fixed, and it is not feasible to perform experiments of much longer duration. Thus, a gain in the efficiency of a factor of ten seemed to be necessary to compensate for the decrease of the production cross section of roughly one order of magnitude for production of  $^{269}\text{Hs}$  in the  $^{248}\text{Cm}(^{26}\text{Mg}, 5n)$  reaction.

## 1.8 Outline of the thesis

First, short-lived Os isotopes were produced at the PHILIPS cyclotron at PSI in heavy-ion induced fusion reactions and were transported from the recoil chamber to the chemistry device using a He/N<sub>2</sub>-carbon aerosol gas-jet (OLGA technique [Gäg91]). These experiments are described at the beginning of Chapter 2. These studies led to the development of a new device for the separation of volatile heavy-ion reaction products, called In situ Volatilization and On-line detection apparatus (IVO). In contrast to the well-known OLGA [Gäg91] the nuclear reaction products are not attached to aerosol particles and transported to the chemistry device with an aerosol-gas-jet [Wol75, Nai89] but volatilized *in situ* within the recoil chamber and transported with the carrier gas in the gas phase. Similar set-ups have already been used earlier in Dubna (see e.g. [Zva66, Zva70]) and also in investigations of Os [Yak99, Yak00]. IVO was tested with short-lived isotopes of Os, which were

---

transformed to OsO<sub>4</sub>, and elemental Hg, again produced at the PHILIPS Cyclotron. This work is published in "Nuclear Instruments and Methods A".

A novel detection system based on the TC principle called Cryo On-Line Detector (COLD) was built, which was then used for the chemical investigation of Hs. A first device of that kind called Cryo-Thermochromatographic Separator (CTS) has previously been developed in Berkeley [Kir02]. In the COLD device, the chromatography column consists of PIN-diodes which form a narrow channel. The diodes register  $\alpha$ - and SF-decaying nuclides adsorbed on the (cooled) surface with a high geometrical efficiency of about 77%, favouring the detection of complete decay sequences (up to 4  $\alpha$ -particles in the case of <sup>269</sup>Hs). Such a IVO-COLD system proved to fulfill the prerequisites for an experiment with Hs.

In Chapter 3, the Hs experiment is described which was performed in May 2001 at the Gesellschaft für Schwerionenforschung mbH (GSI) in Darmstadt, Germany. Long-lived Hs isotopes were produced using an intense <sup>26</sup>Mg beam in the reaction <sup>248</sup>Cm(<sup>26</sup>Mg, 5,4n)<sup>269,270</sup>Hs and the decay of these isotopes was registered in the COLD device. This experiment is described in two papers. One has been submitted to "The European Physical Journal A", the second is accepted for publication in "Nature".

In order to interpret the measured properties of Hs, the stability and adsorption behavior of the group 8 tetroxides were theoretically modelled using two different approaches. First, the trends established by RuO<sub>4</sub> and OsO<sub>4</sub> were extrapolated to HsO<sub>4</sub>. In the second approach, the adsorption of HsO<sub>4</sub> on the active surface of the COLD system was interpreted in terms of a pure physisorption process of a non-polar molecule on a dielectric surface. This work, contained in Chapter 4, is published in the "Journal of Physical Chemistry B".

Chapter 5 contains concluding remarks and a short outlook. In the Appendix, some pictures of the experiment can be found.

---

**References of Chapter 1**

- [Aud95] Audi, G. *et al.* The 1995 update to the atomic mass evaluation. *Nucl. Phys.* **A595**, 409 (1995).
- [Bäc71] Bächmann, K. *et al.* Chemische Probleme bei der Darstellung überschwerer Elemente durch Kernreaktionen. *Radiochim. Acta* **15**, 153 (1971).
- [Bas74] Bass, R. Fusion of heavy nuclei in a classical model. *Nucl. Phys.* **A231**, 45 (1974).
- [Boh36] Bohr, N. Neutron capture and nuclear constitution. *Nature* **137**, 344 (1936).
- [Boh98] Bohr, A. *et al.* *Nuclear structure*. World scientific: Singapore, 1998; Vol. 1
- [Buc91] Buck, B. *et al.* Ground state to ground state alpha decays of heavy even-even nuclei. *J. Phys. G.* **17**, 1223 (1991).
- [Che85] Chepigin, V.I. *et al.* Search of alpha-active isotopes of element 108 in the reaction  $^{249}\text{Cf}+^{22}\text{Ne}$  with fast chemical isolation. Abstract School-Seminar on Heavy Ion Physics 1985, Report P7-86-322, JINR, Dubna (1986) p. 15 (in Russian).
- [Cwi96] Cwiok, S. *et al.* Shell structure of the superheavy elements. *Nucl. Phys.* **A611**, 211 (1996).
- [Cwi99] Cwiok, S. *et al.* Structure of odd-N superheavy elements. *Phys. Rev. Lett.* **83**, 1108 (1999).
- [Cze94] a) Czerwinski, K.R. *et al.* Solution chemistry of element 104: Part I. Liquid-liquid extractions with trisooctylamine. *Radiochim. Acta* **64**, 23 (1994).  
b) Czerwinski, K.R. *et al.* Solution chemistry of element 104: Part II. Liquid-liquid extractions with tributylphosphate. *Radiochim. Acta* **64**, 29 (1994).
- [Des73] Desclaux, J.P. Relativistic Dirac-Fock expectation values for atoms with  $Z=1$  to  $Z=120$ . *At. Data Nucl. Data Tab.* **12**, 311 (1973).
- [Dom84] a) Domanov, V.P. *et al.* Continuous-flow thermochromatographic separation of unsupported radioisotopes of platinum elements in a stream of air from nuclear reaction products in an accelerator heavy-ion beam. Translated from *Radiokhimiya* **26**, 770 (1984).  
b) Domanov, V.P. *et al.* Chromatographic behavior of oxygen-containing compounds of iridium and platinum in ultrasmall quantities. Translated from *Radiokhimiya* **26**, 66 (1984).
- [Dou87] Dougan, R.J. *et al.* OSCAR: An apparatus for on-line gas-phase separations. Lawrence Livermore National Laboratory, Nuclear Chemistry Division, Ann. Rep. FY 87, UCAR 10062/87, p. 4-17 (1987). (unpublished)
- [Dre99] Dressler, R. Synthese neutronenreicher Isotope schwerster Elemente in xn- und  $\alpha$ -xn-Reaktionen. Doctoral thesis, Universität Bern, Bern, 1999.

- 
- [EiB82] Eichler, B. *et al.* Evaluation of the enthalpy of adsorption from thermochromatographical data. *Radiochim. Acta* **30**, 233 (1982).
- [EiR00] a) Eichler, R. *et al.* Chemical characterization of bohrium (element 107). *Nature* **407**, 63 (2000).  
b) Eichler, R. Die chemische Charakterisierung des Transactinoids Bohrium (Bh, Element 107). Doctoral Thesis, Universität Bern, Bern, 2000.
- [Fri75] Fricke, B. Superheavy elements - A prediction of their chemical and physical properties. *Structure and bonding* **21**, 90 (1975).
- [Gäg91] Gäggeler, H.W. *et al.* OLGA II, an on-line gas chemistry apparatus for application in heavy element research. *Nucl. Instrum. Meth.* **A309**, 201 (1991).
- [Gäg92] Gäggeler, H.W. *et al.* Gas phase chromatography experiments with bromides of tantalum and element 105. *Radiochim. Acta* **57**, 93 (1992).
- [Gäg97] Gäggeler, H.W. Fast chemical separation procedures for transactinides. *Proceedings of the Robert A. Welch Foundation, 41st Conference on Chemical Research, The Transactinide Elements*; The Robert A. Welch Foundation: Houston, 1997; p. 43.
- [Gäg98] Gäggeler, H.W. Chemistry gains a new element: Z=106. *J. Alloys. Comp.* **271-273**, 277 (1998).
- [Ghi95] a) Ghiorso, A. *et al.* Evidence for the possible synthesis of element 110 produced by the  $^{59}\text{Co}+^{209}\text{Bi}$  reaction. *Phys. Rev. C* **51**, R2293 (1995).  
b) Ghiorso, A. *et al.* Evidence for the synthesis of  $^{267}110$  produced by the  $^{59}\text{Co}+^{209}\text{Bi}$  reaction. *Nucl. Phys.* **A583**, 861 (1995).
- [Gia00] Giardina, G. *et al.* Effects of the entrance channel on the synthesis of superheavy elements. *Eur. Phys. J. A* **8**, 205 (2000).
- [Gre88] Gregorich, K.E. *et al.* Aqueous chemistry of element 105. *Radiochim. Acta* **43**, 223 (1988).
- [Gri67] Griffith, W.P. *The chemistry of the rarer platinum metals (Os, Ru, Ir and Rh)*. Interscience publishers, John Wiley and Sons: London, 1967.
- [Gri80] Griffith, W.P. *et al.* in *Gmelin Handbuch der anorganischen Chemie*. Osmium Supplement Vol. 1, Springer-Verlag: Berlin, 1980; p.74
- [Gui89] Guillaumont, R. *et al.* Kinetic and thermodynamic aspects of tracer-scale and single atom chemistry. *Radiochim. Acta* **46**, 169 (1989).
- [Gun70] Gundersen, G. *et al.* Molecular structure of xenon tetroxide,  $\text{XeO}_4$ . *J. Chem. Phys.* **52**, 812 (1970).
- [Gup97] Gupta, R.K. *et al.* Structure of  $^{294,302}120$  nuclei using the relativistic mean-field method. *Mod. Phys. Lett. A* **12**, 1727 (1997).
- [Hab01] Haba, H. *et al.* Startup of transactinide chemistry in JAERI. *Radiochim. Acta* **89**, 733 (2001).
- [Her88] Herrmann, G. Synthese schwerster chemischer Elemente - Ergebnisse und Perspektiven. *Angew. Chem.* **100**, 1471 (1988).

- 
- [Hil92] Hildenbrand, D.L. *et al.* Thermochemistry of the gaseous osmium oxides. *J. Phys. Chem.* **96**, 2325 (1992).
- [Hof95] Hofmann, S. *et al.* Production and decay of  $^{269}\text{110}$ . *Z. Phys. A.* **350**, 277 (1995).
- [Hof96] Hofmann, S. *et al.* The new element 112. *Z. Phys. A* **354**, 229 (1996).
- [Hof00] Hofmann, S. *et al.* The discovery of the heaviest elements. *Rev. Mod. Phys.* **72**, 733 (2000).
- [Hof01] Hofmann, S. *et al.* The new isotope  $^{270}\text{110}$  and its decay products  $^{266}\text{Hs}$  and  $^{262}\text{Sg}$ . *Eur. Phys. J. A* **10**, 5 (2001).
- [Hoff71] Hoffman, D.C. *et al.* Detection of plutonium-244 in nature. *Nature* **234**, 132 (1971).
- [Hoff96] Hoffman, D.C. Chemistry of the heaviest elements. *Radiochim. Acta* **72**, 1 (1996).
- [Hoff99] Hoffman, D.C. *et al.* Chemistry of the heaviest elements - one atom at a time. *J. Chem. Educ.* **76**, 331 (1999).
- [Hüb01] Hübener, S. *et al.* Physico-chemical characterization of seaborgium as oxide hydroxide. *Radiochim. Acta* **89**, 737 (2001).
- [Hul80] Hulet, E.K. *et al.* Chloride complexation of element 104. *J. Inorg. Nucl. Chem.* **42**, 79 (1980).
- [Hul87] Hulet, E.K. *et al.* Search for  $^{272}\text{[109]}$  in a new region of stability. Lawrence Livermore National Laboratory, Nuclear Chemistry Division, Ann. Rep. FY 87, UCAR 10062/87, p. 4-9 (1987). (unpublished)
- [Iwa96] Iwamoto, A. *et al.* Collisions of deformed nuclei: A path to the far side of the superheavy island. *Nucl. Phys.* **A596**, 329 (1996).
- [Kac96] a) Kacher, C.D. *et al.* Chemical studies of rutherfordium (element 104): Part II. Solvent extraction studies into tributylphosphate from HBr solutions. *Radiochim. Acta* **75**, 127 (1996).  
b) Kacher, C.D. *et al.* Chemical studies of rutherfordium (element 104): Part III. Solvent extraction studies into triisooctylamine from HF solutions. *Radiochim. Acta* **75**, 135 (1996).
- [Kad96] Kadkhodayan, B. *et al.* On-line gas chromatographic studies of chlorides of rutherfordium and homologs Zr and Hf. *Radiochim. Acta* **72**, 169 (1996).
- [Kel84] Keller, O.L. Chemistry of the heavy actinides and light transactinides. *Radiochim. Acta* **37**, 169 (1984).
- [Kir02] Kirbach, U.W. *et al.* The Cryo-Thermochromatographic Separator (CTS): A new rapid separation and  $\alpha$ -detection system for on-line chemical studies of highly volatile osmium and hassium ( $Z=108$ ) tetroxides. *Nucl. Instrum. Meth.* **A484**, 587 (2002).
- [Kra89] Kratz, J.V. *et al.* Chemical properties of element 105 in aqueous solution: Halide complex formation and anion exchange into triisooctyl amine. *Radiochim. Acta* **48**, 121 (1989).

- 
- [Kra99] Kratz, J.V. Chemical properties of the transactinides. In *Heavy elements and related new phenomena*, Greiner, W., Gupta, R.K., Eds; World scientific: Singapore, 1999; Chapter 4
- [Kru00] Kruppa, A.T. *et al.* Shell corrections of superheavy nuclei in self-consistent calculations. *Phys. Rev. C* **61**, 034313 (2000).
- [Lan96] Lane, M.R. *et al.* Spontaneous fission properties of  $^{262}\text{Rf}$ . *Phys. Rev. C* **53**, 2893 (1996).
- [Laz94] Lazarev, Yu.A. *et al.* Discovery of enhanced nuclear stability near the deformed shells  $N=162$  and  $Z=108$ . *Phys. Rev. Lett.* **73**, 624 (1994).
- [Laz95] Lazarev, Yu.A. *et al.* New nuclide  $^{267}108$  produced by the  $^{238}\text{U} + ^{34}\text{S}$  reaction. *Phys. Rev. Lett.* **75**, 1903 (1995).
- [McM40] McMillan, E. *et al.* Radioactive element 93. *Phys. Rev.* **57**, 1185 (1940).
- [Mel67] Meldner, H. Predictions of new magic regions and masses for superheavy nuclei from calculations with realistic shell model single particle hamiltonians. *Ark. Fys.* **36**, 593 (1967).
- [Mer61] Merinis, J. *et al.* Séparation par volatilisation des radioisotopes de mercure, de platine, d'iridium, d'osmium et de rhénium formés par spallation dans une cible d'or. *Anal. Chim. Acta* **25**, 498 (1961).
- [Möl87] Möller, P. *et al.* Calculated fission properties of the heaviest elements. *Nucl. Phys.* **A469**, 1 (1987).
- [Möl88] a) Möller, P. *et al.* Nuclear masses from a unified macroscopic-microscopic model. *At. Data Nucl. Data Tab.* **39**, 213 (1988).  
b) Möller, P. *et al.* Nuclear mass formula with a finite-range droplet model and a folded-yukawa single-particle potential. *At. Data Nucl. Data Tab.* **39**, 225 (1988).
- [Möl89] Möller, P. *et al.* New developments in the calculation of heavy-element fission barriers. *Nucl. Phys.* **A492**, 349 (1989).
- [Möl94] Möller, P. *et al.* Stability of heavy and superheavy elements. *J. Phys. G* **20**, 1681 (1994).
- [Möl97] Möller, P. *et al.* Nuclear properties for astrophysical and radioactive-ion-beam applications. *At. Data Nucl. Data Tab.* **66**, 131 (1997).
- [Mün84] Münzenberg, G. *et al.* The identification of element 108. *Z. Phys. A* **317**, 235 (1984).
- [Mün86] Münzenberg, G. *et al.* Evidence for  $^{264}108$ , the heaviest known even-even isotope. *Z. Phys. A* **324**, 489 (1986).
- [Mün87] Münzenberg, G. *et al.* Observation of the isotopes  $^{264}108$  and  $^{265}108$ . *Z. Phys. A* **328**, 49 (1987).
- [Mye66] Myers, W.D. *et al.* Nuclear masses and deformations. *Nucl. Phys.* **81**, 1 (1966).
- [Mye96] Myers, W.D. *et al.* Nuclear properties according to the Thomas-Fermi model. *Nucl. Phys.* **A601**, 141 (1996).

- [Nai89] Nai-Qi, Y. *et al.* The saphir gas-jet and a first application to an on-line separation of niobium. *Radiochim. Acta* **47**, 1 (1989).
- [Nik65] Nikol'skii, A.B. *et al.* The thermodynamic properties and stability of ruthenium and osmium oxides. *Russ. J. Inorg. Chem.* **10**, 1 (1965).
- [Nil69] Nilsson, S.G. *et al.* On the nuclear structure and stability of heavy and superheavy elements. *Nucl. Phys.* **A131**, 1 (1969).
- [Oga99] a) Oganessian, Yu.Ts. *et al.* Search for new isotopes of element 112 by irradiation of  $^{238}\text{U}$  with  $^{48}\text{Ca}$ . *Eur. Phys. J. A* **5**, 63 (1999).  
b) Oganessian, Yu.Ts. *et al.* Synthesis of nuclei of the superheavy element 114 in reactions induced by  $^{48}\text{Ca}$ . *Nature* **400**, 242 (1999).  
c) Oganessian, Yu.Ts. *et al.* Synthesis of superheavy nuclei in the  $^{48}\text{Ca} + ^{244}\text{Pu}$  reaction. *Phys. Rev. Lett.* **83**, 3154 (1999).
- [Oga00] a) Oganessian, Yu.Ts. *et al.* Observation of the decay of  $^{292}116$ . *Phys. Rev. C* **63**, 011301(R) (2000).  
b) Oganessian, Yu.Ts. *et al.* Synthesis of superheavy nuclei in the  $^{48}\text{Ca} + ^{244}\text{Pu}$  reaction:  $^{288}114$ . *Phys. Rev. C.* **62**, 041604(R) (2000).
- [Omt02] Omtvedt, J.P. *et al.* SISAK liquid-liquid extraction experiments with pre-separated  $^{257}\text{Rf}$ . *J. Nucl. Radiochem. Sci.* **3**, 121 (2002).
- [Opp98] Oppermann, H. *et al.* Untersuchungen zum thermischen Verhalten der Osmiumoxide. *Z. Naturforsch.* **53 b**, 1352 (1998).
- [Pat89] Patyk, Z. *et al.* Potential energy and spontaneous-fission half-lives for heavy and superheavy nuclei. *Nucl. Phys.* **A502**, 591c (1989).
- [Pat91] a) Patyk, Z. *et al.* Main deformed shells of heavy nuclei studied in a multidimensional deformation space. *Phys. Lett. B* **256**, 307 (1991).  
b) Patyk, Z. *et al.* Ground state properties of the heaviest nuclei analyzed in a multidimensional deformation space. *Nucl. Phys.* **A533**, 132 (1991).
- [Pau99] Paulus, W. *et al.* Chemical properties of element 105 in aqueous solution: Extraction of the fluoride-, chloride-, and bromide complexes of the group-5 elements into an aliphatic amine. *Radiochim. Acta* **84**, 69 (1999).
- [Per96] Pershina, V.G. Electronic structure and properties of the transactinides and their compounds. *Chem. Rev.* **96**, 1977 (1996).
- [Per01] Pershina, V. *et al.* The electronic structure and properties of group 8 oxides  $\text{MO}_4$ , where  $\text{M}=\text{Ru}$ ,  $\text{Os}$ , and element 108,  $\text{Hs}$ . *J. Chem. Phys.* **115**, 792 (2001).
- [Pyy79] Pyykkö, P. *et al.* Relativity and the periodic system of the elements. *Acc. Chem. Res.* **12**, 276 (1979).
- [Pyy88] Pyykkö, P. Relativistic effects in structural chemistry. *Chem. Rev.* **88**, 563 (1988).
- [Rar85] Rard, J.A. Chemistry and thermodynamics of ruthenium and some of its inorganic compounds and aqueous species. *Chem. Rev.* **85**, 1 (1985).
- [Rei92] Reisdorf, W. *et al.* How well do we understand the synthesis of heavy elements by heavy-ion induced fusion? *Z. Phys. A* **343**, 47 (1992).

- 
- [Ren96] Ren, Z. *et al.* Relativistic mean-field study of even-even nuclei near  $Z=108$  and  $N=162$ . *J. Phys. G* **22**, 1793 (1996).
- [Roy02] Royer, G. *et al.* On the formation and alpha decay of superheavy elements. *Nucl. Phys.* **A699**, 479 (2002).
- [Rut97] Rutz, K. *et al.* Superheavy nuclei in self-consistent nuclear calculations. *Phys. Rev. C* **56**, 238 (1997).
- [Sag99] Sagajdak, R.N., private communication, 1999
- [Schä89] Schädel, M. *et al.* ARCA II - A new apparatus for fast, repetitive HPLC separations. *Radiochim. Acta* **48**, 171 (1989).
- [Schä96] a) Schädel, M. Chemistry of the transactinide elements. *Radiochim. Acta* **70-71**, 207 (1995).  
b) Schädel, M. *et al.* Prospects for the discovery of new elements. *J. Radioanal. Nucl. Chem.* **203**, 283 (1996).
- [Schä97] a) Schädel, M. *et al.* Chemical properties of element 106 (seaborgium). *Nature* **388**, 55 (1997).  
b) Schädel, M. *et al.* First aqueous chemistry with seaborgium (element 106). *Radiochim. Acta* **77**, 149 (1997).
- [Schä98] a) Schädel, M. First aqueous chemistry with seaborgium (element 106). *J. Alloys Comp.* **271-273**, 312 (1998).  
b) Schädel, M. *et al.* Aqueous chemistry of seaborgium ( $Z=106$ ). *Radiochim. Acta* **83**, 163 (1998).
- [Schä01] Schädel, M. Aqueous chemistry of transactinides. *Radiochim. Acta* **89**, 721 (2001).
- [Schm84] Schmidt, K.H. *et al.* Some remarks on the error analysis in the case of poor statistics. *Z. Phys. A* **316**, 19 (1984).
- [Schu98] Schumann, D. *et al.* Sorption behaviour of rutherfordium and thorium from HCl/Hf containing aqueous solution. *J. Alloys Comp.* **271-273**, 307 (1998).
- [Schw98] P. Schwerdtfeger *et al.* Relativistic Effects of the Superheavy Elements. In *Encyclopedia of Computational Chemistry*, Wiley: New York, 1998; Vol. 4, 2480-2499
- [Sea58] Seaborg, G.T. *The transuranium elements*. New Haven Yale University Press, 1958.
- [Sil70] Silva, R. *et al.* Chemical separation of rutherfordium. *Inorg. Nucl. Chem. Lett.* **6**, 871 (1970).
- [Smo95] a) Smolanczuk, R. Properties of the hypothetical spherical superheavy nuclei. *Phys. Rev. C* **56**, 812 (1997).  
b) Smolanczuk, R. *et al.* Spontaneous-fission half-lives of deformed superheavy nuclei. *Phys. Rev. C* **52**, 1871 (1995).

- 
- [Smo96] Smolanczuk, R. *et al.* Masses and half-lives of superheavy elements. In "Extremes of nuclear structure". *Proceedings of the International Workshop XXIV on Gross Properties of Nuclei and Nuclear Excitations*, Hirschegg, Austria, January 15-20, 1996, edited by H. Feldmeier, J. Knoll and W. Nörenberg (GSI, Darmstadt, 1996) p. 35-42.
- [Smo97] Smolanczuk, R. Properties of the hypothetical spherical superheavy nuclei. *Phys. Rev. C* **56**, 812 (1997).
- [Sob01] Sobiczewski, A. *et al.* Problem of "deformed" superheavy nuclei. *Phys. Rev. C* **63**, 034036 (2001).
- [Spa88] Spanier, L. *et al.* A modified Bethe-Weizsacker mass formula with deformation and shell corrections and few free parameters. *At. Data Nucl. Data Tab.* **39**, 259 (1988).
- [Str00] Strub, E. *et al.* Fluoride complexation of rutherfordium (Rf, element 104). *Radiochim. Acta* **88**, 265 (2000).
- [Süm84] Sümmerer, K. *et al.* ROMA - A Rotating wheel Multidetector Apparatus used in experiments with  $^{254}\text{Es}$  as a target. GSI Annual Report 1983, 84-1 (1984) p. 246. (unpublished)
- [Swi82] Swiatecki, W.J. The dynamics of the fusion of two nuclei. *Nucl. Phys.* **A376**, 275 (1982).
- [Syl00] Sylwester, E.R. *et al.* On-line gas chromatographic studies of Rf, Zr, and Hf bromides. *Radiochim. Acta* **88**, 837 (2000).
- [Tim96] Timokhin, S.N. *et al.* Chemical identification of element 106 by thermochromatography. *J. Radioanal. Nucl. Chem. Lett.* **212**, 31 (1996).
- [Tru02] Trubert, D. *et al.* Chemical isolation of dubnium (element 105) in fluoride media. *Radiochim. Acta* **90**, 127 (2002).
- [Tsy02] Tsyganov, Yu.S. *et al.* Real-time mode detection of heavy ion-induced nuclear reaction products. *Nucl. Instrum. Meth.* **A477**, 406 (2002).
- [Tür92] Türler, A. *et al.* Gas phase chromatography of halides of elements 104 and 105. *J. Radioanal. Nucl. Chem. (Articles)* **160**, 327 (1992).
- [Tür96] a) Türler, A. *et al.* On-line gas phase chromatography with chlorides of niobium and hahnium (element 105). *Radiochim. Acta* **73**, 55 (1996).  
b) Türler, A. Gas phase chemistry experiments with transactinide elements. *Radiochim. Acta* **72**, 7 (1996).
- [Tür98] a) Türler, A. *et al.* Decay properties of  $^{265}\text{Sg}(Z=106)$  and  $^{266}\text{Sg}(Z=106)$ . *Phys. Rev. C* **57**, 1648 (1998).  
b) Türler, A. *et al.* Evidence for relativistic effects in the chemistry of element 104. *J. Alloys Comp.* **271-273**, 287 (1998).
- [Tür99] Türler, A. *et al.* First measurement of a thermochemical property of a seaborgium compound. *Angew. Chem. Int. Ed.* **38**, 2212 (1999).

- 
- [vZw01] v. Zweidorf, A. *et al.* Deposition and detection of volatile oxides on metallic surfaces with CALLISTO. GSI Scientific Report 2000, Gesellschaft für Schwerionenforschung mbH, Darmstadt 2001-1 (2001). p. 171
- [Wil00] Wilk, P.A. *et al.* Evidence for new isotopes of element 107:  $^{266}\text{Bh}$  and  $^{267}\text{Bh}$ . *Phys. Rev. Lett.* **85**, 2697 (2000).
- [Wol75] Wollnik, G. *et al.* The improvement of a gas-jet system by the use of an aerosol generator. *Nucl. Instrum. Meth.* **127**, 539 (1975).
- [Yak96] Yakushev, A.B. *et al.* Comparative study of oxochlorides of molybdenum, tungsten and element 106. *J. Radioanal. Nucl. Chem.* **205**, 63 (1996).
- [Yak99] Yakushev, A.B. *et al.* On-line experiments with short-lived osmium isotopes as a test of the chemical identification of the element 108 - hassium. 1<sup>st</sup> Int. Conf. on the Chemistry and Physics of the Transactinide Elements, TAN99. Sept. 26-30, 1999, Seeheim, Germany. Extended Abstracts P-M-17.
- [Yak00] Yakushev, A.B. *et al.* On-line experiments with short-lived osmium isotopes as a test for the chemical identification of the element 108 hassium. Joint Inst. Nucl. Res., Flerov Lab. of Nucl. Reactions, Scientific Report 1997-1998, Heavy Ion Physics, Dubna, 2000. p. 186
- [Yak01] Yakushev, A.B. *et al.* First attempt to chemically identify element 112. *Radiochim. Acta* **89**, 743 (2001).
- [Yak02] Yakushev, A.B. *et al.* On the way to chemically identify element 112. Contribution to the Workshop on Recoil Separator for Superheavy Element Chemistry, GSI Darmstadt, Germany, March 20-21, 2002.
- [Zhu85] a) Zhuikov, B.L. *et al.* Experiments for chemical isolation and detecting of spontaneously fissioning and  $\alpha$ -active isotopes of element 108. Dubna 1985. Unpublished report.  
b) Zhuikov, B.L. *et al.* Possibilities of chemical identification of short-lived element 108 isotopes. Abstract School-Seminar on Heavy Ion Physics 1985, Report P7-86-322, JINR, Dubna (1986) p. 26 (in Russian).
- [Zhu89] Zhuikov, B.L. *et al.* Is element 104 (kurchatovium) a p-element? I. Chromatography of atoms with hydrogen as carrier gas. *Radiochim. Acta* **46**, 113 (1989).
- [Zub02] Zubov, A.S. *et al.* Survival probability of superheavy nuclei. *Phys. Rev. C* **65**, 024308 (2002).
- [Zud93] Zude, F. *et al.* Thermochromatography of platinum elements in oxygen: Radiochemical studies of the behaviour of rhodium, palladium, osmium and platinum. *Radiochim. Acta* **62**, 61 (1993).
- [Zva66] Zvara, I. *et al.* Khimiceskie svoistva elementa 104. *Atom. Energija* **21**, 83 (1966) (in Russian).

- 
- [Zva70] Zvara, I. *et al.* Experiments on the chemistry of element 104 - kurchatovium. V. Adsorption of kurchatovium chloride from the gas stream on surfaces of glass and potassium chloride. *J. Inorg. Nucl. Chem.* **32**, 1885 (1970).
- [Zva71] Zvara, I. *et al.* Chemical separation of kurchatovium. *Inorg. Nucl. Chem. Lett.* **7**, 1109 (1971).
- [Zva76] Zvara, I. *et al.* Chemical isolation of nilsbohrium as ekatantalum in the form of the anhydrous bromide. II. Experiments with a spontaneously fissioning isotope of nilsbohrium. Translated from *Radiokhimiya* **18**, 371 (1976).
- [Zva85] Zvara, I. Simulation of thermochromatographic processes by the Monte Carlo method. *Radiochim. Acta* **38**, 95 (1985).
- [Zva90] Zvara, I. Thermochromatographic method of separation of chemical elements in nuclear and radiochemistry. *Isotopenpraxis* **26**, 251 (1990).
- [Zva98] Zvara, I. *et al.* Chemical identification of element 106 (thermochromatography of oxochlorides). *Radiochim. Acta* **81**, 179 (1998).

## 2. Development of the IVO-COLD system

In this chapter, experiments with short-lived Os isotopes produced on the PHILIPS cyclotron at PSI in different heavy-ion induced fusion reactions, e.g.  $^{162}\text{Er}(^{18}\text{O}, xn)^{180-x}\text{Os}$ , or  $^{156}\text{Dy}(^{22}\text{Ne}, xn)^{178-x}\text{Os}$ , are described. These were carried out to investigate the behavior of single atoms of Os with half-lives comparable to that of  $^{269}\text{Hs}$  ( $T_{1/2} \sim 10$  s). The conditions necessary for a fast and quantitative formation of  $\text{OsO}_4$  were evaluated as well as the possibilities of its detection via the nuclear decay of the radioisotopes. Using IC, the adsorption enthalpy of  $\text{OsO}_4$  on quartz was evaluated.

### 2.1 Experiments using a carbon aerosol gas-jet

In a first experiment in the reaction  $^{156}\text{Dy}(^{22}\text{Ne}, xn)^{178-x}\text{Os}$  at a beam energy of  $E_{\text{Lab}} = 128$  MeV in the middle of the target, the isotopes  $^{172}\text{Os}$  ( $E_{\alpha} = 5.100$  MeV,  $T_{1/2} = 19.2$  s) and  $^{173}\text{Os}$  ( $E_{\alpha} = 4.938$  MeV,  $T_{1/2} = 22.4$  s) were produced. The set-up shown in Figure 2-1 was used.

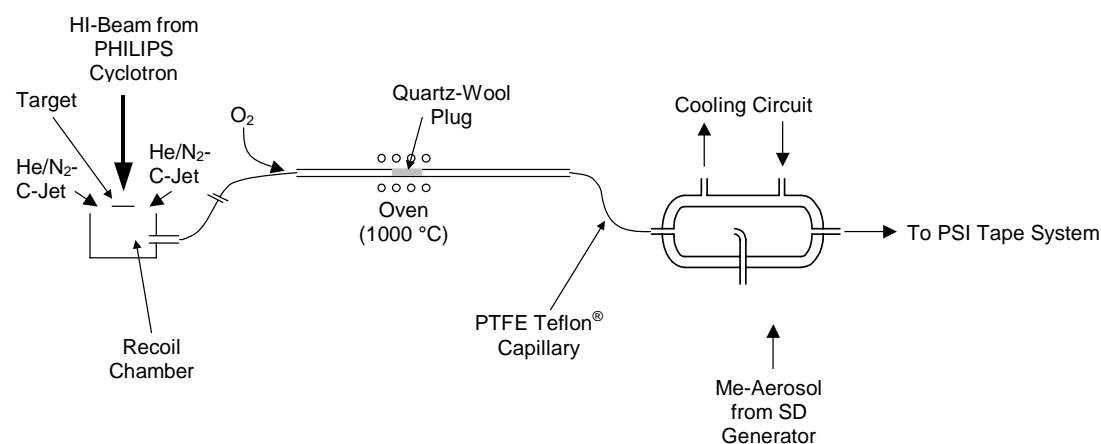


Fig. 2-1 Set-up used for feasibility studies of different metal aerosols for the absorption of  $\text{OsO}_4$ .

The target - recoil-chamber system described in [Pig95] was used and the recoiling Os isotopes were attached to carbon aerosol particles produced via spark discharge (SD). The aerosol particles were transported via a gas-jet (1 l/min He, 20 ml/min N<sub>2</sub>) through a polyethylene capillary (i.d. 2 mm, 10 m length) to a reaction zone, where 20-100 ml/min O<sub>2</sub> was added to the carrier gas and a temperature of 1000 °C applied to burn carbon particles and

release the Os isotopes which were immediately oxidized to OsO<sub>4</sub>. After passing a 30 cm long quartz column (i.d. 3 mm) and a 30 cm long PTFE Teflon<sup>®</sup> capillary (i.d. 2 mm), the OsO<sub>4</sub> molecules were fed into a so-called recluster chamber (i.d. 30 mm, 95 mm length) where a second gas-jet (1 l/min Ar) containing metal aerosol particles was injected. Four different metals (Pb, Fe, Ag, and Cu) were used to check the influence of the metal surface on the absorption efficiency. The aerosol was generated by spark discharge (SD) using electrodes of the respective metal. After the SD-generator, a <sup>85</sup>Kr source was installed to reach charge equilibration. Using this second gas-jet, the Os isotopes were transported to the PSI Tape detection system [Gäg91]. The particles were impacted on a commercial magnetic tape as used for computer data storage which was moved every 20 s to position the sample in front of four consecutive PIPS-detectors to register the  $\alpha$ -particle decay of the Os isotopes. The yield relative to a direct catch, where the He/N<sub>2</sub>-C gas-jet fed through the recoil chamber was directly injected into the deposition position of the PSI tape system, is summarized in Table 2-1.

Tab. 2-1 Observed yield of <sup>172</sup>Os (T<sub>1/2</sub>=19.2 s) adsorbed on different metal surfaces normalized to a direct-catch experiment where a He/N<sub>2</sub>-C gas-jet was directly deposited on the PSI tape system.

Metal	Yield <sup>172</sup> Os [%]
Pb	27
Fe	7
Ag	6
Cu	6

The optimum yield was reached when Pb aerosol particles were used. OsO<sub>4</sub> was probably reduced on the Pb surface to non-volatile lower oxides. This assumption is further supported by the observation that the yield was only optimal when the carrier gas of the recluster aerosol jet was purified from trace amounts of O<sub>2</sub> with a Ta-getter kept at 950 °C. However, as has already been observed in the Bh experiment [EiR00], the He/N<sub>2</sub>-C jet was not very stable and the transport yield of Os isotopes from the target chamber to the quartz column (about 20% only) was lower than that of the second gas-jet where 27 % was reached without any further optimization of the Ar/Pb

aerosol. Therefore an apparatus was developed (Chapter 2.3) where the first gas-jet worked without aerosol particles.

## 2.2 Optimization of a Ar/Pb aerosol

Besides production of a Ar/Pb aerosol via SD, another technique was tested: primary Pb particles were produced from molten lead in a stainless steel crucible. The primary particles were fed into a so-called coagulation vessel with an adjustable volume of 1-7 l. Depending on the size of the vessel and the gas flow rate, different residence times of up to several minutes permitted coagulation to larger agglomerates. Using a differential mobility analyzer (DMA) in connection with a condensation particle counter (CPC), the aerosol particle number concentration and mean particle diameter as a function of the crucible temperature and the volume were measured as shown in Figures 2-2 and 2-3.

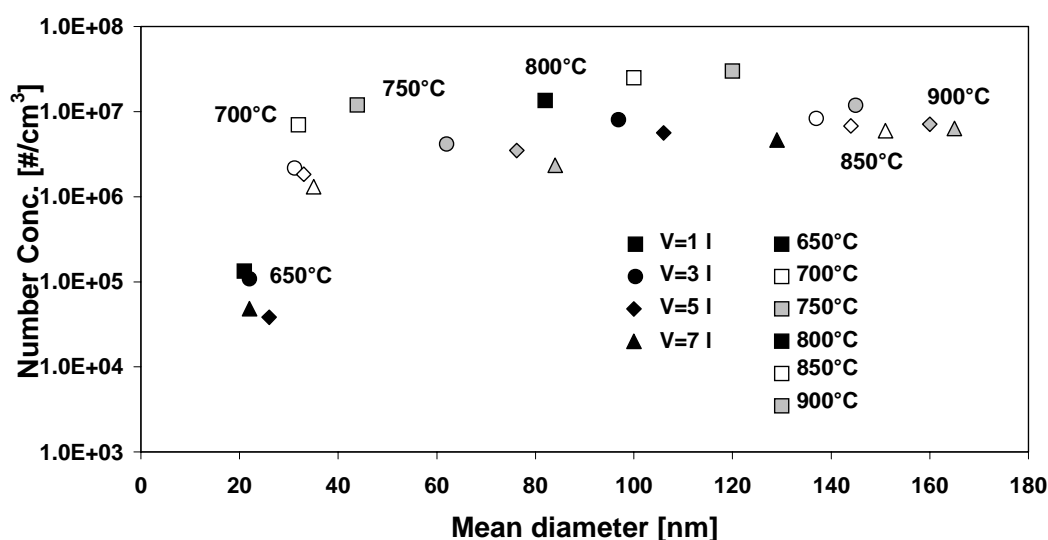


Fig. 2-2 Particle number concentration and mean particle diameter of a Ar/Pb aerosol (500 ml/min Ar) as a function of crucible temperature and coagulation vessel volume.

For efficient transport in a gas-jet, a mean particle diameter of about 100-300 nm and a particle number concentration of about  $5 \cdot 10^6$ - $1 \cdot 10^7$   $\text{cm}^{-3}$  proved to be ideal [Web92]. When using a rotating wheel detection system such as ROMA [Süm84], the particles accumulate on the foils and the resolution obtained in the back detectors is strongly affected by large amounts of Pb on the foils. Therefore, an aerosol with a mean particle diameter of only 100 nm and a particle number concentration  $< 10^7$   $\text{cm}^{-3}$  was considered ideal. Such an aerosol could be produced at a crucible temperature of about 800 °C and a coagulation vessel volume of 3 l. A DMA spectrum of such an aerosol is shown in Figure 2-3.

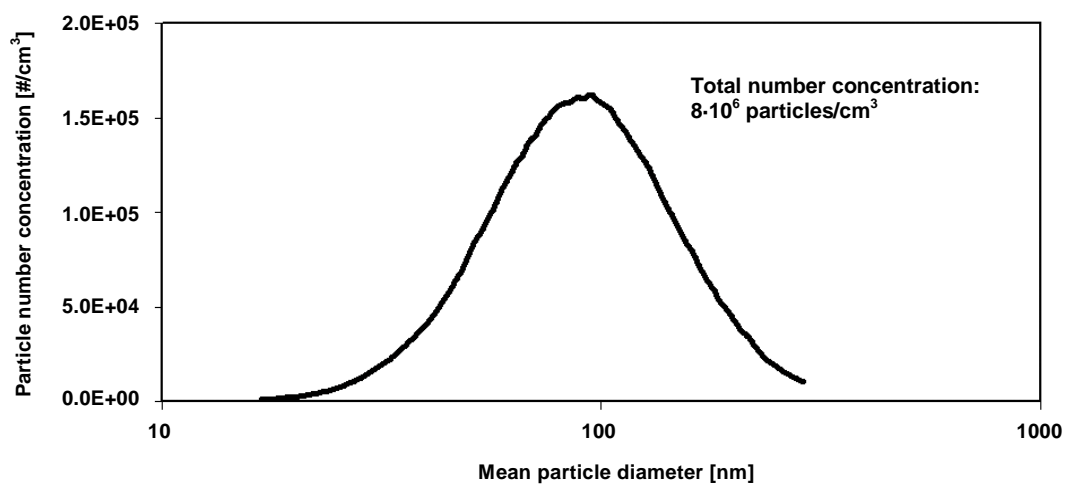


Fig. 2-3 DMA spectrum of a Ar/Pb aerosol (500 ml/min Ar) obtained at a crucible temperature of 800 °C and a coagulation vessel volume of 3 l.

---

## 2.3 IVO, a device for In-situ Volatilization and On-line detection of products from heavy ion reactions

Ch.E. Düllmann<sup>1,2</sup>, B. Eichler<sup>2</sup>, R. Eichler<sup>1,2</sup>, H.W. Gäggeler<sup>1,2</sup>, D.T Jost<sup>2</sup>,  
D. Piguet<sup>2</sup>, A. Türler<sup>1,2</sup>

<sup>1</sup>Department of Chemistry and Biochemistry, University of Berne, CH-3012  
Berne, Switzerland

<sup>2</sup>Paul Scherrer Institute, CH-5232 Villigen, Switzerland

Published in:

*Nuclear Instruments and Methods in Physics Research* **A479**, 631-639  
(2002).

## Abstract

A new gaschromatographic separation system to rapidly isolate heavy ion reaction products in the form of highly volatile species is described. Reaction products recoiling from the target are stopped in a gas volume and converted *in-situ* to volatile species, which are swept by the carrier gas to a chromatography column. Species that are volatile under the given conditions pass through the column. In a cluster chamber, which is directly attached to the exit of the column, the isolated volatile species are chemically adsorbed to the surface of aerosol particles and transported to an on-line detection system. The whole setup was tested using short-lived osmium (Os) and mercury (Hg) nuclides produced in heavy ion reactions to model future chemical studies with hassium (Hs, Z=108) and element 112.

By varying the temperature of the isothermal section of the chromatography column between room temperature and -80 °C, yield measurements of given species can be conducted, yielding information about the volatility of the investigated species.

### 2.3.1 Introduction

Investigations of the nuclear decay properties of the heaviest elements (transactinides,  $Z \geq 104$ ) require fast on-line separators with high separation factors and overall yields. Due to the generally very low production rates of such elements in heavy ion induced fusion reactions, presently reaching levels as low as one atom per month [1], any suitable device has to act as a filter for the much more abundant, unwanted by-products from transfer reactions and to detect final products with an efficiency close to 100 %.

Two different classes of devices have successfully been applied, physical separators and chemical set-ups.

Physical separators for instance take advantage of the different velocities of wanted fusion products and interfering transfer products. This may be achieved by a velocity filter (Wien filter) [2] or a gas-filled magnetic separator

---

[3], in which velocity dependent charge states of the ions lead to different trajectories.

Chemical separators employ the difference in chemical properties of the element to be separated from any unwanted element. Hence, chemical separators are Z specific. So far, only one on-line technique proved to be able to continuously isolate the desired transactinide element and forward it to an on-line detection system. This technique is called on-line isothermal gas chromatography. Two devices based on this principle have been developed, the On-Line Gas chemistry Apparatus (OLGA) [4] and the Heavy Element Volatility Instrument (HEVI) [5], a modified version of OLGA.

Reaction products recoiling from a target are thermalized in helium (He) gas and adsorbed to the surface of carbon aerosol particles ( $\approx 10^6 \text{ cm}^{-3}$ ) suspended in the He. Within a few seconds, the products are continuously transported through a thin capillary from the recoil chamber to the OLGA chemistry device, where the particles are collected on a quartz wool filter kept at an elevated temperature of up to 1000 °C. Reactive gases and oxygen (O<sub>2</sub>) are added to convert the carbon aerosol particles to CO<sub>2</sub> and to form volatile molecules with the reaction products. The chromatographic separation takes place in the adjoining isothermal section of the column (usually quartz), kept at a cooler temperature. Depending on the isothermal temperature setting, only species reaching a threshold volatility pass through the column. At the exit of the column, the products are re-attached to new aerosol particles and then transported to a counting device where the nuclear decay of the separated nuclides is registered. Rotating wheel systems such as the Rotating wheel Multidetector Analyzer (ROMA) [6] or the MG-wheel [7], but also tape devices [8] have proven to be well suited. Typical separation times with the current version of OLGA, OLGA III [9] are about 5 seconds.

One obvious shortcoming of this on-line gas chemistry system is the large number of steps involved, each having a yield less than 100 %. These include the thermalization of highly energetic reaction products in a gas, the attachment of the products in ionic or atomic form to the surface of sub-micrometer particles, the transport of these particles through a capillary, a

chemical reaction of the attached species with reactive gases to form volatile compounds, a gas adsorption chromatography of the compounds with the surface of the chromatography column, a re-attachment of the molecules leaving the column to new aerosol particles followed by a transport to the detection system, and, finally, the deposition of the particles on thin foils via impaction. The overall yield of all these processes reaches values of only 10 to 20 %.

From this point of view it is highly desirable to develop a technique with a much simpler reaction scheme between synthesis and detection of final products. In this work such a device was developed.

### **2.3.2 IVO, a device for in-situ volatilization and on-line detection**

One obvious shortcoming of the OLGA technique is the aerosol-borne transport of reaction products from the recoil chamber at the irradiation position to the chromatography set-up. The adsorption of the thermalized products to the surface of aerosol particles is poorly understood. The yield of this process and the efficiency for the aerosol particles to exit the recoil chamber depend on several parameters such as i) plasma effects caused by the beam, ii) particle number concentration and size distribution of the aerosol particles and iii) geometrical constraints (shape and size) of the recoil chamber.

It is therefore highly desirable to perform the chemical synthesis of volatile molecules *in-situ* in the recoil chamber. This approach has already been used in the very first chemical studies of transactinides [10]. Chlorinating and brominating agents were added to a carrier gas in order to form volatile halides of the d elements. Behind the recoil chamber the species entered a thermochromatography column with a stationary longitudinal negative temperature gradient. The surface of the column (glass or quartz) served both for the separation of volatile species as well as for the detection of spontaneously-fissioning (SF) nuclides via track detection. After each experiment the tracks were revealed by etching and served as position markers where molecules which contained SF-nuclides were deposited.

---

Obviously, such a technique has the disadvantage of not yielding any on-line information during an ongoing experiment. Also, it is now well known that most of the isotopes of transactinides decay via  $\alpha$ -particle emission, a decay mode which is not detectable with the track technique (at least with quartz surfaces). In addition, no unambiguous identification of the isolated nuclides is possible.

To overcome these obvious disadvantages, we developed a new device - named IVO – where a chromatography column with a cluster unit is directly coupled to the recoil and reaction chamber. As an option, an additional chromatography column can be attached which can be cooled to investigate the volatility of the species by the method of isothermal gas adsorption chromatography.

### 2.3.2.1 Technical description of IVO

A schematic drawing of the set-up is shown in Figure 2-4. The heavy ion beam passes a thin ( $\approx 0.5$ - $1 \text{ mg/cm}^2$ ) target ( $\phi=6 \text{ mm}$ ) and induces nuclear reactions. Similar to other gas-jet devices, the reaction products are recoiling out of the target into a gas volume (He), called recoil chamber, which is made of titanium, where they are thermalized. According to the chemical species to be synthesized, reactive gases, e. g.  $\text{O}_2$ , may be added. Typical recoil ranges of reaction products are of the order of a few centimetres. The length and diameter of the cylindrical recoil chamber were adjusted to the expected recoil ranges and straggling angles of the reaction products ( $\phi=2.8 \text{ cm}$ ; length= $4.5 \text{ cm}$ ). Beam particles passing through the recoil chamber are dumped in a  $3.0 \text{ cm}$  thick graphite cylinder, covered by a  $5 \text{ }\mu\text{m}$  thick aluminium (Al) foil. This foil prevents formation of graphite particles by sputtering processes, which may act as aerosols and interfere with *in-situ* chemical reactions, i.e. preventing the formation of oxides due to their reducing surface. It was experimentally observed that Al does not form significant amounts of transportable aerosol particles. The whole device is electrically insulated in order to enable monitoring of the beam current.

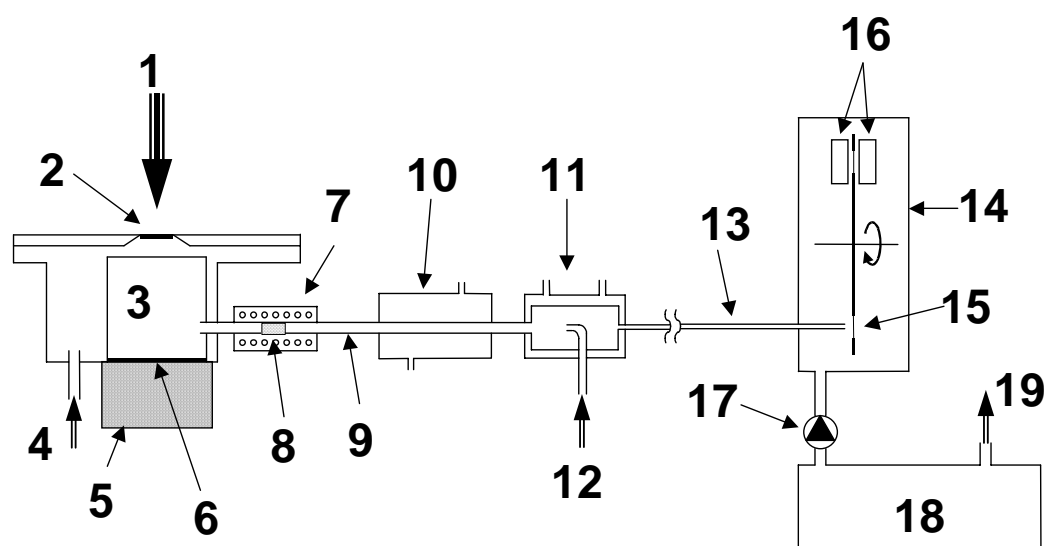


Fig. 2-4 Schematic drawing of IVO: (1) heavy ion beam, (2) target, (3) recoil chamber (titanium), (4) carrier gas and reactive gas inlet, (5) beam stop (graphite), (6) Al foil (5 $\mu$ m), (7) oven ( $T_{\max}$ =900 °C), (8) quartz wool plug, (9) quartz column (i.d.=2 mm), (10) optional cooling, (11) thermostated cluster chamber (length=95 mm, i.d.=30 mm), (12) cluster aerosol inlet, (13) teflon capillary, (14) ROtating wheel Multidetector Analyzer ROMA, (15) PE-foil (30  $\mu$ g/cm<sup>2</sup>), (16) PIPS  $\alpha$  detectors, (17) vacuum pump, (18) scrubber, (19) exhaust.

The carrier and reactive gases are fed into the recoil chamber through a small slit close to the target position. Volatile products, which are formed *in-situ* inside the chamber, are swept out through an open quartz chromatography column, located at a distance of 3.0 cm from the target. The entrance to the quartz column reaches a few mm into the recoil chamber.

The length of the quartz column (i.d. 2 mm) is 30 cm in order to fit into the glove box containing the entire set-up at the irradiation position.

Some chemical reactions, e.g. the formation of OsO<sub>4</sub>, require elevated temperatures. Therefore, an oven with a length of 8.0 cm is installed at a distance of 2.5 cm from the recoil chamber, which can be heated up to 900 °C. A quartz wool plug may be placed inside the quartz tube at the position of maximum temperature. This plug i) serves as a first barrier to retain non-volatile interfering species, ii) is a filter to remove small amounts of aerosol

---

particles which may be produced in the recoil chamber and could transport non-volatile species to the detection system and iii) removes target material which is sputtered from the target. Beam stop, target chamber, oven and the rear end of the quartz capillary are water cooled.

In order to further transport the volatile molecules to a counting device, the well established gas-jet technique is applied, which bases on the fact that small aerosol particles of about 100 nm size can easily be transported with high yield through capillaries and then deposited via impaction on surfaces. Therefore, a so-called cluster chamber is attached to the exit of the quartz column. A cluster aerosol, typically KCl or CsCl in He or argon (Ar), is injected into the chamber and mixed with the carrier gas containing the volatile species. The latter are then adsorbed onto the surface of the particles. The cluster chamber can be heated up to 200 °C in order to overcome a possible activation energy of the adsorption reaction. Through a PTFE or PFA teflon capillary (i.d. 2 mm) the particles are then transported to a detection system, usually ROMA [6] or the PSI tape system [8] where the radioactive decay of the isolated nuclides is registered. The pressure in the counting chamber is about 5 mbar.

Aerosol particles can also be injected directly into the recoil chamber instead of the cluster chamber, thus transporting all nuclear reaction products to the detection system. By comparing yields of different species, information on the decontamination factor of IVO can be gained. Usually, carbon aerosol particles generated via spark discharge between two graphite electrodes ( $\phi=3$  mm) are used. The distance between the electrodes is 2 mm. A 12.5 kV/2.5 mA high voltage supply is used. The current is limited to 2 mA resulting in a discharge frequency of ~5 Hz. In order to generate a sufficient number concentration ( $10^6$  particles/cm<sup>3</sup>), two generator units are coupled in series. The particles, which are highly charged, are then fed through a cylindrical vessel containing in its center a 74 MBq <sup>85</sup>Kr source sealed in a small copper tube where the charge is equilibrated to minimize the loss of particles in the polyethylene (PE) tubes used to transport the aerosol particles to the cluster chamber.

---

In order to determine the overall yield of IVO a catcher foil was mounted behind the target to measure the absolute yield of a given reaction channel.

As an option, an additional quartz column (length=1.5 m; i.d.=2 mm), which can be cooled between ambient temperature and -80 °C, can be coupled to the exit of the chromatography column described above. With this device it is possible to measure the retention time of the volatile species and thus obtain information on the adsorption behavior on a quartz surface.

The whole system is assembled as a modular set-up, to be easily adaptable to specific needs of an experiment.

### **2.3.3 First experiments with volatile osmium tetroxide (OsO<sub>4</sub>) to model a chemistry with Hs (element 108)**

The transactinide element hassium (Hs, Z=108) is expected to be a member of group 8 of the periodic table of the elements and thus a homologue of osmium (Os) and ruthenium (Ru). The longest-lived known isotope which decays by emission of a  $\alpha$  particle is <sup>269</sup>Hs with a half-life of about 10 s and a  $\alpha$ -particle energy of 9.2 MeV [11]. It can be produced by the reaction <sup>248</sup>Cm(<sup>26</sup>Mg, 5n) with an estimated production cross section of about 7 pb [12]. If the chemical properties of Hs are comparable to those of Os and Ru, it should form a very volatile tetroxide, HsO<sub>4</sub>. Thus, IVO seems to be an ideal device for separation and study of HsO<sub>4</sub>. On-line investigations of Os-oxides, which made use of different techniques, had already been conducted earlier, e.g. at Dubna [13], Berkeley [14] or Darmstadt [15].

#### **2.3.3.1 Experimental**

In experiments with IVO at the PSI-PHILIPS cyclotron short-lived Os isotopes with half-lives of about 20 s were produced by irradiation of a dysprosium (Dy) target (0.5 mg/cm<sup>2</sup> Dy, <sup>156</sup>Dy 20 % enriched) with <sup>22</sup>Ne in the reaction <sup>156</sup>Dy(<sup>22</sup>Ne, 6,5n)<sup>172,173</sup>Os. The target was electrochemically deposited on a 3.3 mg/cm<sup>2</sup> thick HAVAR foil. The <sup>22</sup>Ne beam energy in the middle of the target was 127 MeV and the beam intensity was 0.083 particle· $\mu$ A. He was used as carrier gas with a flow rate of 500 ml/min. An admixture of 10 % O<sub>2</sub>

---

served as chemical reagent to synthesize  $\text{OsO}_4$  *in-situ*. Volatile compounds were transported with the carrier gas flow through the quartz chromatography column to the cluster chamber. Heating the reaction oven at the beginning of the column to 600 °C significantly improved the yield of volatile  $\text{OsO}_4$ . Obviously, not all Os-oxides reaching the reaction oven have already been oxidized to the tetroxide in the recoil chamber.

For further transport an aerosol was produced from molten lead (Pb) in Ar (500 ml/min), since earlier experiments at FLNR in Dubna [16] and also at PSI have shown that a lead surface strongly adsorbs  $\text{OsO}_4$ , presumably via its reducing surface to form less volatile Os compounds.

Optimum transport yields of  $\text{OsO}_4$  were found if the molten Pb was kept at 820 °C and then passed through a container of 3 l volume in order to allow the formation of agglomerates of appropriate size.

After transport through a 6 m long PTFE teflon capillary, the particles were impacted on 30  $\mu\text{g}/\text{cm}^2$  polyethylene (PE) foils mounted on the circumference of a rotating wheel system (ROMA [6]) and moved every 20 s between four consecutive pairs of PIPS-detectors to register the  $\alpha$ -particle decays of the Os isotopes from the front and the back side of the PE-foils, which were thin enough to enable  $\alpha$  spectroscopy in a  $4\pi$  counting geometry. In addition, a HPGe-detector was mounted in one of the counting positions to assess  $\gamma$  emitting nuclides.

In order to determine the decontamination factor of the IVO-setup, an experiment was carried out where all nuclear reaction products were transported out of the target chamber directly to the detection system without any specific chemical reaction (except attachment to the surface of the gas-jet aerosol). Therefore, carbon aerosol particles ( $\sim 10^6 \text{ cm}^{-3}$ ) in 1000 ml/min He were fed into the recoil chamber.

In another experiment,  $^{173,174}\text{Os}$  was produced in the reaction  $^{162}\text{Er}(^{18}\text{O}, 6-7n)$  at a beam energy of 116 MeV in the middle of the target and beam intensities of 100 particle-nA. The experimental conditions as e.g. gas flow rates were

---

the same as in the experiment described above. Again, OsO<sub>4</sub> was formed *in-situ* in the recoil chamber. The compounds were transported via the first chromatography column and a 5 m long PFA teflon capillary (i.d.=2 mm) to a second chromatography column (length=1.5 m, i.d.=2 mm) kept at a variable isothermal temperature. After passing through this column, the molecules were transported through a 2 m long PFA teflon capillary (i.d. 2 mm) to the cluster chamber where they were adsorbed on Pb aerosol particles and transported to ROMA for final counting. The isothermal temperature of the chromatography (IC) column was varied between ambient temperature and -80 °C to evaluate the enthalpy of adsorption  $\Delta H_{\text{ads}}$  of OsO<sub>4</sub> on quartz.

### 2.3.3.2 Results and Discussion

Figure 2-5 shows an  $\alpha$ -particle spectrum of the first front detector of an experiment where a He/carbon aerosol was used to transport all nuclear reaction products out of the recoil chamber directly to the ROMA. The following nuclides were identified [17]: <sup>172</sup>Os ( $T_{1/2}$ =19.2 s,  $E_{\alpha}$ =5.100 MeV); <sup>173</sup>Os ( $T_{1/2}$ =22.4 s,  $E_{\alpha}$ =4.938 MeV); <sup>197</sup>Po ( $T_{1/2}$ =56 s,  $E_{\alpha}$ =6.281 MeV); <sup>197m</sup>Po ( $T_{1/2}$ =26 s,  $E_{\alpha}$ =6.385 MeV); <sup>198</sup>Po ( $T_{1/2}$ =1.76 min,  $E_{\alpha}$ =6.185 MeV); <sup>199m</sup>Po ( $T_{1/2}$ =4.2 min,  $E_{\alpha}$ =6.059 MeV); <sup>200</sup>Po ( $T_{1/2}$ =11.5 min,  $E_{\alpha}$ =5.863 MeV) and <sup>201m</sup>Po ( $T_{1/2}$ =8.9 min,  $E_{\alpha}$ =5.786 MeV). Formation of the Os isotopes occurred in the reaction <sup>156</sup>Dy(<sup>22</sup>Ne, 6,5n)<sup>172,173</sup>Os whereas Po isotopes were produced in the reaction <sup>nat</sup>W(<sup>22</sup>Ne, xn)<sup>197-201m</sup>Po from the W contained in the HAVAR target backing.

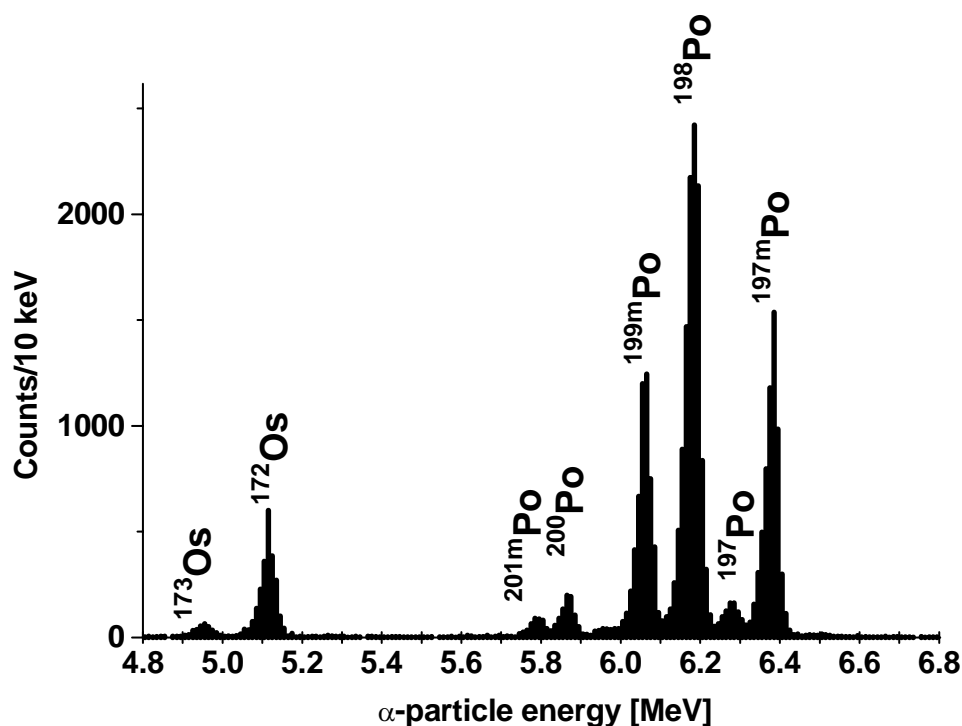


Fig. 2-5  $\alpha$ -particle spectrum for the reaction  $^{156}\text{Dy}+^{22}\text{Ne}$ . The spectrum was obtained in a direct catch experiment where all reaction products were transported out of the recoil chamber by means of a He/carbon gas-jet.  $\alpha$  lines of  $^{172,173}\text{Os}$  produced in the reaction  $^{156}\text{Dy}(^{22}\text{Ne}, 6,5n)^{172,173}\text{Os}$  and  $^{197-201m}\text{Po}$  are visible. Po isotopes originate from the reaction of the beam with W contained in the HAVAR target backing.

Figures 2-6 (a) and (b) show the  $\alpha$ -particle spectra of the first detector pair of an experiment where IVO was used as a chemical separator. The spectrum (a) has been acquired with the front detector, and (b) with the back detector. Only peaks at 5.100 MeV ( $^{172}\text{Os}$ ) and 4.938 MeV ( $^{173}\text{Os}$ ) were observed. The energy resolution of the detectors for 5 MeV  $\alpha$ -particles was about 35 keV and 75 keV full width at half maximum (FWHM) for the front and back detector, respectively. No Po was observed under the given conditions. Only very few events in the range between 5.70-6.60 MeV were detected. If all of these events are assigned to the decay of Po isotopes, a lower limit for the decontamination factor with respect to Po of  $2 \times 10^4$  is calculated. The chemical yield of the separator was about 50 %.

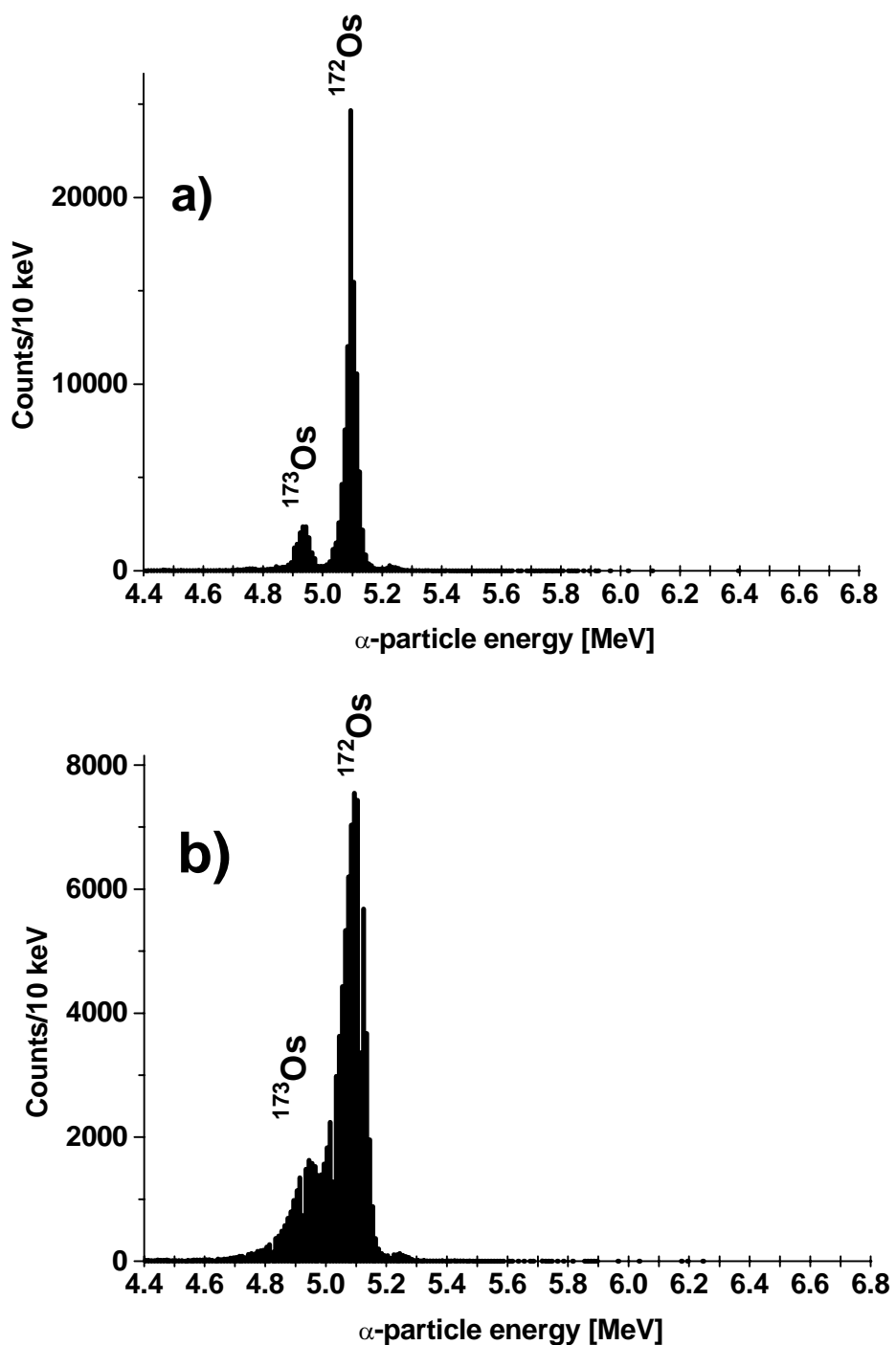


Fig. 2-6  $\alpha$ -particle spectra from the reaction  $^{156}\text{Dy}+^{22}\text{Ne}$  from an experiment where IVO was used as chemical preseparator. Only the lines of the Os isotopes appear, Po was not volatile under the given conditions and did not reach the detection system. (a)  $\alpha$ -particle spectrum of the first front detector. (b)  $\alpha$ -particle spectrum of the first back detector.

In another set of experiments, short-lived Os was produced in the reaction  $^{162}\text{Er}(^{18}\text{O}, 7,6n)^{173,174}\text{Os}$ . By means of a coolable second chromatography column, the method of isothermal chromatography (IC) was applied to study the adsorption behavior of  $\text{OsO}_4$  on quartz. Using the nuclear half-lives of  $^{173,174}\text{Os}$  as an internal clock allowed the measurement of the retention time of the molecules in the column. The retention time in the IC column depends on the volatility of the compound, which is usually expressed by the enthalpy of adsorption on the column material  $\Delta H_{\text{ads}}$ . At the temperature where the yield reaches 50 % of the maximum yield, the retention time in the IC column equals the half-life of the radioactive nuclide contained in the molecule. Hence, a yield vs. isothermal temperature curve was measured (Figure 2-7).

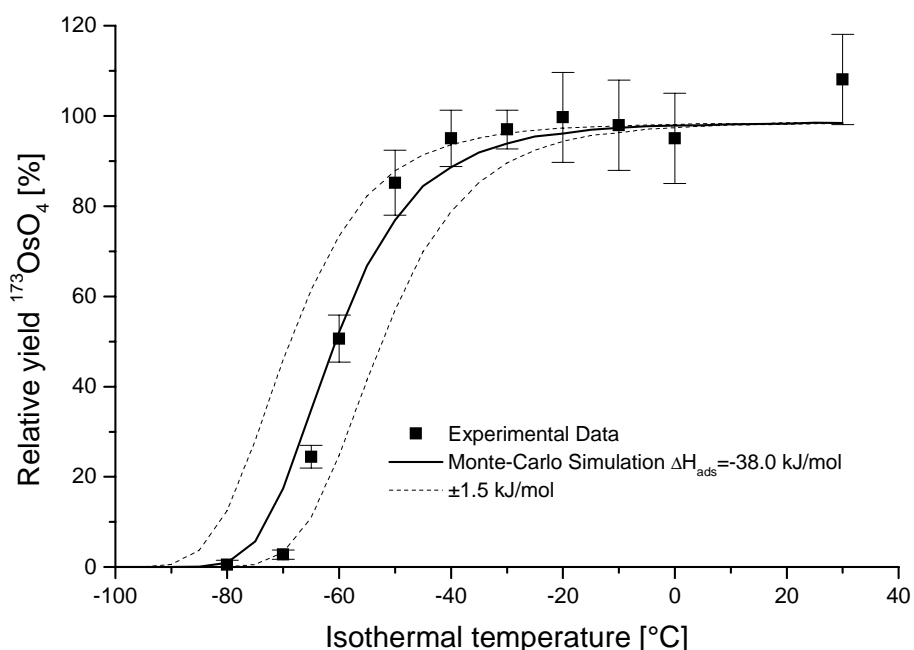


Fig. 2-7 Relative yield vs. isothermal temperature curve for  $^{173}\text{OsO}_4$  ( $T_{1/2}=22.4$  s). The solid line is the result of a Monte-Carlo simulation of the experiment assuming an enthalpy of adsorption  $\Delta H_{\text{ads}}$  of  $-38.0$  kJ/mol. The dashed lines indicate the  $1\sigma$ -error range of  $1.5$  kJ/mol.

$\Delta H_{\text{ads}}$  of  $\text{OsO}_4$  on quartz was evaluated using a thermodynamic method [18] and a microscopic model using a Monte-Carlo technique [19]. A value of  $\Delta H_{\text{ads}}=(-38.0\pm 1.5)$  kJ/mol was evaluated in this way. This value is in good

agreement with an on-line thermochromatographic investigation of the same compound by Domanov et al. [13]. Reevaluation of these experiments with the analysis procedure that has been applied in our experiments yields  $\Delta H_{\text{ads}}=(-39\pm 1)$  kJ/mol.

The yields of  $^{173,174}\text{OsO}_4$  were measured at an isothermal temperature of  $-30$  °C at different beam currents of 0.1, 0.2, 0.3 and 0.4 particle- $\mu\text{A}$ , respectively (Figure 2-8). The observed linear correlation has a correlation coefficient of  $>0.99$ . This observation is in contrast to [20], where decreasing  $\text{OsO}_4$  yields were observed with increasing beam intensities.

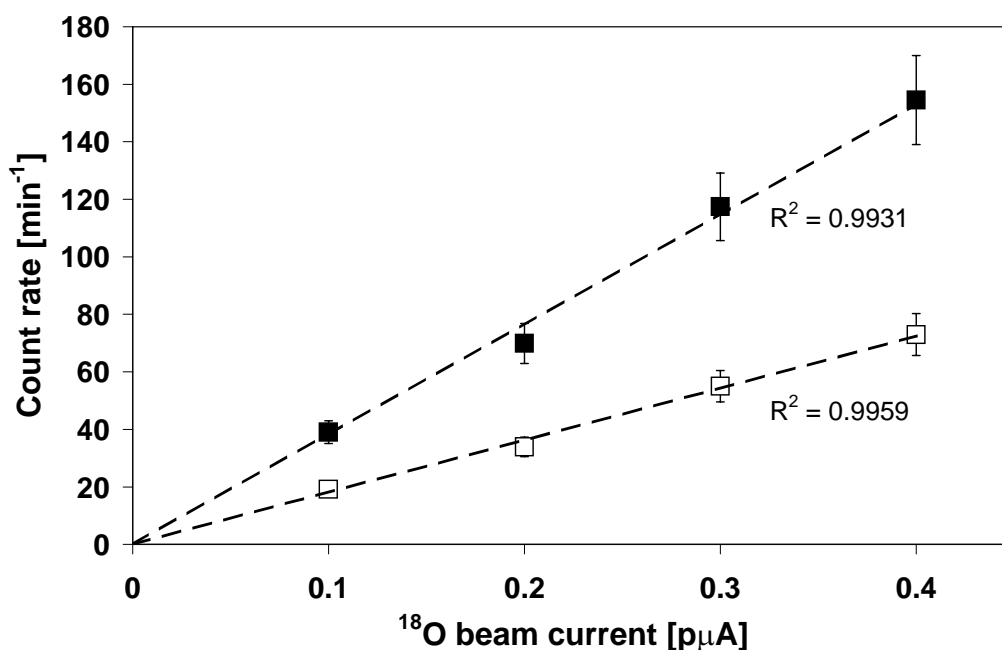


Fig. 2-8 Dependency of the yield of Os-isotopes vs. beam intensity in the reaction  $^{18}\text{O}+^{162}\text{Er}$  (■  $^{174}\text{OsO}_4$ ; □  $^{173}\text{OsO}_4$ ). The measured points can be fitted by linear regression lines with an intercept of 0 with correlation coefficients of  $R^2=0.9931$  ( $^{174}\text{OsO}_4$ ) and  $R^2=0.9959$  ( $^{173}\text{OsO}_4$ ), respectively.

### 2.3.4 First experiments with mercury (Hg) to model a chemistry with elements 112 and 114

Recent experiments gave evidence that elements  $Z=112$  [21] and 114 [22] have neutron-rich isotopes with lifetimes long enough for their chemical

---

characterization. These elements are presumably very noble metals and expected to be highly volatile. Gas adsorption chromatographic investigations in the elemental state seem to be feasible [23, 24]. These superheavy elements are predicted to have rather high adsorption enthalpies on metal surfaces such as palladium (Pd) or platinum (Pt) [23].

Therefore, on-line experiments with Hg nuclides, serving as a model element for element 112, and Pd aerosol particles were carried out to investigate the adsorption, transport, and sample preparation.

Pd is the favoured adsorption material for volatile s- and p-metals (thus also for elements 112 and 114) if stable surface bonding is essential [25]. The calculated enthalpy of adsorption  $\Delta H_{\text{ads}}(\text{calc})$  of Hg on a Pd surface amounts to -194.4 kJ/mol [26]. In thermochromatographic experiments with carrier-free amounts of Hg  $\Delta H_{\text{ads}} = -171 \pm 5$  kJ/mol [25] was determined.

The aerosol was generated by spark discharge between two Pd electrodes in a He/Ar gas flow (500 ml/min each). A single generator unit was used. The electrodes consisted of rolled Pd foils with a thickness of 100  $\mu\text{m}$  and had a diameter of 2 mm.

Suitable Hg nuclides were produced by irradiation of an ytterbium (Yb) target ( $^{168}\text{Yb}$ , 21 % enriched) with  $^{22}\text{Ne}$  ( $E=129$  MeV, 0.083 particle- $\mu\text{A}$ ) at the PSI-PHILIPS cyclotron in the IVO set-up in the reaction  $^{168}\text{Yb}(^{22}\text{Ne}, xn)^{190-x}\text{Hg}$ . The recoiling Hg isotopes were thermalized in He atmosphere and swept through the isothermal quartz column ( $T_{\text{reaction oven}}=800$  °C) by the carrier gas (600 ml/min). The gas flow reached the cluster chamber where it was mixed with the aerosol carrier gas (500 ml/min He and 500 ml/min Ar) containing Pd aerosol particles. Adsorbed to the Pd aerosol particles, Hg could be transported to the detection device (ROMA) through a PTFE teflon capillary (length=6 m, i.d.=2 mm), impacted on 30  $\mu\text{g}/\text{cm}^2$  PE-foils in the collection position and turned periodically to the detection position. Collection and measuring times were 10 s; one experiment lasted 30 min.

Figure 2-9 shows an  $\alpha$ -particle spectrum from the first front detector. The following nuclides were identified [17]:  $^{183}\text{Hg}$  ( $T_{1/2}=8.8$  s,  $E_{\alpha}=5.905$  MeV);  $^{184}\text{Hg}$  ( $T_{1/2}=30.6$  s,  $E_{\alpha}=5.54$  MeV) and  $^{185}\text{Hg}$  ( $T_{1/2}=49$  s,  $E_{\alpha}=5.65$  MeV). A resolution of 40 keV FWHM and 90 keV FWHM was achieved in the front and the back detectors, respectively.

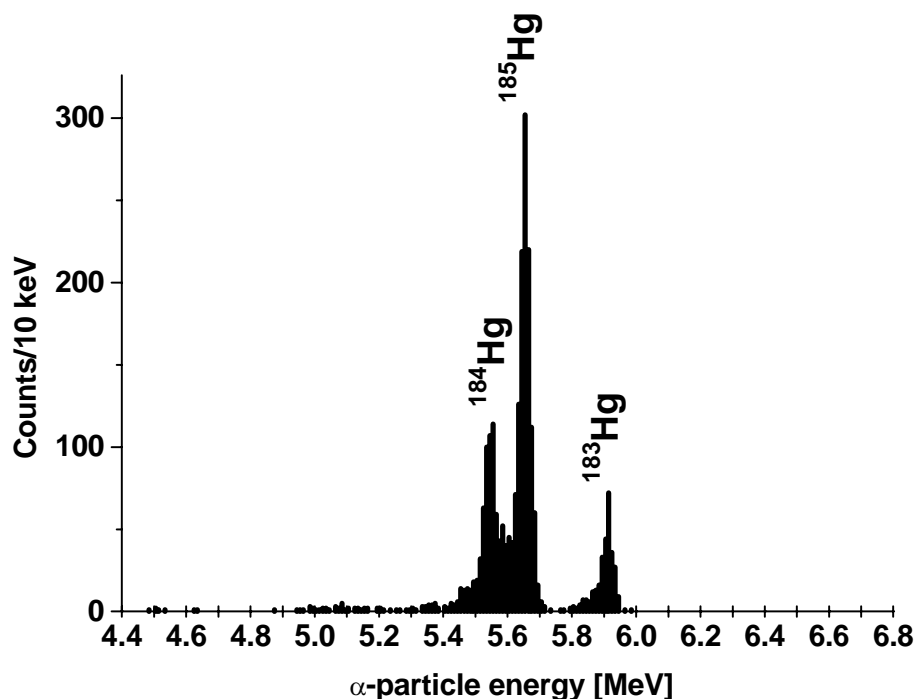


Fig. 2-9  $\alpha$ -particle spectrum from the reaction  $^{168}\text{Yb}+^{22}\text{Ne}$ . The isotopes  $^{183-185}\text{Hg}$  produced in the reaction  $^{168}\text{Yb}(^{22}\text{Ne}, 5-7n)$  are visible. No other  $\alpha$ -particle emitting nuclides with  $\alpha$  energies in the range between 3.0 and 10.0 MeV were detected.

These model experiments proved that:

- highly volatile metals such as Hg can be transported in He gas flow systems without aerosol particles and then rapidly and irreversibly adsorbed on metal aerosol particles if the enthalpy of adsorption is sufficiently large (as e.g. for Hg on Pd) and

- the bonding of Hg to the surface of Pd is sufficiently strong to enable gas-jet transport and  $\alpha$  spectroscopic measurements at low pressures (5 mbar) at room temperature.

---

We therefore consider such a technique suitable for experimental investigations of chemical and nuclear decay properties of other d- and p-elements including the transactinides with  $Z=112-117$ , provided a high overall yield can be achieved.

### 2.3.5 Conclusions

A new chemical separator set-up was built to separate volatile elements or molecules containing short-lived nuclides produced in heavy ion reactions which was tested with short-lived nuclides of Os and Hg in the form of  $\text{OsO}_4$  and elemental Hg, which served as model species for  $\text{HsO}_4$  and element 112, respectively. The chemical yield of the separator in the Os experiment was about 50 % and the lower limit of the decontamination factor from Po was  $2 \times 10^4$ . According to the test results, the apparatus is expected to be well suited for the isolation of transactinides produced in heavy-ion induced fusion reactions from interfering byproducts.

### Acknowledgments

The preparation of the targets by Mrs. E. Rössler and the delivery of a stable beam by the operators of the PSI cyclotron are highly appreciated. This work was supported by the Swiss National Science Foundation.

### References

- [1] Yu.Ts. Oganessian, V.K. Utyonkov, Yu.V. Lobanov, F.Sh. Abdullin, A.N. Polyakov, I.V. Shirokovsky, Yu.S. Tsyganov, G.G. Gulbekian, S.L. Bogomolov, B.N. Gikal, A.N. Mezentsev, S. Iliev, V.G. Subbotin, A.M. Sukhov, G.V. Buklanov, K. Subotic, M.G. Itkis, K.J. Moody, J.F. Wild, N.J. Stoyer, M.A. Stoyer, R.W. Lougheed, Phys. Rev. Lett. 83 (1999) 3154
- [2] G. Münzenberg, W. Faust, S. Hofmann, P. Armbruster, K. Grüttner, H. Ewald, Nucl. Instr. Meth. 161 (1979) 65
- [3] A. Ghiorso, S. Yashita, M.E. Leino, L. Frank, J. Kalnins, P. Armbruster, J.-P. Dufour, P.K. Lemmertz, Nucl. Instr. Meth. A269 (1988) 192

- 
- [4] H.W.Gäggeler, D.T. Jost, U. Baltensperger, A. Weber, A. Kovacs, D. Vermeulen, A. Türler, Nucl. Instr. Meth. A309 (1991) 201
- [5] B. Kadkhodayan, A. Türler, K.E. Gregorich, M.J. Nurmia, D.M. Lee, D.C. Hoffman, Nucl. Instr. Meth. A317 (1992) 254-261
- [6] K. Sümmerer, M. Brügger, W. Bröchle, H. Gäggeler, E. Jäger, M. Schädel, D. Schardt, E. Schimpf, GSI Ann. Rep. 1983, 84-1 (1984) 246 (unpublished)
- [7] D.C. Hoffman, D. Lee, A. Ghiorso, M. Nurmia, K. Aleklett, Phys. Rev. C 22 (1980) 1581
- [8] D.T. Jost, D. Vermeulen, IEEE Tans. Nucl. Sci. 39 (1992) 186
- [9] A. Türler, Radiochim. Acta 72 (1996) 7
- [10] I. Zvara, Yu.T. Tschuburkov, P. Zaletka, T.S. Zvarova, M.P. Chalajevskij, B.V. Chilov, Atomnaja energija 21 (1966) 83
- [11] S. Hofmann, V. Ninov, F.P. Hessberger, P. Armbruster, H. Folger, G. Münzenberg, H.J. Schött, A.G. Popeko, A.V. Yeremin, S. Saro, R. Janik, M. Leino, Z. Phys. A 354 (1996) 229
- [12] J.V. Kratz, Proc. R. A. Welch Foundation, 41st Conf. on Chem. Research, The Transactinide Elements, October 27-28, 1997, Houston Texas, p. 65
- [13] V.P. Domanov, I. Zvara, Radiokhimiya 26 (1984) 770 (in Russian)
- [14] R.J. Dougan, K.J. Moody, E.K. Hulet, G.R. Bethune, LLNL Ann. Rep. FY 87, UCAR 10062/87, p. 4-17
- [15] A. v. Zweidorf, J.V. Kratz, N. Trautmann, M. Schädel, A. Nähler, E. Jäger, B. Schausten, W. Bröchle, E. Schimpf, R. Angert, Z. Li, G. Wirth, 1st International Conference on the Chemistry and Physics of the Transactinide Elements, TAN, September 26-30, 1999, Seeheim, Germany, Extended Abstracts, 1999
- [16] B.L. Zhuikov, V.I. Chepigin, H. Kruz, G.M. Ter-Akopian, I. Zvara, Report JINR Dubna, USSR, P7-86-322, 1986

- 
- [17] G. Pfennig, H. Klewe-Nebenius, W. Seelmann-Eggebert, Karlsruher Nuklidkarte, Forschungszentrum Karlsruhe, 6. Auflage 1995, korrigierter Nachdruck 1998
- [18] B. Eichler, I. Zvara, *Radiochim. Acta* 30 (1982) 233
- [19] I. Zvara, *Radiochim. Acta* 38 (1985) 95
- [20] A. von Zweidorf, R. Angert, W. Bröchle, E. Jäger, J.V. Kratz, A. Kronenberg, G. Langrock, Zongwei Li, M. Schädel, B. Schausten, E. Schimpf, E. Stiel, E. Strub, N. Trautmann, G. Wirth, Universität Mainz, Institut für Kernchemie, Ann. Rep. 1999, ISSN 0932-7622 (2000) 16 (unpublished)
- [21] Yu.Ts. Oganessian, A.V. Yeremin, G.G. Gulbekian, S.L. Bogomolov, V.I. Chepigin, B.N. Gikal, V.A. Gorshkov, M.G. Itkis, A.P. Kabachenko, V.B. Kutner, A. Yu. Lavrentev, O.N. Malyshev, A.G. Popeko, J. Roháč, R.N. Sagaidak, S. Hofmann, G. Münzenberg, M. Veselsky, S. Saro, N. Iwasa, K. Morita, *Eur. Phys. J. A* 5 (1999) 63
- [22] Yu.Ts. Oganessian, A.V. Yeremin, A.G. Popeko, S.L. Bogomolov, G.V. Buklanov, M.L. Chelnokov, V.I. Chepigin, B.N. Gikal, V.A. Gorshkov, G.G. Gulbekian, M.G. Itkis, A.P. Kabachenko, A.Yu. Lavrentev, O.N. Malyshev, J. Rohac, R.N. Sagaidak, S. Hofmann, S. Saro, G. Giardina, K. Morita, *Nature* 400 (1999) 242
- [23] B. Eichler, *Kernenergie* 19/10 (1976) 307
- [24] B. Eichler, H. Rossbach, *Radiochim. Acta* 33 (1983) 121
- [25] B. Eichler, S.C. Kim, report JINR Dubna, USSR, P12-83-206, 1983 (in Russian)
- [26] B. Eichler et al. *Isotopenpraxis* 21 (1985) 180

---

## 2.4 The Cryo On-Line Detector COLD

Usually only few events are recorded in transactinide experiments. IC requires experiments at different temperatures. A first experiment is usually conducted at a temperature higher than the expected  $T_{50\%}$ . It is assumed that the retention time at this experimental temperature is short enough to ensure that almost each species of interest entering the column reaches its exit. In another experiment, the temperature is lowered to prevent any of the atoms or compounds of the element under investigation from reaching the detection system. Hence, chemical information is only gained at the expense of information on the decay properties. Since the absence of only one expected atom is not statistically significant, a great amount of (expensive) beam time is "sacrificed" to measure "zero".

In contrast, in a TC experiment every single decaying species yields chemical information, namely the deposition temperature on the surface material. However, it is usually impossible to apply an on-line detection system in TC experiments due to the maximum detector operating temperature of about 40 °C. Therefore, on-line TC can only be used to investigate highly volatile species. This condition is fulfilled in the case of  $\text{OsO}_4$  and presumably also  $\text{HsO}_4$  and it seemed advantageous to attempt to investigate  $\text{HsO}_4$  using the TC technique. The major drawback is that the lifetime of the mother nuclide cannot be measured because there is no initial signal of its deposition.

In past transactinide experiments where TC was applied [Zva66, Zva71, Zva76, Tim96, Zva98] the chromatography column usually consisted of mica (or quartz), and SF decaying short-lived nuclides were identified by etching the chromatography column after an experiment to make the fission fragment tracks visible. However,  $\alpha$ -decaying nuclides could not be detected. SF is an unspecific decay mode and a definite proof that none of the much more abundant SF decaying transfer products caused these tracks was very difficult. In the past these facts led to controversies, e.g. in the discovery of element 104 [Bar92].

---

With the availability of high-resolution  $\alpha$ -particle/fission-fragment detectors in various geometries and with inert surface, the development of an on-line TC apparatus working in a temperature range between ambient temperature and  $-100\text{ }^{\circ}\text{C}$  became possible. The idea of using an on-line TC set-up for chemical identification was first proposed at a LBNL workshop in Berkeley by Türler [Tür97]. As a consequence a first device was then developed by Kirbach [Kir02]. This device was called Cryo-Thermochromatographic Separator (CTS) and permitted on-line detection of  $\alpha$ - and SF-decaying nuclides. The inner surface of CTS consisted of a narrow channel formed by silicon PIN photodiodes serving both as chromatography column and detectors for registering the nuclear decay of the investigated species. In test experiments with short-lived Os isotopes, CTS was shown to quantitatively adsorb  $\text{OsO}_4$  and detect its nuclear decay with rather high efficiency [Kir02]. Based on these encouraging results, an improved version called Cryo On-Line Detector (COLD) was built. The schematic of COLD is shown in Figure 2-10. Volatile tetroxides formed in IVO are transported through a PFA Teflon<sup>®</sup> capillary (1) and enter the chromatography column installed inside a copper bar (2). Along this bar a negative longitudinal temperature gradient is established by means of a heat medium circuit (3) controlled by a thermostat kept at  $-20\text{ }^{\circ}\text{C}$  on the "warm" entrance side and a container (4) filled with liquid nitrogen ( $\text{LN}_2$ ). This is connected via a vacuum insulated cold finger (5) to the copper bar at the exit resulting in a minimum temperature of  $\approx -170\text{ }^{\circ}\text{C}$ . The container was vacuum insulated. The temperature profile was monitored by means of five thermocouples installed along the copper bar. To prevent the formation of ice layers inside the column and freezing of the electrical contacts, the whole device was placed inside a vacuum tight housing (6) flushed with dry  $\text{N}_2$  purge gas with a water vapor concentration below 1 ppm.

The enlarged cut-out (Figure 2-10) on the right shows the construction of the column. A PTFE Teflon<sup>®</sup> coated copper bar (2) with 36 recesses suited to hold pairs of PIN-photodiodes with an active surface of  $1 \times 1\text{ cm}^2$  manufactured by DT Detection Technology, Inc, Micropolis (Finland). The outermost layer of

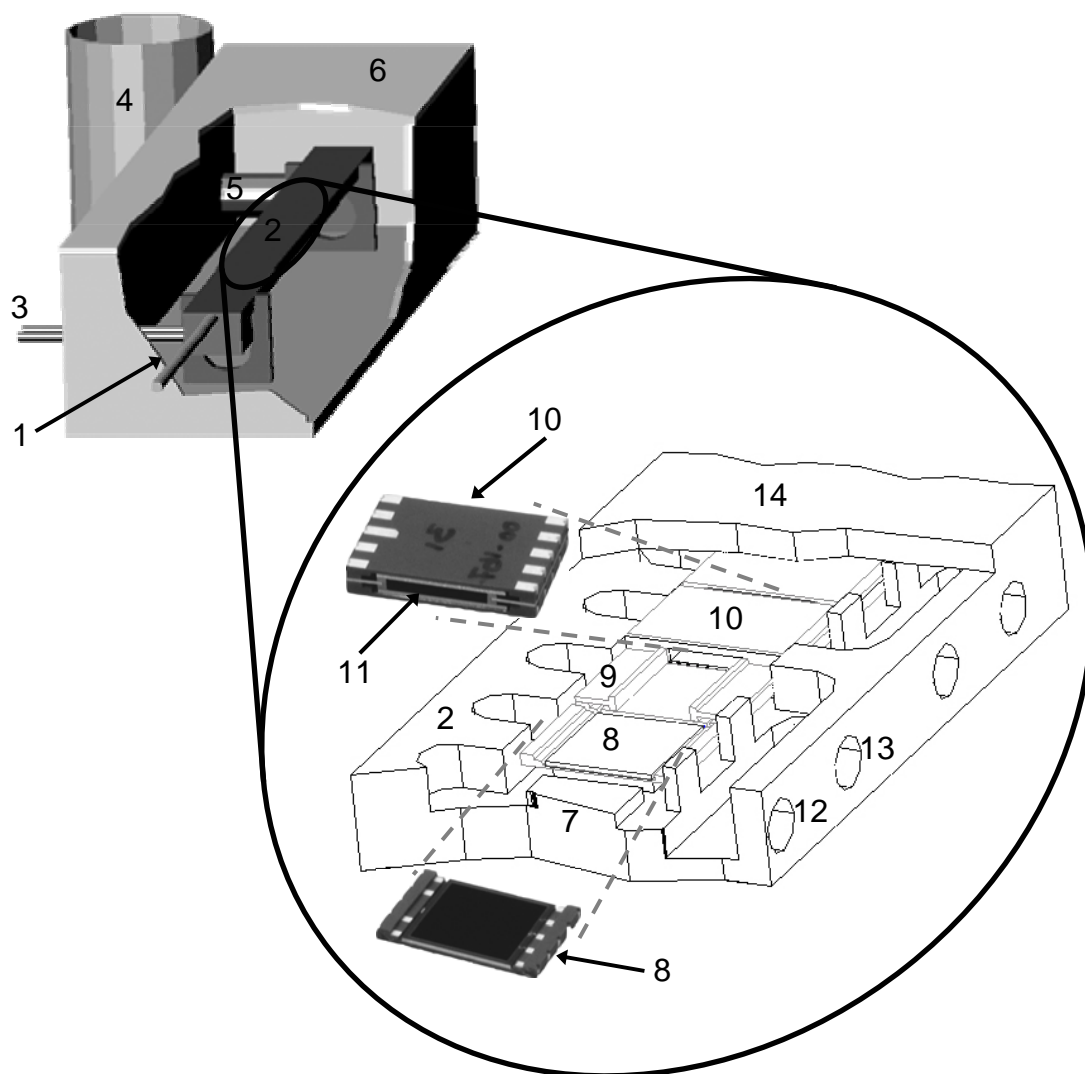


Fig. 2-10 Schematic of the Cryo On-Line Detector COLD. For explanation see text.

the active surface consisted of  $\text{Si}_3\text{N}_4$ . One diode pair was placed in each recess. The diodes were placed on uncoated supportings (7) of  $9.3 \times 10.6 \text{ mm}^2$  with a height of 0.3 mm to ensure proper thermal contact. The second recess shows a silicon PIN-Photodiode (8). Another PIN-diode was glued on top (10) with an insulating epoxy glue specially tailored for low temperature application in semiconductor technology using two T-shaped spacers (9) made of silicon (as shown in the third recess) thus forming a narrow channel (11) of  $8.6 \times 1.5 \text{ mm}^2$  cross section. A series of 36 pairs of diodes was mounted in the copper bar. By means of the spacers, the gas flow was confined to the active detector surface. Every three consecutive top (T) or bottom (B) diodes were electronically connected, forming one spectroscopy

channel. COLD therefore consisted of 12 detector pairs. Each spectroscopy channel had one SMC connector for the T detector (12) and another for the B detector (13) for connecting it to the electronics system. The cover of the bar (14) was made of PTFE Teflon<sup>®</sup> coated copper and was screwed with 26 screws to the bar.

The geometrical efficiency for detecting a single  $\alpha$ -particle emitted by a species adsorbed within the detector array was 77 %, corresponding to the following probabilities to see x  $\alpha$ -particles of a  $\alpha$ - $\alpha$ - $\alpha$ - $\alpha$ -decay chain:

Tab. 2-2 Probabilities to detect x  $\alpha$ -particles of a 4- $\alpha$ -particles decay chain in COLD.

x	Probability [%]
4	35
3	42
2	19
1	4
0	0

The detectors of the COLD array were on-line calibrated with  $\alpha$ -decaying <sup>219</sup>Rn and its daughters <sup>215</sup>Po and <sup>211</sup>Bi using a <sup>227</sup>Ac source. The determined energy resolution was about 50-70 keV (FWHM) for detectors 1 to 8 and about 80-110 keV (FWHM) for detectors 9 to 12.

## 2.5 Test experiments with COLD

### 2.5.1 Short-lived $\alpha$ -decaying Os isotopes

In several experiments, the proper functioning of COLD was demonstrated. In the reaction  $^{156}\text{Dy}(^{20}\text{Ne}, \text{xn})^{176-x}\text{Os}$ , short lived Os isotopes were produced. They were converted to OsO<sub>4</sub> and forwarded to COLD using IVO. The gas composition was 1.4 l/min He and 100 ml/min O<sub>2</sub>. Figure 2-11 shows the obtained thermochromatogram and the integrated chromatogram for the two nuclides <sup>168</sup>Os (T<sub>1/2</sub> = 2.1 s) and <sup>173</sup>Os (T<sub>1/2</sub> = 22.4 s). The enthalpies of adsorption were determined to (-37±1) kJ/mol for <sup>168</sup>Os and (-39.5±1.5) kJ/mol for <sup>173</sup>Os. Both values agree well with the value determined in Chapter 2.3 of

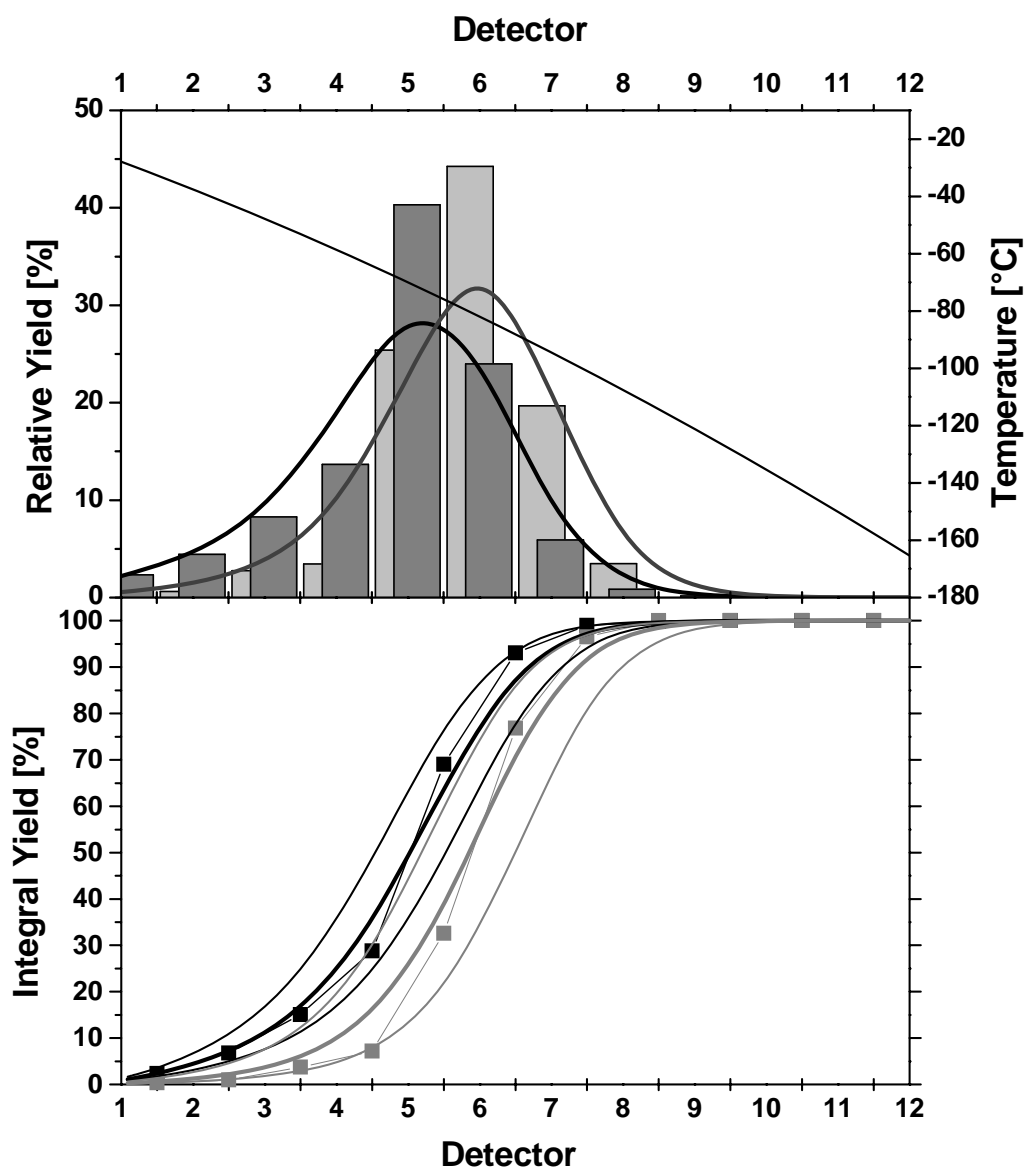


Fig. 2-11 TC and integrated TC of  $^{168}\text{Os}$  ( $T_{1/2} = 2.1$  s) and  $^{173}\text{Os}$  ( $T_{1/2} = 22.4$  s) at a total gas flow rate of 1.5 l/min. The bars (TC) and squares (integrated TC) represent experimental values: dark grey:  $^{168}\text{Os}$ ; light grey:  $^{173}\text{Os}$ . The thick lines represent the results of Monte Carlo simulations (details on this method are given in Chapter 3.4.1) assuming an enthalpy of adsorption of -37 kJ/mol ( $^{168}\text{Os}$ , black) and -39.5 kJ/mol ( $^{173}\text{Os}$ , grey). The thin lines indicate the error margins of  $\pm 1$  kJ/mol ( $^{168}\text{Os}$ ) and  $\pm 1.5$  kJ/mol ( $^{173}\text{Os}$ ), respectively. The thin solid line in the TC represents the temperature gradient (right hand scale).

( $-38.0 \pm 1.5$ ) kJ/mol and with literature values [Dom84, Kir02] determined under similar experimental conditions (on-line experiments). The influence of a different surface ( $\text{Si}_3\text{N}_4$  in COLD,  $\text{SiO}_2$  in all other experiments) seems minimal. This is to be expected, since for physisorption processes on dielectric surfaces, such as silicon oxides or nitrides, the influence of the surface material should be negligible.

Although the half-life of both nuclides differs by a factor of ten and that of  $^{168}\text{Os}$  is as short as 2.1 s, the obtained peak-shape indicates that a chromatographic process has taken place within the column, and COLD is applicable to nuclides with half-lives of a few seconds or even less.

### 2.5.2 Detection of fission fragments of $^{252}\text{Cf}$

Fission fragments originating from spontaneously fissioning  $^{252}\text{Cf}$  were measured with a PIN-diode as used in the COLD. The experiment was performed at ambient temperature. The obtained spectrum is shown in Figure 2-12.

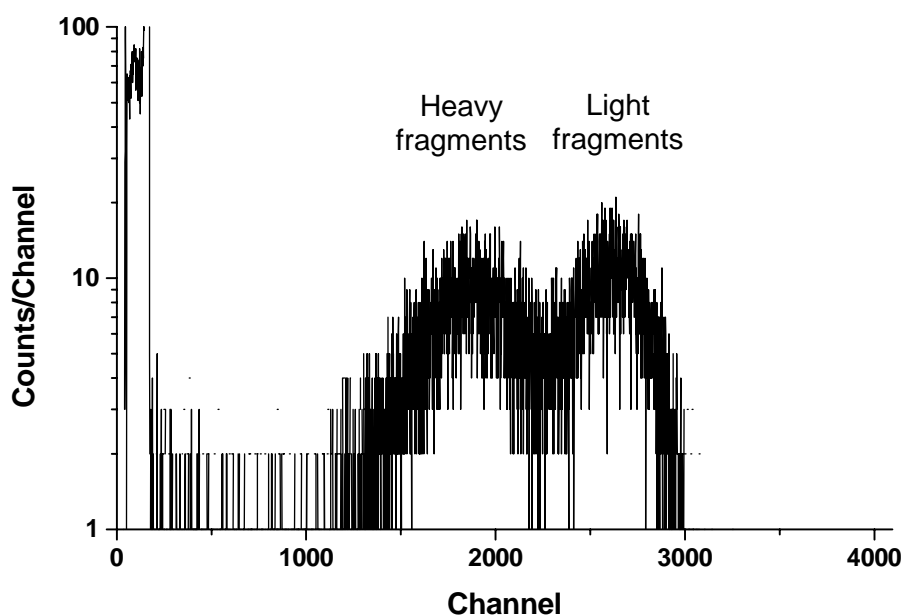


Fig. 2-12 Intensity vs. fragment energy spectrum of  $^{252}\text{Cf}$  fission fragments acquired with a single PIN diode as used in COLD at room temperature.

The obtained spectrum resolves the double humped distribution which proves that the diodes register the full energy of the fission fragments.

---

**References of Chapter 2**

- [Bar92] Barber, R.C. *et al.* Discovery of the transfermium elements. *Prog. Part. Nucl. Phys.* **29**, 453 (1992).
- [Dom84] Domanov, V.P. *et al.* Continuous-flow thermochromatographic separation of unsupported radioisotopes of platinum elements in a stream of air from nuclear reaction products in an accelerator heavy-ion beam. Translated from *Radiokhimiya* **26**, 770 (1984).
- [EiR00] Eichler, R. Die chemische Charakterisierung des Transactinoids Bohrium (Bh, Element 107). Doctoral Thesis, Universität Bern, Bern, 2000.
- [Gäg91] Gäggeler, H.W. *et al.* OLGA II, an on-line gas chemistry apparatus for application in heavy element research. *Nucl. Instrum. Meth.* **A309**, 201 (1991).
- [Kir02] Kirbach, U.W. *et al.* The Cryo-Thermochromatographic Separator (CTS): A new rapid separation and  $\alpha$ -detection system for on-line chemical studies of highly volatile osmium and hassium (Z=108) tetroxides. *Nucl. Instrum. Meth.* **A484**, 587 (2002).
- [Pig95] Piguet, D. *et al.* A double-window gas-jet target for applications in heavy ion induced reactions. Paul Scherrer Institut, Annual Report 1994, Annex IIIA (1995) p. 86 (unpublished)
- [Süm84] Sümmerer, K. *et al.* ROMA - A ROtating wheel Multidetector Apparatus used in experiments with  $^{254}\text{Es}$  as a target. GSI Annual Report 1983, 84-1 (1984) p. 246. (unpublished)
- [Tim96] Timokhin, S.N. *et al.* Chemical identification of element 106 by thermochromatography. *J. Radioanal. Nucl. Chem. Lett.* **212**, 31 (1996).
- [Tür97] Türler, A. BGS as preseparator for chemical studies. Proceedings of the Workshop on the physics using compound nucleus separators, Lawrence Berkeley National Lab, April 10-20, 1997. K.E. Gregorich, Editor, LBNL-40483/CONF-9704118/UC-412, 1997.
- [Web92] Weber, A.P. Characterization of the geometrical properties of agglomerated aerosol particles. PSI-Bericht 129, ISSN 1019-0643, Dezember 1992 (unpublished).
- [Zva66] Zvara, I. *et al.* Khimiceskie svoistva elementa 104. *Atom. Energija* **21**, 83 (1966) (in Russian).
- [Zva71] Zvara, I. *et al.* Chemical separation of kurchatovium. *Inorg. Nucl. Chem. Lett.* **7**, 1109 (1971).
- [Zva76] Zvara, I. *et al.* Chemical isolation of nilsbohrium as ekatantalum in the form of the anhydrous bromide. II. Experiments with a spontaneously fissioning isotope of nilsbohrium. Translated from *Radiokhimiya* **18**, 371 (1976).
- [Zva98] Zvara, I. *et al.* Chemical identification of element 106 (Thermochromatography of oxochlorides). *Radiochim. Acta* **81**, 179 (1998).

### 3. The experimental identification of hassium

In the following, the Hs experiment is described as well as its analysis. It was conducted in May 2001 at GSI.

#### 3.1 The IVO-COLD set-up

The IVO-COLD system as described in Chapter 2 was used. The test experiments were performed at PSI using a stationary target in contrast to the Hs experiment at GSI where a rotating target was used. The distance from the target to the exit of the quartz column was 40 mm in the Hs experiment at GSI, resulting in a slightly larger volume of the recoil chamber (34 ml, compared to 28 ml at PSI) due to an adapter flange inserted to connect IVO to the GSI beamline.

##### 3.1.1 Calibration of COLD

A  $^{227}\text{Ac}$  source which permanently emanated  $^{219}\text{Rn}$  ( $T_{1/2} = 3.96$  s) was installed in a by-pass of the gas line before IVO. It was periodically switched on to

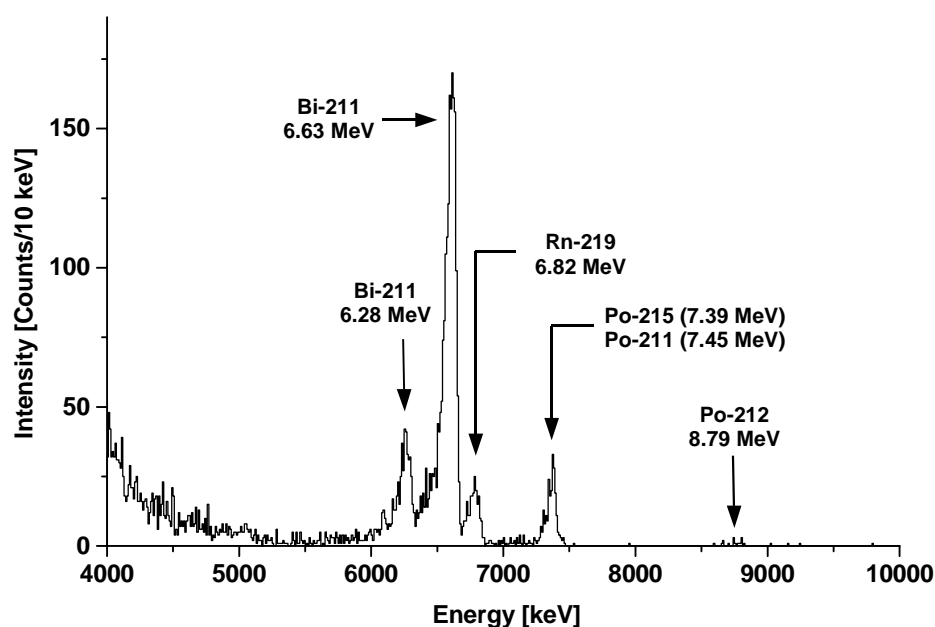


Fig. 3-1 Calibration spectrum of the COLD. Detectors 2 to 9. Resolution at 6500 keV (FWHM) for single units:  $\sim 80$  keV.

---

enable a thorough calibration of each detector. The daughters of  $^{219}\text{Rn}$ ,  $^{215}\text{Po}$  and  $^{211}\text{Bi}$ , are both non-volatile and decay at the same place where the Rn precursor did. Therefore, in all detectors a pattern similar to the one shown in Figure 3-1 was visible. The few events observed at about 8.8 MeV are assigned to  $^{212}\text{Po}$  originating in environmental  $^{220}\text{Rn}$ .

### 3.1.2 Operation of the IVO-COLD system

Using an adaptation flange, IVO was installed at an irradiation position of the UNILAC at GSI. COLD was connected via a 10 m long PFA Teflon<sup>®</sup> capillary installed inside of a PA tube flushed with  $\text{N}_2$  with a water vapor content  $<1$  ppm. In order to prevent the diffusion of water into COLD, a slight overpressure ( $\sim 30$  mbar) was maintained inside the COLD using a butterfly valve at the exit. The whole system was flushed for at least 30 min (but usually  $>1$  h) with dry gas (as used as carrier gas in the experiment) before COLD was cooled down. As soon as the temperature was stable, data acquisition was started and the beam switched on.

The experiment was twice interrupted in order to defrost COLD. The dew point of the carrier gas was always below  $-75$  °C (corresponding to a water vapor concentration  $<1$  ppm). Formation of layers of ice would have been observable causing deterioration of the energy resolution. No such effects were observed, not even at a temperature corresponding to the dew point. However, the current of the respective diodes was higher than usual, indicating that trace amounts of water had deposited on the diodes. No such effects were observed at temperatures above  $-75$  °C.

Data was acquired during 64.2 h. A total of  $10^{18}$  Mg particles passed through the  $^{248}\text{Cm}$  target (isotopic composition  $^{248}\text{Cm}$  95.8%,  $^{246}\text{Cm}$  4.2%) having an average thickness of  $554 \mu\text{g}/\text{cm}^2$ . The beam energy inside the target material was 143.7-146.8 MeV. The target system is described in detail in Chapter 3.3.

### 3.1.3 Data acquisition

The data acquisition software TANDEM [Schl89] was used. It allowed for a quasi on-line control of the experiment.

The continuously acquired data was stored on a harddisk. Every four hours acquisition was stopped and the respective file closed. A new file was created and the acquisition instantly resumed. Thus, a first rough data analysis and preliminary search for correlated events could be performed immediately after acquisition.

## 3.2 Analysis of the data and identification of Hs isotopes

After the experiment, a thorough calibration of all spectra was performed and correlated decay sequences were looked for. Since detector unit 1 B did not operate due to a technical failure, section 1 was excluded from the data analysis.

### 3.2.1 Alpha spectra

The following figures show cumulative spectra of detectors 2T and 2B (Figure 3-2), 3T and 3B (Figure 3-3) and 2 to 9 (T and B detectors) (Figure 3-5). Detectors 2T and 2B: Visible are  $\alpha$ -lines of  $^{219}\text{Rn}$  and its daughters  $^{215}\text{Po}$  and  $^{211}\text{Bi}$ . These nuclides originate in the  $^{227}\text{Ac}$  source. In addition,  $^{211}\text{At}$  ( $T_{1/2} = 7.2$  h) and its daughter  $^{211}\text{Po}$  are visible.  $^{211}\text{At}$  is formed in a transfer reaction of  $^{26}\text{Mg}$  with  $^{248}\text{Cm}$ .

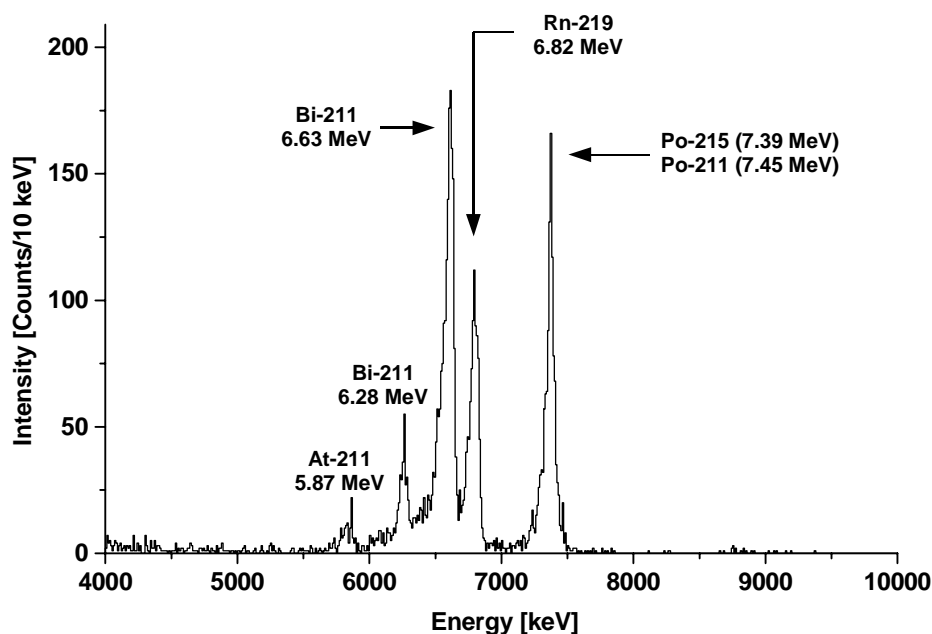


Fig. 3-2 Cumulative  $\alpha$ -spectrum of detectors 2T and 2B (Beam dose:  $10^{18}$  Mg particles).

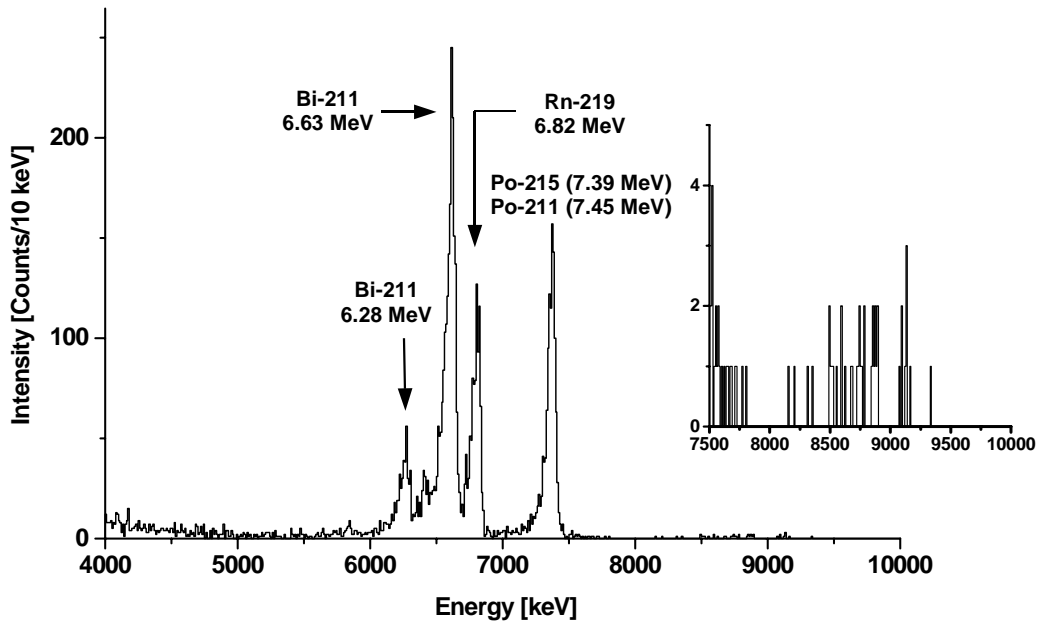


Fig. 3-3 Cumulative  $\alpha$ -spectrum of detectors 3T and 3B (Beam dose:  $10^{18}$  Mg particles).

Detectors 3T and 3B: Again, the nuclides originating in the  $^{227}\text{Ac}$  source are identified. Hardly any  $^{211}\text{At}$  is observed. The spectra of the detectors 4 to 9 were similar. The temperatures of detectors 11 and 12 were low enough to partly adsorb Rn. A TC of Rn (identified via the  $\alpha$ -line of the daughter  $^{215}\text{Po}$  which is separated from all other  $\alpha$ -lines) is shown in Figure 3-4.

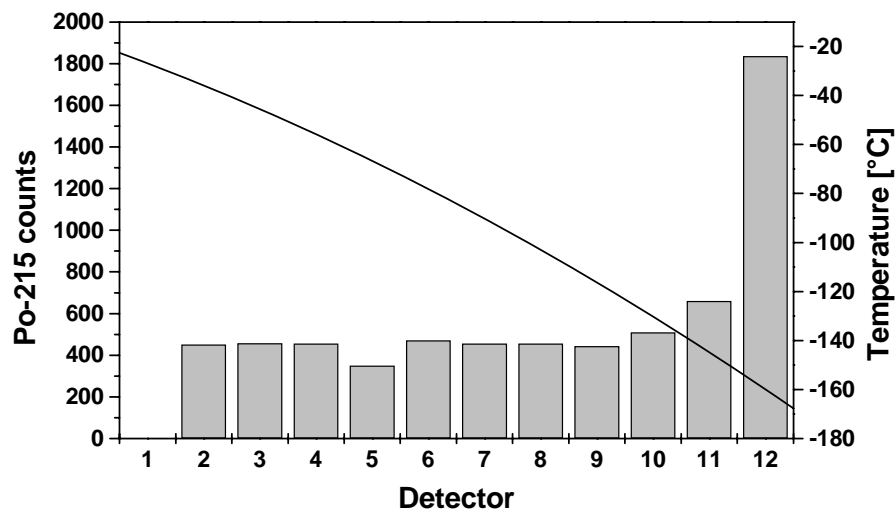


Fig. 3-4 Thermochromatogram of  $^{215}\text{Po}$ , the daughter of  $^{219}\text{Rn}$ .

No other  $\alpha$ -decaying nuclide was detected. In Figure 3-5, the sum spectrum of detectors 2 to 9 is shown.

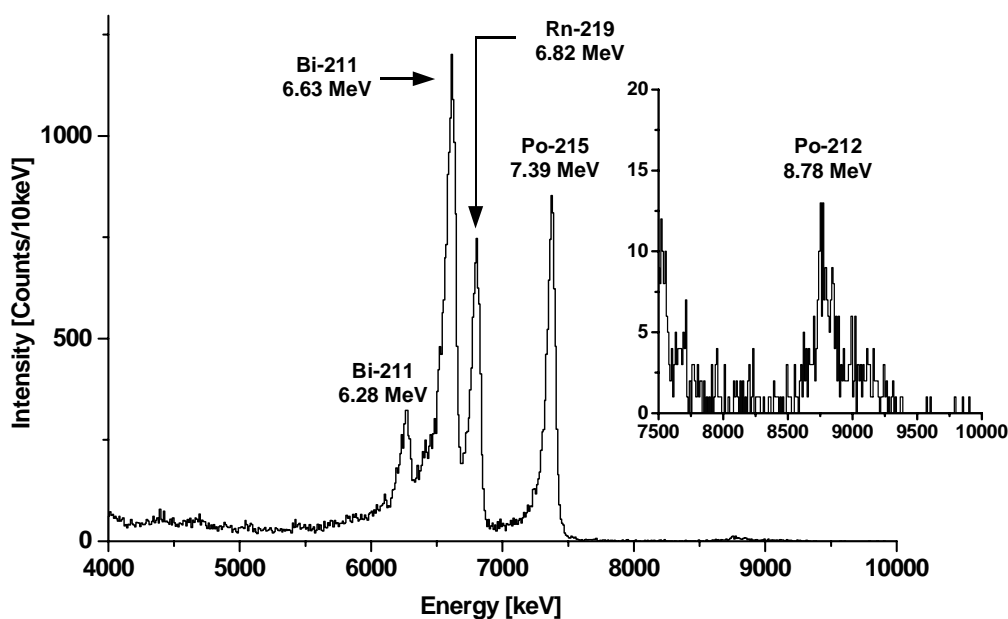


Fig. 3-5 Cumulative  $\alpha$ -spectrum of detectors 2 to 9 (T and B). Beam dose:  $10^{18}$  Mg particles.

Small amounts of  $^{212}\text{Po}$  originating in environmental  $^{220}\text{Rn}$  are visible. However, the interesting energy range  $>8.0$  MeV was relatively clean.

### 3.2.2 Fission fragments

Throughout the whole experiment, only very few fission fragments were detected. A threshold value of 50 MeV was set for an event to be considered as originating from a fission fragment. Four coincident fissions (i.e. one fragment in a T detector in coincidence with a fission fragment in the corresponding B detector) and 5 single fragments were observed. All these events occurred in detectors 2 to 4. All other detectors registered zero fission fragments, except for one fission fragment being observed in the operating side of detector 1.

Tab. 3-1 Observed fission fragments.

---

Date	Time	Detector	Fragment energy [MeV]
12-May-2001	02:33:34	2T / 2B	94 / 93
12-May-2001	14:43:12	4T	85
12-May-2001	14:51:08	4T / 4B	88 / 80
12-May-2001	14:59:42	4B	53
12-May-2001	17:09:23	4T / 4B	94 / 92
12-May-2001	18:42:33	2T	106
12-May-2001	21:50:43	4B	62
12-May-2001	22:00:45	3T / 3B	94 / 85
12-May-2001	23:22:50	1T	60
14-May-2001	07:09:04	3T	108

---

In the following publication, the result of the correlation analysis and the decay chains assigned to Hs isotopes is described.

---

### 3.3 Decay properties of $^{269}\text{Hs}$ and evidence for the new nuclide $^{270}\text{Hs}$

A. Türler<sup>1,2</sup>, Ch.E. Düllmann<sup>1,2</sup>, H.W. Gäggeler<sup>1,2</sup>, U.W. Kirbach<sup>3</sup>, A.B. Yakushev<sup>4</sup>, M. Schädel<sup>5</sup>, W. Bröchle<sup>5</sup>, R. Dressler<sup>1</sup>, K. Eberhardt<sup>6</sup>, B. Eichler<sup>1</sup>, R. Eichler<sup>5</sup>, T.N. Ginter<sup>3</sup>, F. Glaus<sup>1</sup>, K.E. Gregorich<sup>3</sup>, D.C. Hoffman<sup>3,7</sup>, E. Jäger<sup>5</sup>, D.T. Jost<sup>1</sup>, D.M. Lee<sup>3</sup>, H. Nitsche<sup>3,7</sup>, J.B. Patin<sup>3,7</sup>, V. Pershina<sup>5</sup>, D. Piguet<sup>1</sup>, Z. Qin<sup>8</sup>, B. Schausten<sup>5</sup>, E. Schimpf<sup>5</sup>, H.-J. Schött<sup>5</sup>, S. Soverna<sup>1,2</sup>, R. Sudowe<sup>3</sup>, P. Thörle<sup>6</sup>, S.N. Timokhin<sup>4</sup>, N. Trautmann<sup>6</sup>, A. Vahle<sup>9</sup>, G. Wirth<sup>5</sup>, P. Zielinski<sup>3,7</sup>

<sup>1</sup>Paul Scherrer Institute, CH-5232 Villigen, Switzerland

<sup>2</sup>Department of Chemistry and Biochemistry, University of Berne, CH-3012 Berne, Switzerland

<sup>3</sup>Nuclear Science Division, Lawrence Berkeley National Laboratory, Berkeley, California 94720

<sup>4</sup>Flerov Laboratory of Nuclear Reactions, Joint Institute for Nuclear Research, 141980 Dubna, Moscow Region, Russia

<sup>5</sup>Gesellschaft für Schwerionenforschung mbH, D-64291 Darmstadt, Germany

<sup>6</sup>Institut für Kernchemie, Universität Mainz, D-55099 Mainz, Germany

<sup>7</sup>Department of Chemistry, University of California, Berkeley, CA 94720-1460

<sup>8</sup>Institute of Modern Physics, Chinese Academy of Sciences, Lanzhou 730000, P.R. China

<sup>9</sup>Research Center Rossendorf e.V., D-01314 Dresden, Germany

Submitted to:

*The European Physical Journal A* (2002)

## Abstract

The nuclides  $^{269}\text{Hs}$  and  $^{270}\text{Hs}$  were produced in bombardments of a  $^{248}\text{Cm}$  target with 143.7-146.8 MeV  $^{26}\text{Mg}$  ions. After chemical isolation, Hs atoms were identified by observing genetically linked nuclear decay chains. Three chains originating from  $^{269}\text{Hs}$  confirmed the decay properties observed previously in the decay of  $^{277}\text{112}$ . Two chains exhibited the characteristics expected for the new nuclide  $^{270}\text{Hs}$ , which was predicted to be the next heavier "doubly-magic" nucleus after  $^{208}\text{Pb}$ . From the measured  $E_{\alpha}=(9.16^{+0.70}_{-0.30}$  MeV) an  $\alpha$ -decay half-life of  $3.6^{+0.8}_{-1.4}$  s was estimated.

Element 108 (hassium, Hs) was discovered in 1984 by Münzenberg et al. [1] using the reaction  $^{208}\text{Pb}(^{58}\text{Fe}, 1n)^{265}\text{Hs}$ . Until today,  $^{264-267}\text{Hs}$  and  $^{269}\text{Hs}$  have positively been identified [1-5]. Furthermore,  $^{263}\text{Hs}$  as a daughter of  $^{267}\text{110}$  [6] and one spontaneous-fission (SF) decay of  $^{277}\text{Hs}$  as decay product of  $^{289}\text{114}$  have been reported [7]. Three decays of  $^{269}\text{Hs}$  have been observed in the decay chain of  $^{277}\text{112}$  [5,8]. In macroscopic-microscopic calculations increased stability was predicted at and near  $N=162$  and  $Z=108$  [9,10]. This new area of increased stability corresponds to gaps in the single-particle spectra which appear only at deformed shapes. By using a larger deformation space and a dynamic treatment of the fission barriers, Patyk et al. [9,10] analyzed the single-particle spectra of heavy nuclei and predicted  $^{270}\text{Hs}$  to be a relatively strongly bound "doubly-magic" deformed nucleus. They predicted rather long SF half-lives in this region. Therefore,  $^{270}\text{Hs}$  is expected to decay predominantly by  $\alpha$ -particle emission with  $Q_{\alpha}=9.44$  MeV [10]. In the most recent work this value was slightly reduced to  $Q_{\alpha}=9.13$  MeV [11], resulting in a partial  $\alpha$ -decay half-life of about 6 s, whereas the partial SF-decay half-life was predicted to be 1.8 h [12]. Decay energies of  $Q_{\alpha}=8.7-9.9$  MeV have been derived from mass models [13-15],  $Q_{\alpha}=9.0$  MeV was calculated in the framework of the relativistic mean-field theory [16]. It is therefore of great interest to experimentally establish the decay properties of this nucleus. We report here on our experiments to chemically identify Hs, which resulted in the observation of  $^{269}\text{Hs}$  and evidence for the production of the new nuclide  $^{270}\text{Hs}$ .

---

In our experiments  $^{270}\text{Hs}$  and  $^{269}\text{Hs}$  were produced via the  $^{248}\text{Cm}(^{26}\text{Mg}, 4n)$  and  $^{248}\text{Cm}(^{26}\text{Mg}, 5n)$  reactions. The Universal Linear Accelerator (UNILAC) at the Gesellschaft für Schwerionenforschung, Darmstadt, provided very intense beams of up to  $6.6\text{-}\mu\text{A}$   $192.7\text{-MeV}$   $^{26}\text{Mg}^{5+}$ . The beam entered the target chamber through a rotating 3 segment  $3.68\text{ mg/cm}^2$  Be vacuum window and the  $2.82\text{ mg/cm}^2$  Be target backing, before passing through the target material. The 3 banana shaped  $^{248}\text{Cm}$  targets ( $^{248}\text{Cm}$  95.8 %,  $^{246}\text{Cm}$  4.2 %) with an average thickness of  $239\text{ }\mu\text{g/cm}^2$ ,  $730\text{ }\mu\text{g/cm}^2$ , and  $692\text{ }\mu\text{g/cm}^2$  were prepared on Be foils by molecular plating. The  $^{248}\text{Cm}$  target material was obtained by chemical separation from a  $^{252}\text{Cf}$  neutron source [17]. The rotating vacuum window allowed for pressures of up to 1.3 atm in the target chamber. The target wheel rotated in the gaseous atmosphere of the target chamber with 2000 rpm. The rotation was synchronized with the beam pulses of the UNILAC in order to evenly distribute each 6-ms beam pulse over one of the three segments of the wheel. The  $192.7\text{-MeV}$  beam energy of  $^{26}\text{Mg}^{5+}$  from the accelerator resulted in projectile energies in the  $^{248}\text{Cm}$  targets of  $143.7\text{-}146.8\text{ MeV}$ .

In order to investigate the chemical properties of Hs, the gas chromatographic separation system IVO (In situ Volatilization and On-line detection) was developed and tested with short-lived  $\alpha$ -particle emitting Os isotopes [18]. Element 108 is expected to belong to group 8 of the periodic table (like Os) and to form stable  $\text{HsO}_4$  molecules, which should be volatile even at room temperature [19]. Nuclear reaction products recoiling from the target are stopped in He containing 7.7%  $\text{O}_2$ . Os and presumably Hs are converted in situ to volatile tetroxides. The recoil chamber was continuously flushed at a flow rate of  $1300\text{ ml/min}$ . At the exit of the recoil chamber the gas passed through a quartz column containing a quartz wool plug which was heated to  $873\text{ K}$ . This quartz wool plug served as a filter for aerosol particles and provided a surface to complete the oxidation reaction of Os and Hs. Volatile species were then transported through a  $10\text{ m}$  long teflon (PFA) capillary (i.d.  $2\text{ mm}$ ) to an on-line detection system.

---

In order to efficiently detect the nuclear decay of isolated Hs nuclides, as well as to obtain chemical information about the volatility of the investigated compounds, a cryo thermochromatography detector was used [20]. The gas mixture containing volatile HsO<sub>4</sub> molecules is flowing through a narrow channel formed by a series of planar silicon diodes. Along this channel a longitudinal negative temperature gradient is established. The position at which the characteristic  $\alpha$ -particle decay chain originating from the decay of a Hs nuclide is registered is indicating the deposition temperature of this molecule on the diode surface. Due to the close proximity of the silicon diodes facing each other, the probability to register a complete decay chain is rather high. A drawback of our method in comparison to kinematic separators is the lack of an initial implantation signal of the mother nucleus, which allows to measure the lifetime of the mother nuclide. In our apparatus the time at which a deposition of a HsO<sub>4</sub> molecule took place could not be detected, only the lifetimes of the daughter nuclei were measured. A cryo thermochromatography system named COLD (Cryo On-Line Detector) using an array of 2x36 PIN-diodes (Positive Implanted N-type silicon, 10x10 mm active area) was built. The COLD detector is an improved version of the Cryo-Thermochromatographic Separator (CTS) [20] which was pioneered at Lawrence Berkeley National Laboratory. Two PIN-diodes mounted on ceramic supports (XRA-100, Detection Technology, Inc.) were glued together facing each other. Two T-shaped spacers made from silicon confined the gas flow to the active surface of the diodes. The gap in the channel was 1.5 mm wide. Always 3 neighboring PIN-diodes were electrically connected to form one detector unit. The COLD array consisted therefore of 12 sections each containing one pair of detector units, denoted with top (T) and bottom (B). The temperature ranged from 243 K down to 93 K. The detector units of the COLD array were calibrated with  $\alpha$ -decaying <sup>219</sup>Rn (and its daughters <sup>215</sup>Po and <sup>211</sup>Bi) emanating from a <sup>227</sup>Ac source. The resolution was about 50-70 keV (FWHM) for detector units 1 through 8 (T and B) and about 80-110 keV (FWHM) for detector units 10 through 12 (T and B). The usually better resolution of PIN-diodes was degraded due to two effects. First, by electrically coupling 3 diodes together and, second, by the fact that about 30% of the

registered  $\alpha$ -particles were emitted by nuclides adsorbed on the opposite detector unit. Therefore, the energy of these  $\alpha$ -particles was degraded by the He/O<sub>2</sub> atmosphere in the gap between the diodes. This energy loss was typically about 40 keV unless the  $\alpha$ -particles were emitted under very shallow angles to the diode surface. The uncertainties of the  $\alpha$ -decay energies in this work amount to typically  $^{+70}_{-30}$  keV. A typical  $\alpha$ -particle spectrum of section 3 is shown in Figure 3-6.

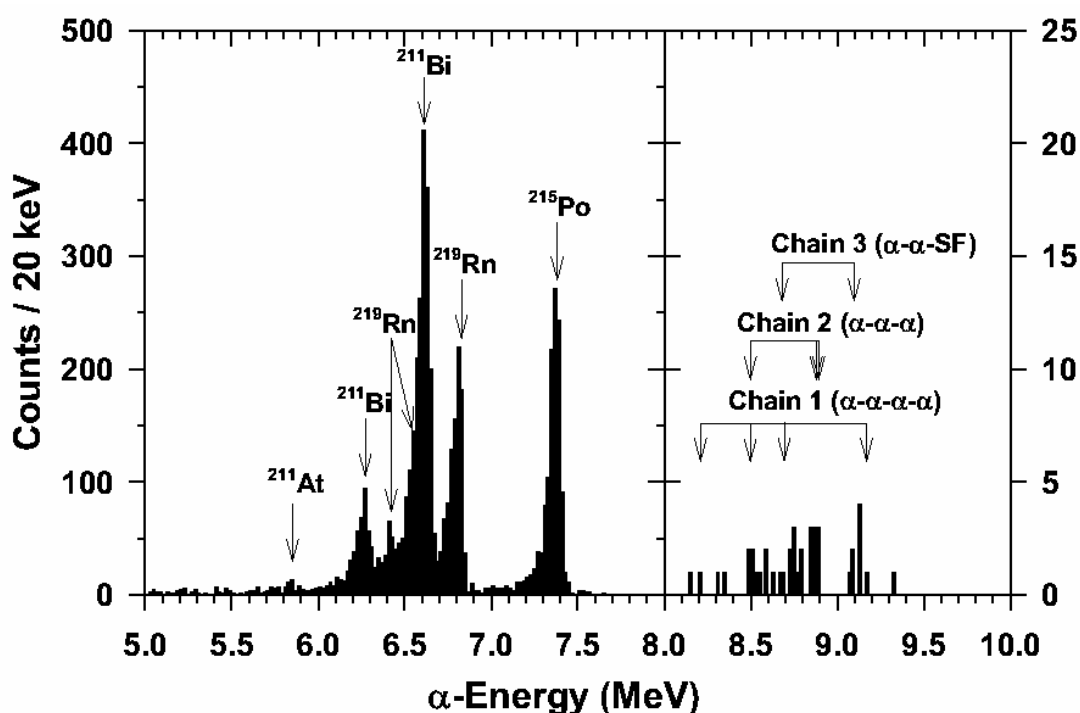


Fig. 3-6  $\alpha$ -particle spectrum of section 3 recorded during 64.2 h of beam ( $1.0 \times 10^{18} \text{ }^{26}\text{Mg}$  ions).

In the course of the experiment, data was collected during 64.2 h and a beam integral of  $1.0 \times 10^{18} \text{ }^{26}\text{Mg}$  ions was accumulated. The count rate in all sections was very low. Only  $^{219}\text{Rn}$ ,  $^{220}\text{Rn}$ ,  $^{211}\text{At}$  and their decay products were identified as background activities. While  $^{211}\text{At}$  and its decay product  $^{211}\text{Po}$  was deposited mainly in the first two sections,  $^{219}\text{Rn}$  and  $^{220}\text{Rn}$  and their decay products accumulated in the last three sections, where the temperature was low enough to condense Rn. Since detector unit 1B was not operating, section 1 was excluded from the data analysis. The average count rate per section was  $0.6 \text{ h}^{-1}$  in the relevant energy window  $E_{\alpha}=8.0\text{-}9.5 \text{ MeV}$  in sections 2

through 10. The data analysis revealed one four-member- and 4 three-member decay chains each having a length  $\leq 70$  s. The four-member decay chain could unambiguously be attributed to the decay of  $^{269}\text{Hs}$ . The remaining 4 three-member decay chains, each having a similarly low probability to be of random origin, must for chemical reasons be attributed to an isotope of Hs. From the calculated excitation functions of the reaction  $^{26}\text{Mg}+^{248}\text{Cm}$  [21] these are  $^{269}\text{Hs}$  or  $^{270}\text{Hs}$  at a beam energy of 143.7-146.8 MeV. Based on the poorly or unknown decay data of  $^{269,270}\text{Hs}$  and their decay products, two of the remaining 4 decay chains were attributed to  $^{269}\text{Hs}$  and two were tentatively assigned to the decay of the new nuclide  $^{270}\text{Hs}$  (Figure 3-7).

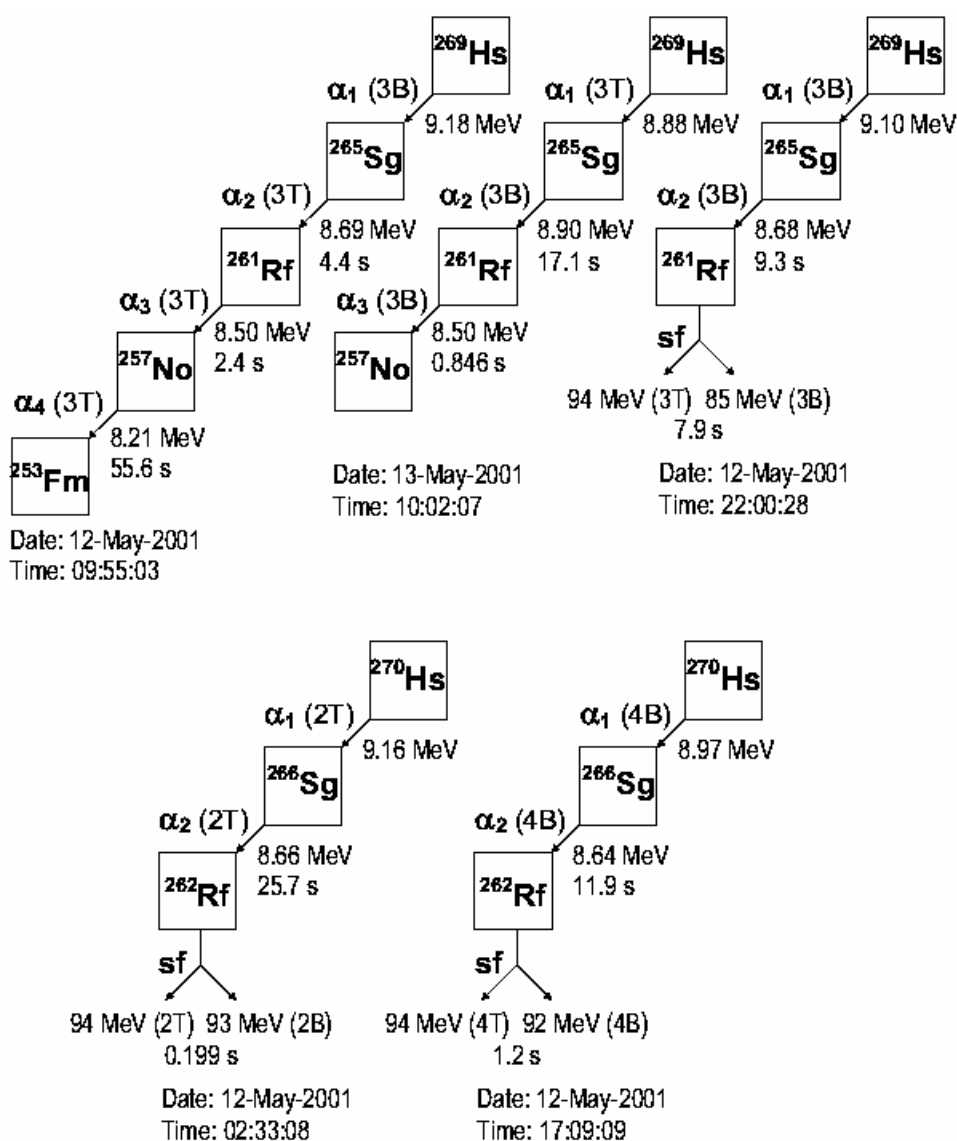


Fig. 3-7 Observed decay chains attributed to the decay of  $^{269}\text{Hs}$  and  $^{270}\text{Hs}$  produced in the reaction  $^{26}\text{Mg}+^{248}\text{Cm}$ .

The first decay chain of  $^{269}\text{Hs}$  consisted of four  $\alpha$ -particles occurring within 62.3 s in section 3. Based on the count rate in the energy window  $E_\alpha=8.0\text{-}9.5$  MeV in this section, the expected number of random four-member decay chains within 62.3 s not related to the decay of  $^{269}\text{Hs}$  was calculated as  $N_R \leq 2 \times 10^{-6}$ . The first  $\alpha$  decay with  $E_\alpha=9.18$  MeV was followed by  $E_\alpha=8.69$  MeV ( $\Delta t=4.4$  s), in good agreement with the expected decay properties of  $^{265}\text{Sg}$ . Decay energies between  $E_\alpha=8.69\text{-}8.94$  MeV and a half-life of  $7.4^{+3.3}_{-2.7}$  s have been measured for this nuclide [22,23]. The chain continued through  $^{261}\text{Rf}$  ( $E_\alpha=8.50$  MeV,  $\Delta t=2.4$  s) and  $^{257}\text{No}$  ( $E_\alpha=8.21$  MeV,  $\Delta t=55.6$  s). The last decay agrees well with literature data for  $^{257}\text{No}$  [24]. However,  $^{261}\text{Rf}$  is known to decay by the emission of  $8.28 \pm 0.02$  MeV  $\alpha$ -particles [25] with a half-life of  $78^{+11}_{-6}$  s [26]. While in these earlier works the observation of 8.5 MeV  $\alpha$ -particles could not be ruled out due to the presence of contaminants, the work of Lazarev et al. [27], where 69  $^{261}\text{Rf}\text{-}^{257}\text{No}$  correlations were registered, clearly showed no evidence for this  $\alpha$ -decay energy. Nonetheless, the properties of our decay chain are in very good agreement with the ones observed for  $^{269}\text{Hs}$  in the first two decay chains of  $^{277}\text{112}$  produced in the reaction  $^{208}\text{Pb}(^{70}\text{Zn}, 1n)$  [5]. There,  $\alpha$ -decay energies of 9.17 and 9.23 MeV were observed for  $^{269}\text{Hs}$ . A striking feature was the observation of  $E_\alpha=8.52$  MeV for  $^{261}\text{Rf}$  in the second  $^{277}\text{112}$  decay chain with a relatively short lifetime of 4.7 s [5], which now has also been observed in this work.

Two further decay chains attributed to  $^{269}\text{Hs}$  were observed in the same section 3, i.e. at the same deposition temperature. In one decay chain the decay of  $^{257}\text{No}$  was missed. This chain started with  $E_\alpha=8.88$  MeV, which is a relatively low decay energy for  $^{269}\text{Hs}$ . Since it was not possible to determine on which side of the detector sandwich  $^{269}\text{HsO}_4$  was deposited, it is conceivable that this  $\alpha$ -particle lost a considerable part of its energy in the He/O<sub>2</sub> atmosphere. The decay chain proceeded through  $^{265}\text{Sg}$  ( $E_\alpha=8.90$  MeV,  $\Delta t=17.1$  s) and through  $^{261}\text{Rf}$  ( $E_\alpha=8.50$  MeV,  $\Delta t=846$  ms) ( $N_R \leq 7 \times 10^{-5}$ ). It appears, as if in the decay of  $^{269}\text{Hs}$  a different state of  $^{261}\text{Rf}$  is populated. This is corroborated by the third observed decay chain, which is very similar to the first one, but is terminated by SF of  $^{261}\text{Rf}$  ( $\Delta t=7.9$  s) ( $N_R \leq 7 \times 10^{-6}$ ). The energies

of the fission fragments have not been corrected for pulse height defects in the detectors and for neutron emission. The decay data of this chain is again in good agreement with a third decay chain observed recently for  $^{277}\text{112}$ , which was also terminated by SF of  $^{261}\text{Rf}$  with a lifetime of 14.5 s [8]. For the so far known 78-s  $^{261}\text{Rf}$  an upper limit for SF of  $\leq 10\%$  was established [25]. Since  $E_\alpha = 8.52$  MeV fits better into the systematics of ground-state  $\alpha$ -decay energies, Hofmann et al. [8] tentatively assigned the two  $\alpha$ -decays and the one SF event measured in their  $^{277}\text{112}$  decay chains to the ground state of  $^{261}\text{Rf}$ . With the three additional events observed in this work, a half-life of  $7.3^{+5.0}_{-2.1}$  s and a SF-branch of about 33 % is calculated for the decay of  $^{261}\text{Rf}$ , whereas the previously known 78-s state should be denoted with  $^{261\text{m}}\text{Rf}$ .

In our experiment, two decay chains exhibiting the expected decay characteristics of  $^{270}\text{Hs}$  were observed. The so far unknown  $^{270}\text{Hs}$  is expected to decay via  $\alpha$ -particle emission to the known nuclide  $^{266}\text{Sg}$  ( $E_\alpha = 8.63 \pm 0.05$  MeV) [22] which decays to  $^{262}\text{Rf}$  ( $T_{1/2} = 2.1 \pm 0.2$  s), a short-lived SF nuclide [28]. The first decay chain with  $E_\alpha = 9.16$  MeV, followed by  $E_\alpha = 8.66$  MeV ( $\Delta t = 25.7$  s) and SF ( $\Delta t = 199$  ms) occurred in section 2 ( $N_R \leq 8 \times 10^{-6}$ ). Nearly identical energies were measured for both fission fragments. A similar decay chain starting with  $E_\alpha = 8.97$  MeV followed by  $E_\alpha = 8.64$  MeV ( $\Delta t = 11.9$  s) and SF ( $\Delta t = 1.2$  s) was observed in section 4 ( $N_R \leq 5 \times 10^{-5}$ ). Again, nearly identical fragment energies were measured. In both decay chains the  $\alpha$ -decay energy attributed to  $^{266}\text{Sg}$  is in agreement with literature data [22]. The short correlation times of both SF events and the symmetric energy division among the fragments point to  $^{262}\text{Rf}$  as terminating nuclide. The nuclide  $^{262}\text{Rf}$  is known to fission symmetrically [28]. From the measured  $E_\alpha = 9.16^{+0.07}_{-0.03}$  MeV attributed to  $^{270}\text{Hs}$ ,  $Q_\alpha = 9.30^{+0.07}_{-0.03}$  MeV was calculated in good agreement with predictions [10,11]. Using the relationship between  $Q_\alpha$  of ground state to ground state  $\alpha$ -decays of even-even nuclides and the nuclear half-life by Buck et al. [29], resulted in  $T_{1/2}^\alpha(^{270}\text{Hs}) = 3.6^{+0.8}_{-1.4}$  s. The formula of Buck et al. [29] reproduces the half-lives of known even-even nuclides within a factor of  $\sim 2$ . Since only about 77% of the inner surface of the COLD channel consisted of active detector surface, detection of a few incomplete decay sequences is

---

expected. Two  $\alpha$ -SF correlations were observed in sections 3 and 4 that still have a rather low random probability, but could not be assigned with certainty to either  $^{269}\text{Hs}$  or  $^{270}\text{Hs}$ . These were in section 3:  $E_\alpha=9.14$  MeV followed by SF (108 MeV, only 1 fragment,  $\Delta t=42.6$  s) ( $N_R \leq 4 \times 10^{-4}$ ) and in section 4:  $E_\alpha=8.72$  MeV followed by SF (53 MeV, only 1 fragment,  $\Delta t=3.1$  s) ( $N_R \leq 2 \times 10^{-4}$ ). Also, 4 uncorrelated SF decays with fragment energies  $\geq 50$  MeV were registered in detectors 2, 3, and 4. All other sections 5 through 12 registered zero SF events. This may point to a SF branch in either  $^{269}\text{Hs}$  or  $^{270}\text{Hs}$ . Also, no three-member  $\alpha$ -decay chains were observed in sections 5 through 10 with a length  $\leq 300$  s.

Assuming an overall efficiency of  $\sim 40\%$ , a production cross section of 4 pb for  $\alpha$ -decaying  $^{270}\text{Hs}$  and of 6 pb for  $\alpha$ -decaying  $^{269}\text{Hs}$  was calculated at 143.7-146.8 MeV beam energy. The cross sections are reported with an estimated accuracy of a factor of  $\sim 3$ . The isotopes  $^{269}\text{Hs}$  and presumably  $^{270}\text{Hs}$  were identified after chemical separation by observing genetically linked decay chains. The lower end of the decay chain of  $^{277}112$  was clearly reproduced and our work strongly supports the claim of Hofmann et al. [5] that in their work indeed the new element 112 had been produced. The efficiency and sensitivity of chemical methods competed favorably with physical separator systems and showed that chemical methods allow to work on the 1 pb cross section level. The chemical implications of our experiment are discussed in a separate publication [30].

### **Acknowledgments**

We thank the staff of the GSI UNILAC and K. Tinschert together with his ECR ion source team for providing stable, very high intensity beams of  $^{26}\text{Mg}$ . We also thank the GSI target laboratory for valuable assistance in providing Be foils for the vacuum windows. K.-H. Behr's help in setting up the beam control system and E. Badura's efforts to provide reliable beam current monitors is appreciated. These studies were supported in part by the Swiss National Science Foundation and the Chemical Sciences Division of the Office of Basic Energy Sciences, U.S. Department of Energy.

**References**

- [1] G. Münzenberg et al., Z. Phys. A 317, 235 (1984).
- [2] G. Münzenberg et al., Z. Phys. A 324, 489 (1986).
- [3] Yu.A. Lazarev et al., Phys. Rev. Lett. 75, 1903 (1995).
- [4] S. Hofmann et al., Eur. Phys. J. A 10, 5 (2001).
- [5] S. Hofmann et al., Z. Phys. A 354, 229 (1996).
- [6] A. Ghiorso et al., Phys. Rev. C 51, R2293 (1995).
- [7] Yu.Ts. Oganessian et al., Phys. Rev. Lett. 83, 3154 (1999).
- [8] S. Hofmann, G. Münzenberg, Rev. Mod. Phys. 72, 733 (2000).
- [9] Z. Patyk, A. Sobiczewski, S. Cwiok, Nucl. Phys. A502, 591c (1989).
- [10] Z. Patyk, A. Sobiczewski, Nucl. Phys. A 533, 132 (1991).
- [11] A. Sobiczewski, I. Muntian, Z. Patyk, Phys. Rev. C 63, 034306 (2001).
- [12] R. Smolanczuk, J. Skalski, A. Sobiczewski, Phys. Rev. C 52, 1871 (1995).
- [13] P. Möller, J.R. Nix, K.-L. Kratz, At. Data Nucl. Data Tab. 66,131 (1997).
- [14] S. Liran, A. Marinov, N. Zeldes, Phys. Rev. C 62, 047301 (2001).
- [15] G. Royer, R.A. Gherghescu, Nucl. Phys. A 699, 479 (2002).
- [16] Z. Ren, Z.Y. Zhu, Y.H. Cai, G. Xu, J. Phys. G. 22,1793 (1996).
- [17] R. Malmbeck et al., Radiochim. Acta 89, 543 (2001).
- [18] Ch.E. Düllmann et al., Nucl. Instrum. Methods A 479, 631 (2002).
- [19] V.G. Pershina et al., J. Chem. Phys. 115, 792 (2001).
- [20] U.W. Kirbach et al., Nucl. Instrum. Methods A 484, 587 (2002).

- 
- [21] W. Reisdorf, M. Schädel, Z. Phys. A 343, 47 (1992).
- [22] Yu.A. Lazarev et al., Phys. Rev. Lett. 73, 624 (1994).
- [23] A. Türler et al., Phys. Rev. C 57, 1648 (1998).
- [24] P. Eskola, K. Eskola, M. Nurmia, A. Ghiorso, Phys. Rev. C 2 ,1058 (1970).
- [25] A. Ghiorso, M. Nurmia, K. Eskola, P. Eskola, Phys. Lett. 32B, 95 (1970).
- [26] B. Kadkhodayan et al., Radiochim. Acta 72, 169 (1996).
- [27] Yu.A. Lazarev et al., Phys. Rev. C 62, 064307 (2000).
- [28] M.R. Lane et al., Phys. Rev. C 53, 2893 (1996).
- [29] B. Buck, A.C. Merchant, S.M. Perez, J. Phys. G 17, 1223 (1991).
- [30] Ch.E. Düllmann et al., Nature (in press).

### 3.4 Evaluation of the enthalpy of adsorption of $\text{HsO}_4$ on the detector surface material ( $\text{Si}_3\text{N}_4$ )

The distribution of the seven decay chains along the TC column of the COLD, as well as the temperature gradient are shown in Figure 3-8. The distribution of  $^{172}\text{OsO}_4$  ( $T_{1/2} = 19.2$  s) is also given.

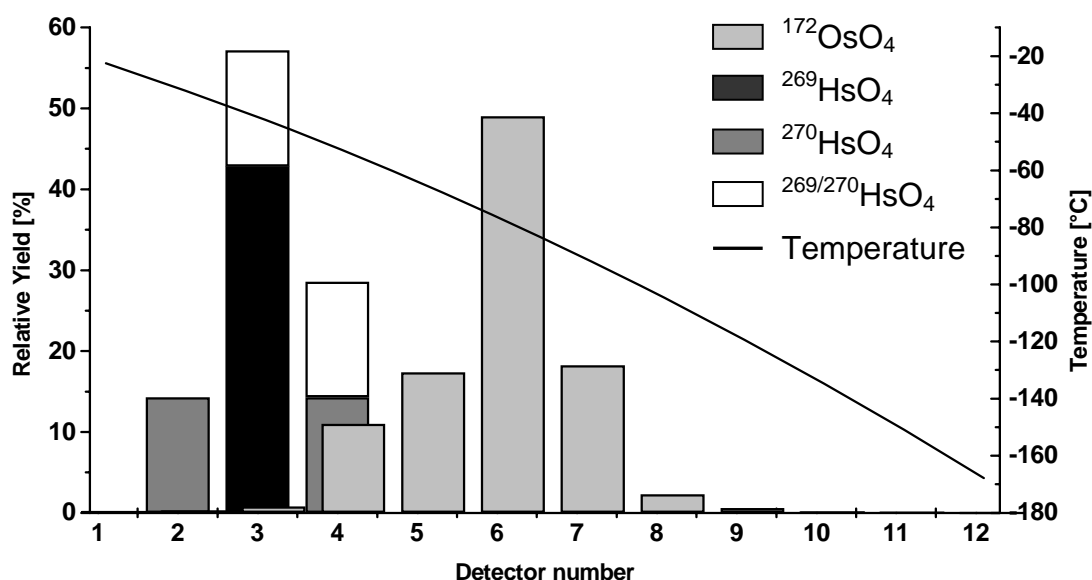


Fig. 3-8 Merged thermochromatogram of  $^{172}\text{OsO}_4$  and the decay chains attributed to  $^{269,270}\text{HsO}_4$ .

The maxima of the deposition distributions were found at temperatures of  $(-82 \pm 7)$  °C for  $^{172}\text{OsO}_4$  and at  $(-44 \pm 6)$  °C for all events attributed to Hs.

Mobile adsorption, without any superimposed chemical reaction, occurs in the case of  $\text{OsO}_4$  on a quartz column as shown in Chapter 2.3.3. Owing to the even greater stability of  $\text{HsO}_4$ , the same transport mechanism was assumed for this compound on  $\text{Si}_3\text{N}_4$ . The enthalpy of adsorption on the column material ( $\text{Si}_3\text{N}_4$ ) was evaluated using two independent models:

- A Monte Carlo simulation (MCS) of the trajectories of single molecules travelling along a chromatography column [Zva85].
- A thermodynamic approach using the model of mobile adsorption [EiB82].

### 3.4.1 Monte Carlo simulation

In this section, a brief introduction to the model is given. A complete description can be found in [Zva85]. Using the Monte Carlo technique, the trajectories of single molecules travelling along a chromatography column are simulated using the real experimental parameters such as temperature profile, gas flow rate or half-life of the species. The chromatographic process is based on the reversible adsorption of the species on the column surface. The mean time  $\bar{\tau}_a$  a molecule spends in the adsorbed state  $\tau_a$  is described by the Frenkel equation [Fre24],

$$\bar{\tau}_a = \tau_0 \cdot \exp(-\Delta H_{\text{ads}}/R \cdot T) \quad (3-1)$$

where  $\tau_0$  is the period of oscillations of the molecule in adsorbed state perpendicular to the surface [s],  $R$  the universal gas constant [J/mol·K], and  $T$  the absolute temperature [K]. The entropy of adsorption  $\Delta S_{\text{ads}}$  is not taken into account in this model, in contrast to the model of mobile adsorption, which is discussed in Chapter 3.4.2. In the desorbed state, the molecule is carried along the column by the carrier gas flow. The probability density distribution of the length of displacements  $\eta$  is approximated by the following physical picture: (i) once the molecule encounters the surface, it generally experiences a series of adsorption-desorption events proceeding without a change in the coordinate along the column length; (ii) these sequences are intermittent with rather long downstream jumps. The mean length of these jumps strongly depends on the diffusion coefficient. The change of the coordinate of the molecule due to (i) is neglected in the simulation; only the time between type (ii) events is taken into account. The probability distribution of the jump length  $\eta$  of type (ii) events is exponentially decreasing:

$$\rho(\eta) = (1/\bar{\eta}) \cdot \exp(-\eta/\bar{\eta}) \quad (3-3)$$

The model proved suitable to describe both off-line and on-line experiments (IC and TC) and is well suited to evaluate thermochemical data from experiments with high gas-flow rates ( $\sim 1$ /min) (see e.g. [Tür96]). However, a circular column is generally assumed and, since a column with a rectangular

---

cross section ( $8.6 \times 1.5 \text{ mm}^2$ ) could not be modeled, simulations assuming different column diameters were performed. The gas flow rate was scaled with the ratio of the real cross section to that used in the simulation. The distribution of  $\text{OsO}_4$  was simulated applying three different parameter sets:

(i) a tube with a diameter of 4.053 mm, corresponding to the same cross section as the COLD channel. The simulated gas flow rate remained unchanged.

(ii) a tube with a diameter of 8.6 mm, corresponding to the length of the COLD channel. The gas flow rate was increased by a factor of 4.503 (corresponding to 5853.9 ml/min) to achieve the same gas flow velocity as in the experiment.

(iii) a tube with a diameter of 1.5 mm, corresponding to the width of the COLD channel. The gas flow rate was scaled down by a factor of 7.300 (corresponding to 178.08 ml/min), again to match the gas flow velocity.

In Figure 3-9, the resulting distribution of 100'000 molecules for each of the three different approaches is shown in comparison to the experimental data. As a result of the MCS the one value for  $\Delta H_{\text{ads}}$  was chosen for which a  $T_{50\%}$  value (shown in the integrated TC) resulted that best described the experimental data.

As can be seen, the results of the simulation (iii) (thick solid line) best describe the experimental data. This result is in agreement with the observations made in experiments with the CTS [Kir02] which seems reasonable because the mean distance from the surface is approximately the same in the COLD column and in a column used in (iii). The resulting value of  $\Delta H_{\text{ads}}(\text{HsO}_4) = (-39 \pm 1) \text{ kJ/mol}$  is again in good agreement with that obtained with the IC method described in Chapter 2.3.3 and with literature values [Dom84, Kir02]. Therefore, this geometry was also used for the evaluation of  $\Delta H_{\text{ads}}(\text{HsO}_4)$ .

An important parameter in the whole simulation process is the half-life of the species. In the present experiment, the lifetime of the mother isotope could not be determined. The half-life of  $^{270}\text{Hs}$  has not yet been measured; a value

of 4 s was estimated by applying  $\alpha$ -systematics [Buc91] (see Chapter 3.3).

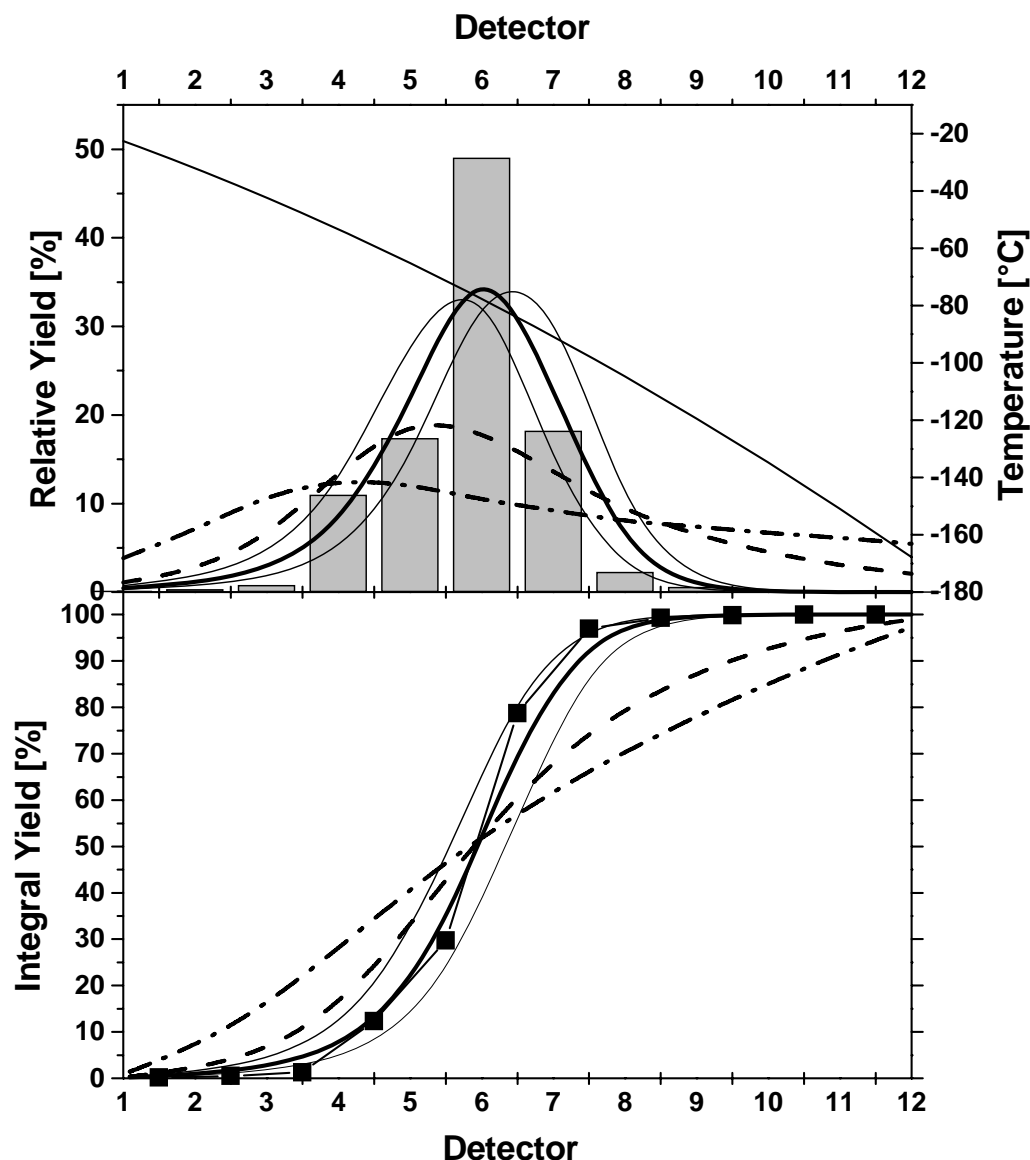


Fig. 3-9 TC and integrated TC of  $^{172}\text{Os}$ . Indicated are the experimental data (bars and squares, respectively). The thin solid line in the upper panel indicates the temperature profile (right-hand scale). The lines are the results of the MCS assuming the following geometries and adsorption enthalpies: assumption (i) (dashed line)  $-43$  kJ/mol, assumption (ii) (dash-dotted line)  $-46.5$  kJ/mol, and assumption (iii) (thick solid line)  $-39$  kJ/mol, respectively. The indicated error margins (thin solid lines) are  $\pm 1$  kJ/mol (for geometry (iii)).

From three detected decay chains, the half-life of  $^{269}\text{Hs}$  was determined to  $11^{+15}_{-4}$  s [Hof96, Hof00]. Therefore, only the three events attributed to  $^{269}\text{Hs}$  were used for the evaluation of  $\Delta H_{\text{ads}}(\text{HsO}_4)$ . The maximum of the deposition distribution of these three events was found at a temperature of  $(-44 \pm 6)$  °C.

Tab. 3-2 Parameters used for the MCS in this work.

Parameter		Value
Mass of the gases [g/mol]	He	4
	O <sub>2</sub>	32
Density of the gases at their boiling points [g/cm <sup>3</sup> ]	He	0.122
	O <sub>2</sub>	0.804
Density [g/cm <sup>3</sup> ]	OsO <sub>4</sub>	4.906
	HsO <sub>4</sub>	6.8 <sup>b</sup>
Molecular weight [g/mol]	<sup>172</sup> OsO <sub>4</sub>	236
	<sup>269</sup> HsO <sub>4</sub>	333
Half-life [s]	<sup>168</sup> Os	2.1
	<sup>172</sup> Os	19.2
	<sup>173</sup> Os	22.4
	<sup>269</sup> Hs	$11^{+15}_{-4}$
Period of oscillation of Si <sub>3</sub> N <sub>4</sub> [s]	Si <sub>3</sub> N <sub>4</sub>	$3.2 \cdot 10^{-13}$ a
	SiO <sub>2</sub>	$2 \cdot 10^{-13}$ a
Length of the column [m]		0.4183
Diameter of the column [m]	(i)	0.004053
	(ii)	0.0086
	(iii)	0.0015
Gas flow rate [ml/min]	(i)	1300
	(ii)	5853.9
	(iii)	178.08
Pressure inside the column [Pa]		760 torr

<sup>a</sup> calculated using the Lindemann-formula from [EiB00]

<sup>b</sup> estimated

For the evaluation of the adsorption enthalpy of  $^{269}\text{HsO}_4$  on the surface material, the MCS routine was slightly modified. The history of only three molecules was simulated and the position where they decayed was registered. If all three decays occurred in detector number 3 (as was the case in the experiment), the respective simulation was considered successful. For each adsorption enthalpy, 100'000 such simulations with 3 molecules each were carried out in steps of  $\Delta H_{\text{ads}}$  of 0.5 kJ/mol. In Figure 3-10, the fraction of successful simulations is given for each value of  $\Delta H_{\text{ads}}$ . Simulations were carried out using a half-life of 11 s (as was determined for  $^{269}\text{Hs}$ ), 7 s ( $T_{1/2} - 1\sigma$ ),

and 26 s ( $T_{1/2}+1\sigma$ ). The results were then superimposed according to the gaussian distribution: The weight of the 11 s-simulation was 1, the weights of the two other simulations were 0.607 ( $=e^{-0.5}$ ) which is the value of the gaussian distribution at 1  $\sigma$ . The result of this superposition is the dotted curve. The solid line is a gaussian fit to this curve. The mean value of the gaussian is -45.91 kJ/mol and the standard deviation  $\sigma=1.83$  kJ/mol. Therefore,  $\Delta H_{\text{ads}}(\text{HsO}_4)=(-46\pm 2)$  kJ/mol (68 % c.i.).

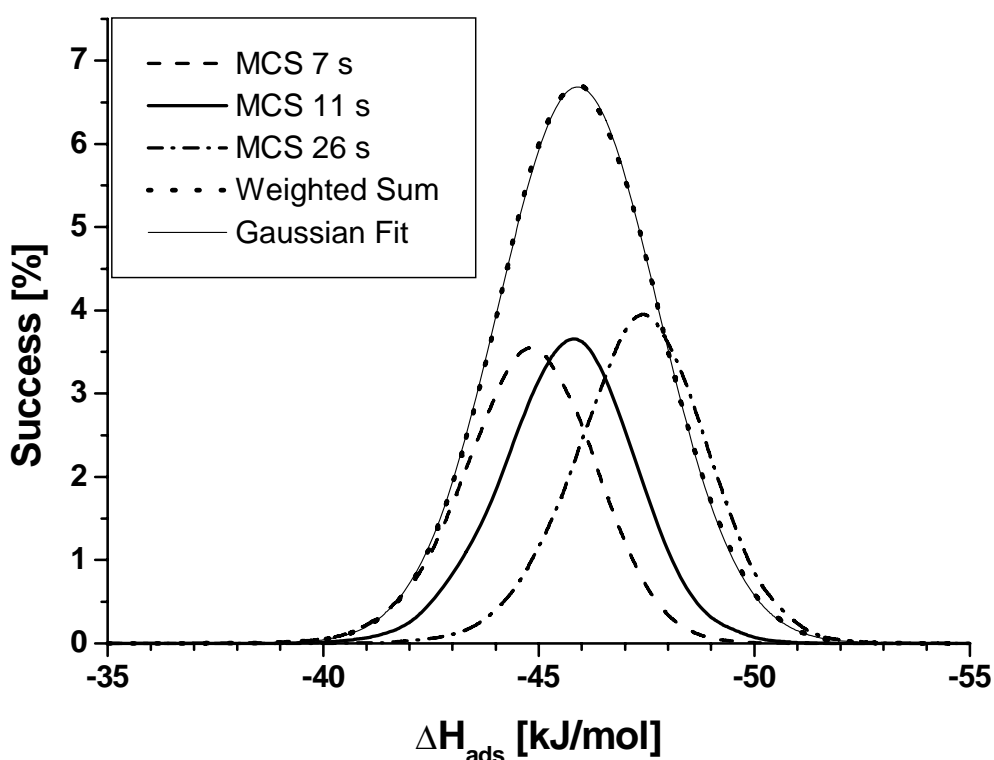


Fig. 3-10 Evaluation of the adsorption enthalpy of  $^{269}\text{HsO}_4$ . For explanations see text.

MCS with 100'000 events using the values -44, -46 and -48 kJ/mol for  $\Delta H_{\text{ads}}(\text{HsO}_4)$  were then performed and are shown with the experimental distribution of  $^{269}\text{Hs}$  in the COLD column (3 events in detector 3) in Figure 3-11.

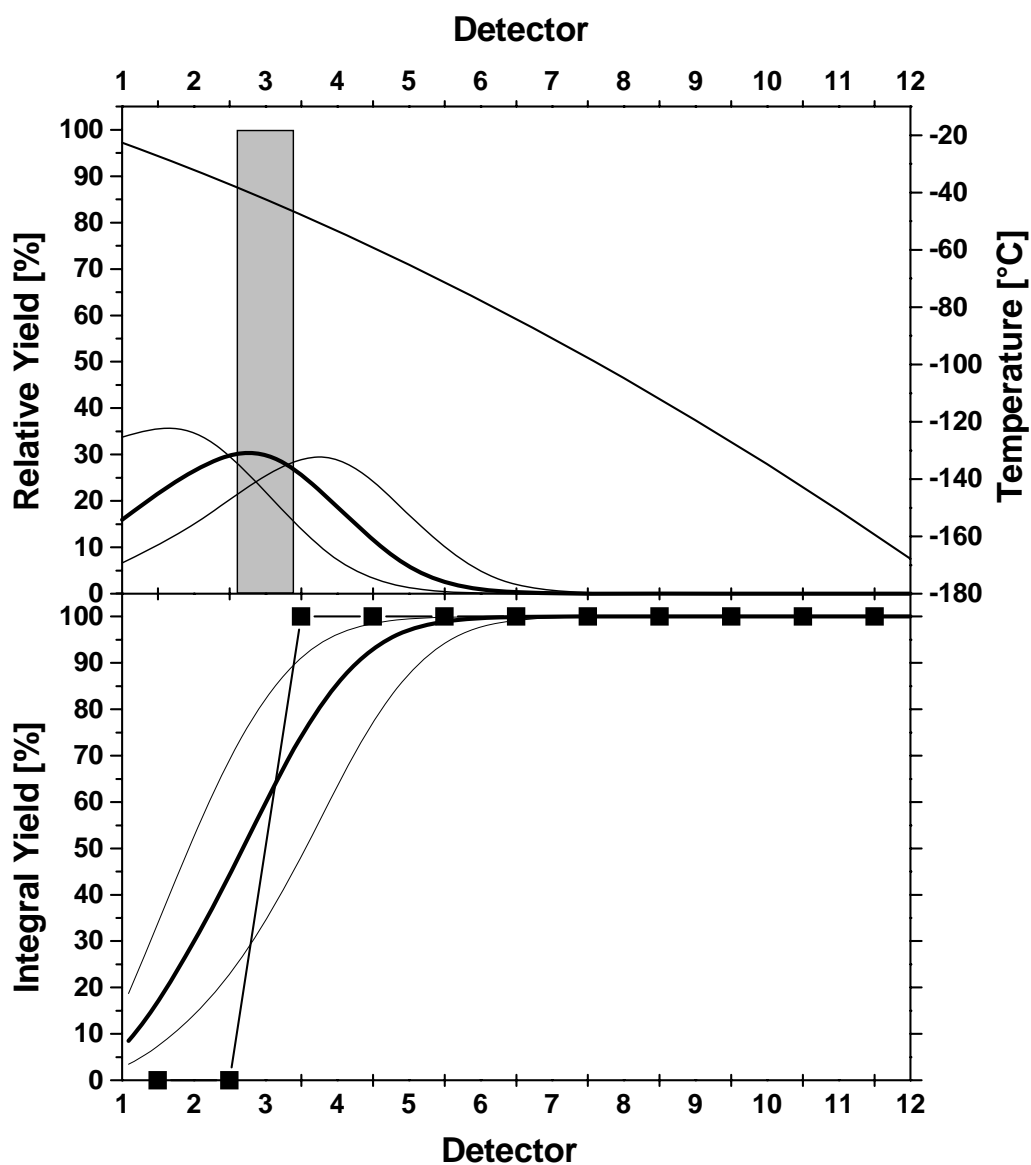


Fig. 3-11 Results of the MCS of  $^{269}\text{HsO}_4$ . Shown are the TC in the upper panel and the integrated TC in the lower panel. Experimental result: gray bar (upper panel) and black squares (lower panel). In the upper panel, the temperature gradient is indicated (right hand scale). The result of the MCS using  $\Delta H_{\text{ads}} = -46$  kJ/mol is represented by the thick solid line, thin solid lines indicate the uncertainty of  $\pm 2$  kJ/mol.

### 3.4.2 Model of mobile adsorption

The application of the model of mobile adsorption [EiB82], a thermodynamic model which describes the adsorption as a transition of a monatomic gas with three transitional degrees of freedom into the adsorbed state with two translational and one vibrational degrees of freedom, is an independent way to evaluate  $\Delta H_{\text{ads}}$  of a species on a column material. The model, as well as its limitations are discussed in detail in [EiB82]. In order to verify the data obtained with the Monte Carlo simulations,  $\Delta H_{\text{ads}}$  was calculated for  $\text{HsO}_4$  and for  $\text{OsO}_4$  using the same three different geometries of the chromatography column. The following parameters were used:

Tab. 3-3 Parameters used for the evaluation of  $\Delta H_{\text{ads}}$  of  $\text{OsO}_4$  and  $\text{HsO}_4$  applying the model of mobile adsorption.

Parameter	$^{172}\text{OsO}_4$	$^{269}\text{HsO}_4$
Standard temperature [K]	298	298
Start temperature [K]	250	250
Deposition temperature [K]	191±7	229±6
Oscillation period of the surface [s] <sup>a</sup>	$3.2 \cdot 10^{-13}$	$3.2 \cdot 10^{-13}$
Molar mass [g/mol]	236	333
Temperature gradient [K/m]:		
Detectors 2-4		-305
Detectors 5-7	-354	
Column diameter [m]	(i) <sup>b</sup>	0.004053
	(ii)	0.0086
	(iii)	0.0015
Gas flow rate [m <sup>3</sup> /s]	(i)	$2.1666 \cdot 10^{-5}$
	(ii)	$9.7565 \cdot 10^{-5}$
	(iii)	$2.968 \cdot 10^{-6}$
Pressure in the column [Pa]	101325	101325
Experiment duration [s] <sup>c</sup>	27.7	$16^{+22}_{-6}$ <sup>d</sup>

<sup>a</sup> calculated using the Lindemann-formula from [EiB00]

<sup>b</sup> geometry used (cf. Chapter 3.4.1)

<sup>c</sup> lifetime of the nuclide

<sup>d</sup> calculated from three measured lifetimes of [Hof96, Hof00]; uncertainties according to [Schm84]

For both compounds,  $\Delta H_{\text{ads}}$  was evaluated using the three different geometries described in Chapter 3.4.1 which are denoted with (i)-(iii). The gradient used was calculated for the region where deposition of the respective

compound was detected, i.e. detectors 2-4 for HsO<sub>4</sub> and detectors 5-7 for OsO<sub>4</sub>. In Table 3-4, the results are summarized.

Tab. 3-4 Evaluated adsorption enthalpies using the model of mobile adsorption including uncertainties of the deposition temperature (OsO<sub>4</sub>, HsO<sub>4</sub>) and the half-life (<sup>269</sup>HsO<sub>4</sub>). (1σ errors are given)

Geometry used	$\Delta H_{\text{ads}}(\text{OsO}_4)$ [kJ/mol]	$\Delta H_{\text{ads}}(\text{HsO}_4)$ [kJ/mol]
(i)	-39.8±1.5	-46.8±1.9
(ii)	-41.1±1.5	-48.3±2.0
(iii)	-38.2±1.5	-44.9±1.9

The entropy of adsorption  $\Delta S_{\text{ads}}$  on silicon nitride was calculated according to model of mobile adsorption (eq. 12 in [EiB82]) to -168.4 J/mol·K.

The difference in  $\Delta H_{\text{ads}}$  of OsO<sub>4</sub> and HsO<sub>4</sub> is about 7 kJ/mol, independent of the geometry used. The results are also in close agreement with those obtained by the MCS method and confirm the validity of the geometry (iii) used.

The half-life of <sup>270</sup>Hs can be estimated as similar to that of <sup>269</sup>Hs from the observed deposition distribution (one event in Detector 2 and one in Detector 4) which is similar to that of <sup>269</sup>Hs (three events in Detector 3).

---

### 3.5 Chemical investigation of hassium (element 108)

Ch.E. Düllmann<sup>1,2</sup>, W. Bröchle<sup>3</sup>, R. Dressler<sup>2</sup>, K. Eberhardt<sup>4</sup>, B. Eichler<sup>2</sup>, R. Eichler<sup>3</sup>, H.W. Gäggeler<sup>1,2</sup>, T.N. Ginter<sup>5</sup>, F. Glaus<sup>2</sup>, K.E. Gregorich<sup>5</sup>, D.C. Hoffman<sup>5,6</sup>, E. Jäger<sup>3</sup>, D.T. Jost<sup>2</sup>, U.W. Kirbach<sup>5</sup>, D.M. Lee<sup>5</sup>, H. Nitsche<sup>5,6</sup>, J.B. Patin<sup>5,6</sup>, V. Pershina<sup>3</sup>, D. Piguet<sup>2</sup>, Z. Qin<sup>7</sup>, M. Schädel<sup>3</sup>, B. Schausten<sup>3</sup>, E. Schimpf<sup>3</sup>, H.-J. Schött<sup>3</sup>, S. Soverna<sup>1,2</sup>, R. Sudowe<sup>5</sup>, P. Thörle<sup>4</sup>, S.N. Timokhin<sup>8</sup>, N. Trautmann<sup>4</sup>, A. Türler<sup>9</sup>, A. Vahle<sup>10</sup>, G. Wirth<sup>3</sup>, A.B. Yakushev<sup>8</sup>, P.M. Zielinski<sup>5</sup>

<sup>1</sup>Departement für Chemie und Biochemie, Universität Bern, CH-3012 Bern, Switzerland

<sup>2</sup>Paul Scherrer Institut, CH-5232 Villigen, Switzerland

<sup>3</sup>Gesellschaft für Schwerionenforschung mbH, D-64291 Darmstadt, Germany

<sup>4</sup>Institut für Kernchemie, Universität Mainz, D-55099 Mainz, Germany

<sup>5</sup>Nuclear Science Division, Lawrence Berkeley National Laboratory, Berkeley, California 94720

<sup>6</sup>Department of Chemistry, University of California, Berkeley, CA 94720-1460

<sup>7</sup>Institute of Modern Physics, Chinese Academy of Sciences, Lanzhou 730000, P.R. China

<sup>8</sup>Flerov Laboratory of Nuclear Reactions, Joint Institute for Nuclear Research, 141980 Dubna, Moscow Region, Russia

<sup>9</sup>Institut für Radiochemie, Technische Universität München, D-85748 Garching, Germany

<sup>10</sup>Research Center Rossendorf e.V., D-01314 Dresden, Germany

Accepted for publication in:

*Nature* (2002)

The periodic table provides a classification of the chemical properties of the elements. However, for the heaviest elements, the transactinides, this role of the periodic table reaches its limits because increasingly strong relativistic effects on the valence electron shells can induce deviations from known trends in chemical properties<sup>1-4</sup>. In the case of the first two transactinides, elements 104 and 105, relativistic effects are indeed influencing their chemical properties<sup>5</sup>, while elements 106 and 107 both behave as expected from their position within the periodic table<sup>6,7</sup>. Here we report the chemical separation and characterization of only seven detected atoms of element 108 (hassium, Hs), which were generated as isotopes <sup>269</sup>Hs (refs. 8,9) and <sup>270</sup>Hs (ref. 10) in the fusion reaction between <sup>26</sup>Mg and <sup>248</sup>Cm. The hassium atoms are immediately oxidized to a highly volatile oxide, presumably HsO<sub>4</sub>, for which we determine an enthalpy of adsorption on our detector surface that is comparable to the adsorption enthalpy determined under identical conditions for the osmium oxide OsO<sub>4</sub>. These results provide evidence that the chemical properties of hassium and its lighter homologue osmium are similar, thus confirming that hassium exhibits properties as expected from its position in group 8 of the periodic table.

The discovery of Hs was reported in 1984 (ref. 11) with the identification of the nuclide <sup>265</sup>Hs with a half-life of  $T_{1/2} = 1.5$  ms (refs. 11,12). In 1996, the much longer-lived isotope <sup>269</sup>Hs, with a half-life of about 10 s, was observed in the  $\alpha$ -decay chain of <sup>277</sup>112 (ref. 8). Recently, evidence for the existence of the neighboring nuclide <sup>270</sup>Hs was found and a half-life of about 4 s deduced from its measured  $\alpha$ -decay energy<sup>10</sup>. The latter two Hs isotopes might be sufficiently long-lived to allow their chemical characterization. Suitable reactions for their direct production are <sup>248</sup>Cm(<sup>26</sup>Mg, 5,4n)<sup>269,270</sup>Hs, for which formation cross sections of a few picobarn have been estimated<sup>13</sup>.

The periodic table suggests that Hs is a member of group 8 and thus chemically similar to its lighter homologues ruthenium (Ru) and osmium (Os), which are known to form highly volatile tetroxides. Therefore, Hs is expected to also form a very volatile tetroxide (HsO<sub>4</sub>) suitable for gas-phase

---

isolation<sup>1,14-16</sup>, even though two earlier attempts to chemically identify Hs in the tetroxide form proved not successful<sup>17,18</sup>.

Fully relativistic density functional calculations<sup>19</sup> for the tetroxides of the group 8 elements indicated that the electronic structure of HsO<sub>4</sub> is very similar to that of OsO<sub>4</sub>, with covalent bonding being somewhat more pronounced in the former. The stability of the gaseous tetroxides was found<sup>19</sup> to increase in the order RuO<sub>4</sub><OsO<sub>4</sub><HsO<sub>4</sub>, in agreement with extrapolations within group 8 of the periodic table<sup>20</sup>. The density functional calculations, in conjunction with a surface interaction model, suggest adsorption enthalpies of HsO<sub>4</sub> and OsO<sub>4</sub> on a quartz surface of (-35.9±1.5) kJ mol<sup>-1</sup> and (-38.0±1.5) kJ mol<sup>-1</sup>, respectively. Extrapolations of the volatility of group 8 tetroxides suggest almost identical adsorption enthalpies of (-46±15) kJ mol<sup>-1</sup> and (-45±15) kJ mol<sup>-1</sup> for HsO<sub>4</sub> and OsO<sub>4</sub>, respectively, while a physisorption model yields identical values of (-47±11) kJ mol<sup>-1</sup> for both tetroxides. Overall, the theoretical values suggest fairly similar adsorption behavior for HsO<sub>4</sub> and OsO<sub>4</sub> on quartz. Although the present experiment uses detectors covered with a silicon nitride layer, we expect a direct analogy between theory and experiment because we observed comparable adsorption interactions of OsO<sub>4</sub> with quartz and silicon nitride.

The expected high volatility of group 8 tetroxides allows excellent separation from heavy actinides and lighter transactinides as well as from Pb, Bi and Po, which is important because several isotopes of these elements are formed with high yield as byproducts of the nuclear fusion reaction. These nuclides often decay via emission of  $\alpha$ -particles and, therefore, severely interfere with the unambiguous detection of the nuclear decay of the investigated Hs nuclide.

On-line investigations of Os oxides have already been conducted earlier<sup>15,21,22</sup>. Using the In situ Volatilization and On-line detection apparatus (IVO) carrier-free <sup>173</sup>OsO<sub>4</sub> (T<sub>1/2</sub>=22.4 s) could be separated and detected with an overall efficiency of (40±10)%. Decontamination from Po ( $\geq 2 \cdot 10^4$ ) was excellent<sup>21</sup>.

---

The experimental set-up, schematically shown in Figure 3-12, involves mounting the  $^{248}\text{Cm}$  target<sup>23</sup> on a rotating wheel and bombarding it with up to  $8 \times 10^{12}$   $^{26}\text{Mg}^{5+}$  particles per second, delivered by the UNILAC accelerator at the Gesellschaft für Schwerionenforschung mbH. The particle beam first passed through a rotating 3 segment  $3.68 \text{ mg/cm}^2$  Be vacuum window which allowed for a pressure up to 1.3 atm in the recoil chamber. The 192.7 MeV beam energy delivered by the UNILAC resulted in  $^{26}\text{Mg}$  projectile energies of 143.7-146.8 MeV inside the  $^{248}\text{Cm}$  target. Nuclear reaction products recoiling from the target were thermalized in the gas volume (34 ml) of the IVO device<sup>21</sup> flushed with dry (measured water vapor concentration <1 ppm) 1.2 l/min helium (He) and 100 ml/min oxygen ( $\text{O}_2$ ). The reaction products were transported with the carrier gas through a 30 cm long quartz column (i.d. 4 mm) containing a quartz wool plug at a distance of 6.5 cm from the recoil chamber. This plug was heated to 600 °C and served as a filter for aerosol particles and provided a surface to complete the oxidation reaction of Os and Hs to their tetroxides, which were further transported through a 10 m long perfluoroalkoxy (PFA) Teflon<sup>®</sup> capillary (i.d. 2 mm) to the detection system. The capillary was installed inside of a polyamide (PA) tube flushed with dry  $\text{N}_2$ .

Using gas phase adsorption thermochromatography<sup>24</sup>, the temperature at which  $\text{HsO}_4$  deposits was measured, using a chromatographic column along which a stationary negative temperature gradient is maintained. The chromatographic column, the Cryo On-Line Detector (COLD), also served as detection system for the identification of decaying atoms of  $^{269,270}\text{Hs}$ . COLD consists of 12 pairs of silicon PIN-photodiodes of  $1 \times 3 \text{ cm}^2$  active area mounted at a distance of 1.5 mm via two spacers made from silicon. PIN diodes are well suited for detection of  $\alpha$ -particles or fission fragments. The diode pairs were installed inside of a copper bar. A temperature gradient from -20 °C to -170 °C was established along the detector array. The efficiency for detecting a single  $\alpha$ -particle emitted by a species adsorbed within the detector array was 77%. To avoid formation of ice layers on the detector surfaces, the whole device was placed inside a vacuum tight housing flushed with dry  $\text{N}_2$ .

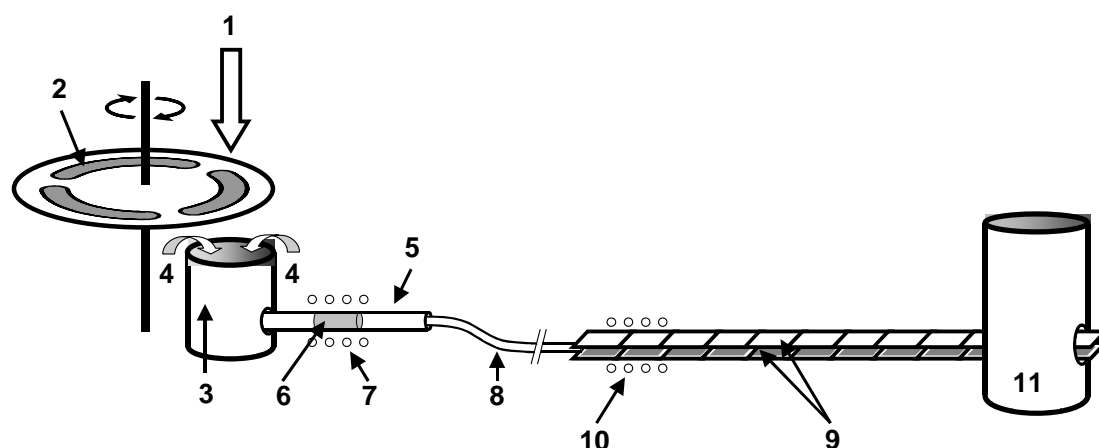


Fig. 3-12. **Schematic drawing of the IVO-COLD set-up used to produce and isolate Hs isotopes in form of the volatile  $\text{HsO}_4$ .**

The  $^{26}\text{Mg}$ -beam (1) passes through the rotating vacuum window and  $^{248}\text{Cm}$ -target (2) assembly. The target consisted of three banana-shaped segments ( $1.9\text{ cm}^2$  area each) covered with  $239\text{ }\mu\text{g}/\text{cm}^2$ ,  $730\text{ }\mu\text{g}/\text{cm}^2$ , and  $692\text{ }\mu\text{g}/\text{cm}^2$   $^{248}\text{Cm}$ , respectively. The  $^{248}\text{Cm}$  (isotopic composition  $^{246}\text{Cm}$ : 4.2%;  $^{248}\text{Cm}$ : 95.8%) was deposited on  $2.82\text{ mg}/\text{cm}^2$  beryllium (Be) backings by molecular plating. The target-window assembly rotated in the adjacent gas volume with 2000 rpm and was synchronized with the beam macrostructure of the accelerator in order to distribute each 6-ms beam pulse evenly over one target segment. In the fusion reaction  $^{269,270}\text{Hs}$  nuclei are formed which recoil out of the target into a gas volume (3) and are flushed with a  $\text{He}/\text{O}_2$  mixture (4) out of the chamber. The gas was passed through a cartridge containing  $\text{P}_2\text{O}_5$  as a drying agent before injecting it into IVO. This way, the water vapor concentration was reduced to a measured value of  $<1\text{ ppm}$  throughout the experiment. The gas was injected into a quartz column (5) containing a quartz wool plug (6) heated to  $600\text{ }^\circ\text{C}$  by an oven (7). There, Hs is converted to  $\text{HsO}_4$  which is volatile at room temperature and transported with the gas flow through a 10 m long perfluoroalkoxy (PFA) Teflon<sup>®</sup> capillary (8) to the COLD detector array registering the nuclear decay ( $\alpha$  and spontaneous

---

fission) of the Hs nuclides. The array consists of 24 detectors arranged in 12 pairs (9). A temperature gradient was established along the detector array by means of a thermostat (10) at the entrance and a liquid nitrogen cryostat (11) at the exit. The temperature was monitored by 5 thermocouples installed along the copper bar. Depending on the volatility of HsO<sub>4</sub>, the molecules adsorb at a characteristic temperature.

COLD is an improved version of a previous set-up called the Cryo-Thermochromatography Separator (CTS) developed at Berkeley<sup>22</sup>.

The detectors of the COLD array were on-line calibrated with  $\alpha$ -decaying <sup>219</sup>Rn and its daughters <sup>215</sup>Po and <sup>211</sup>Bi using a <sup>227</sup>Ac source. The determined energy resolution was 50-70 keV (FWHM) for detectors 1 through 8 and 80-110 keV (FWHM) for detectors 9 through 12.

The proper functioning of the IVO-COLD system was checked at the beginning and after the end of the Hs experiment by mounting a 800  $\mu\text{g}/\text{cm}^2$  <sup>152</sup>Gd (32% enr.) target to produce short-lived Os isotopes in the reaction <sup>152</sup>Gd(<sup>26</sup>Mg, 6n)<sup>172</sup>Os. The beam intensity was  $1 \times 10^{12} \text{ s}^{-1}$  and the beam energy in the middle of the target 153 MeV. All other experimental parameters including gas composition and flow rate were identical to those of the Hs experiment. In the COLD detector array the  $\alpha$ -decay of <sup>172</sup>Os was registered. <sup>172</sup>Os has a half-life of 19.2 s and a 1.0%  $\alpha$ -decay branch with  $E_{\alpha} = 5.10 \text{ MeV}$ .

The experiment to produce Hs isotopes lasted 64.2 h during which a total of  $1.0 \times 10^{18}$  <sup>26</sup>Mg-particles passed through the target. Only  $\alpha$ -lines originating from <sup>211</sup>At, <sup>219,220</sup>Rn and their decay products were identified. While <sup>211</sup>At and its decay product <sup>211</sup>Po were deposited mainly in the first two detectors, <sup>219,220</sup>Rn and their decay products accumulated in the last three detectors, where the temperature was sufficiently low to partly adsorb Rn. One side of detector pair 1 did not operate due to a technical failure and, therefore, this detector unit was excluded from the data analysis. During the experiment, 7 correlated decay chains were detected (see Figure 3-13). All correlated  $\alpha$ -decay chains were observed in detectors 2 through 4 and assigned to the

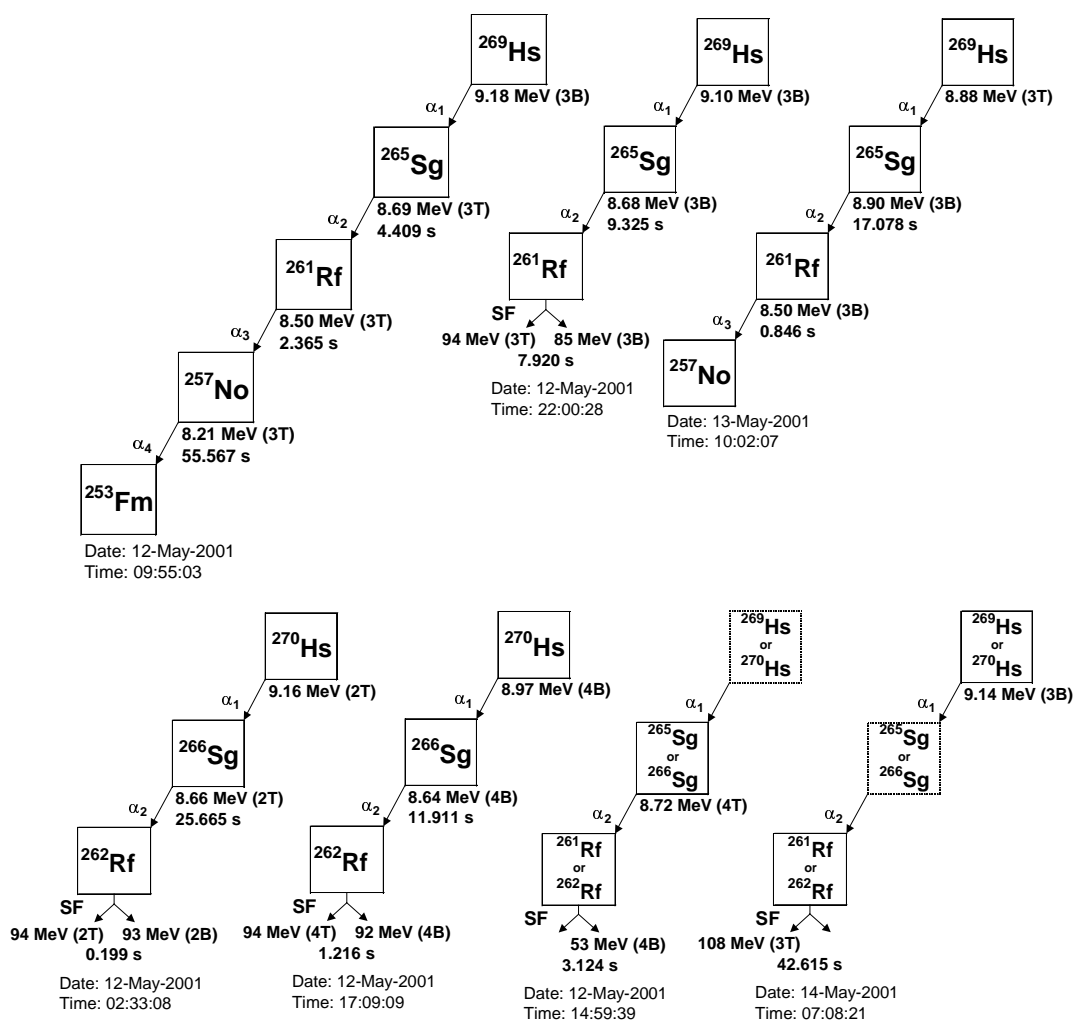


**Fig. 3-13 The seven nuclear decay chains originating from Hs isotopes that were detected in the course of the experiment allowing an unambiguous identification of hassium after chemical separation.**

Indicated are the energies of  $\alpha$ -particles and fission fragments in megaelectronvolts (MeV) and the lifetimes in seconds (s). The detector in which the decay was registered is indicated in parenthesis where T stands for top detector and B for bottom detector. For each chain the date and time of its registration are given. The lifetime of the mother isotope could not be determined with the applied thermochromatography technique since the deposition time is not measured.

decay of  $^{269}\text{Hs}$  or  $^{270}\text{Hs}$ . The characteristics of the first three decay chains agree well with literature data<sup>8,9</sup> on  $^{269}\text{Hs}$  and its daughter nuclides, while two other decay chains can be attributed<sup>10</sup> to the decay of  $^{270}\text{Hs}$ . The last two decay chains were incomplete and a definite assignment to  $^{269}\text{Hs}$  or  $^{270}\text{Hs}$  could not be made. No additional three-member decay chains within  $\leq 300$  s were registered in detectors 2 through 10. The background count-rate of  $\alpha$ -particles with energies between 8.0 and 9.5 MeV was about  $0.6 \text{ h}^{-1}$  per detector, leading to very low probabilities of  $\leq 7 \times 10^{-5}$  and  $\leq 2 \times 10^{-3}$  for any of the first five chains and any of the last two chains, respectively, being of random origin. In addition, four uncorrelated fission fragments with energies  $> 50$  MeV were registered in detectors 2 through 4. All other detectors registered no fission fragments, except for one fission fragment being observed in the operating side of detector 1.

As depicted in Figure 3-14, the  $\alpha$ -decay of one Hs atom was registered in detector 2, the decay of four atoms in detector 3 and the decay of two atoms in detector 4. The maximum of the Hs distribution was found for a temperature of  $(-44 \pm 6) \text{ }^\circ\text{C}$ . The deposition distribution of  $\text{OsO}_4$  measured before and after the experiment revealed a maximum in detector 6 at  $(-82 \pm 7) \text{ }^\circ\text{C}$ . The adsorption enthalpy ( $\Delta H_{\text{ads}}$ ) of the compound on the stationary phase is extracted from the measured deposition distribution by using Monte Carlo simulations of the trajectories of single molecules as they move along the column under real experimental conditions<sup>25</sup>. The only free parameter in the simulations is  $\Delta H_{\text{ads}}$ , but the half-life of the nuclide is a crucial parameter. For this reason, and because the half-life of  $^{270}\text{Hs}$  has not yet been measured, only decays assigned to  $^{269}\text{Hs}$  were used to evaluate the adsorption enthalpy of the compound on the silicon nitride surface. The results that best reproduce the experimental data are shown in Figure 3-14 (solid lines) and suggest a value of  $\Delta H_{\text{ads}} = (-46 \pm 2) \text{ kJ mol}^{-1}$  (68% c.i.), which was inferred using a  $T_{1/2}$  value of  $11^{+15}_{-4} \text{ s}$  for  $^{269}\text{Hs}$  (refs. 8,9). The given uncertainty reflects the width of the measured deposition peak. The adsorption enthalpy of  $\text{OsO}_4$  on silicon nitride deduced from this experiment was  $(-39 \pm 1) \text{ kJ mol}^{-1}$ , which is in good agreement with the adsorption enthalpy obtained in earlier investigations using quartz surfaces<sup>15,21,22</sup>.

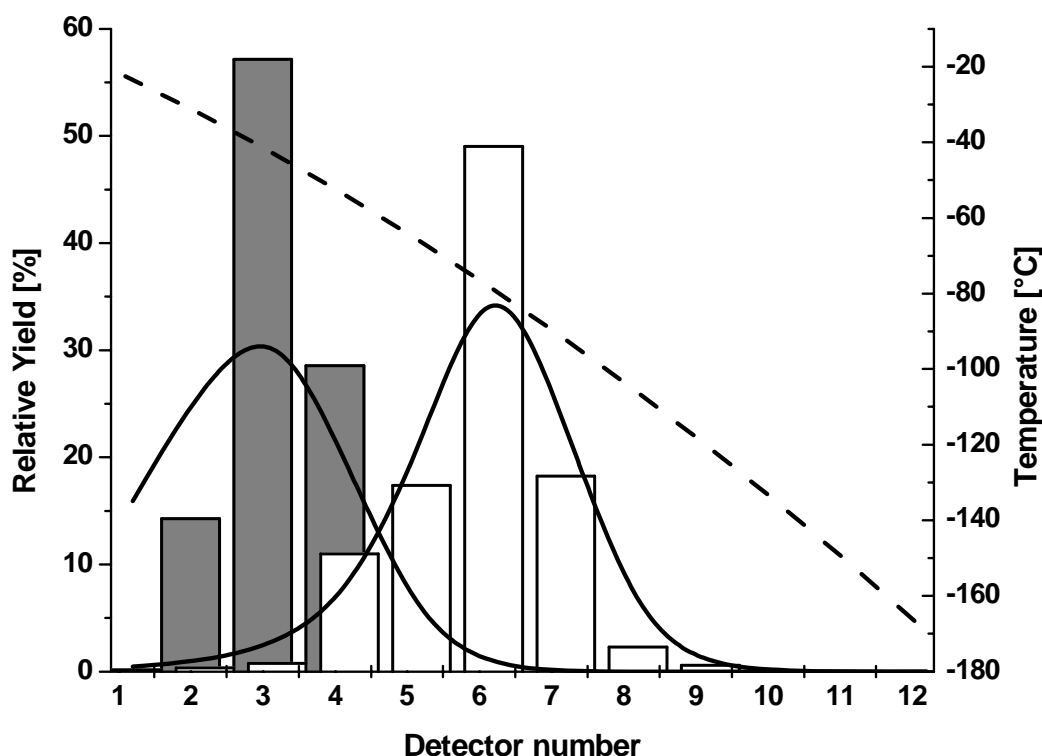


Fig. 3-14 **Merged thermochromatogram of HsO<sub>4</sub> and OsO<sub>4</sub>.**

Indicated are the relative yields of HsO<sub>4</sub> and OsO<sub>4</sub> for each of the 12 detector pairs. Measured values are represented by bars: HsO<sub>4</sub>: dark grey; OsO<sub>4</sub>: white. For Hs, the following distribution was measured: <sup>269</sup>Hs: 3 events (all in detector 3); <sup>270</sup>Hs: 2 events (one in detector 2 and one in detector 4); Hs (isotope unknown): 2 events (one in detector 3 and one in detector 4). For Os, the distribution of  $1 \times 10^5$  events of <sup>172</sup>OsO<sub>4</sub> is given. The dashed line indicates the temperature profile (right-hand scale). The maxima of the deposition distributions were evaluated as  $(-44 \pm 6)$  °C for HsO<sub>4</sub> and  $(-82 \pm 7)$  °C for OsO<sub>4</sub> where the uncertainties indicate the temperature range covered by the detector which registered the maximum of the deposition distribution. Solid lines represent results of a Monte Carlo simulation of the migration process of the species along the column with standard adsorption enthalpies of  $-46.0 \text{ kJ mol}^{-1}$  for <sup>269</sup>HsO<sub>4</sub> and  $-39.0 \text{ kJ mol}^{-1}$  for <sup>172</sup>OsO<sub>4</sub>.

The experimentally derived adsorption enthalpy of HsO<sub>4</sub> is thus lower than that of OsO<sub>4</sub>, while the predictions suggest either similar values<sup>20</sup> or a slightly

higher value<sup>19</sup> for HsO<sub>4</sub>. However, the theoretical values and experimental values have associated uncertainties. Moreover, the low value of the  $\Delta H_{\text{ads}}$  determined for the hassium oxide species clearly suggests that it is HsO<sub>4</sub>, given that by analogy with the known properties of the Os oxides, other Hs oxides are all expected to be less volatile and unable to reach the detection system. The observed formation of a very volatile Hs molecule, presumably HsO<sub>4</sub>, in a mixture of oxygen and helium thus provides strong qualitative evidence that Hs is an ordinary member of group 8 of the periodic table that behaves similar to its lighter homologue Os.

### Acknowledgements

We thank the staff of the Laboratory for Micro- and Nanotechnology at PSI for manufacturing the PIN-diode sandwiches for the COLD array. We thank the staff of the GSI UNILAC for providing stable, highly intense beams of <sup>26</sup>Mg as well as the GSI target laboratory for Be foils for the vacuum windows. The support from the European Commission Institute for Transuranium Elements, Karlsruhe, for long-term storage of <sup>252</sup>Cf and the chemical separation of <sup>248</sup>Cm is highly appreciated. These studies were supported in part by the Swiss National Science Foundation and the Chemical Sciences Division of the Office of Basic Energy Sciences, U.S. Department of Energy.

### References

1. Fricke, B. Superheavy elements. *Structure and bonding* **21**, 90-144 (1975).
2. Pyykkö, P. & Desclaux, J.-P. Relativity and the periodic system of elements. *Acc. Chem. Res.* **12**, 276-281 (1979).
3. Pershina, V.G. Electronic structure and properties of the transactinides and their compounds. *Chem. Rev.* **96**, 1977-2010 (1996).
4. Schwerdtfeger, P. & Seth, M. Relativistic effects of the superheavy elements. In *Encyclopedia of Computational Chemistry* Vol. **4**, 2480-2499 (Wiley, New York, 1998).

- 
5. Kratz, J. V. in Heavy Elements and Related New Phenomena Ch. 4 (eds Greiner, W. & Gupta, R. K.) 129-193 (World Scientific, Singapore, 1999).
  6. Schädel, M. *et al.* Chemical properties of element 106 (seaborgium). *Nature* **388**, 55-57 (1997).
  7. Eichler, R. *et al.* Chemical characterization of bohrium (element 107). *Nature* **407**, 63-65 (2000).
  8. Hofmann, S. *et al.* The new element 112. *Z. Phys. A* **354**, 229-230 (1996).
  9. Hofmann, S. & Münzenberg, G. The discovery of the heaviest elements. *Rev. Mod. Phys.* **72**, 733-766 (2000).
  10. Türler, A. *et al.* Decay properties of  $^{269}\text{Hs}$  and evidence for the new nuclide  $^{270}\text{Hs}$ . *Eur. Phys. J. A* (submitted).
  11. Münzenberg, G. *et al.* The identification of element 108. *Z. Phys. A* **317**, 215-216 (1984).
  12. Hofmann, S. *et al.* Production and decay of  $^{269}\text{110}$ . *Z. Phys. A* **350**, 277-280 (1995).
  13. Schädel, M. & Hofmann, S. Prospects for the discovery of new elements. *J. Radioanal. Nucl. Chem.* **203**, 283-300 (1996).
  14. Bächmann, K. & Hoffmann, P. Chemische Probleme bei der Darstellung überschwerer Elemente durch Kernreaktionen. *Radiochim. Acta* **15**, 153-163 (1971).
  15. Domanov, V.P. & Zvara, I. Continuous-flow thermochromatographic separation of unsupported radioisotopes of platinum elements in a stream of air from nuclear reaction products in an accelerator heavy-ion beam. Translated from *Radiokhimiya* **26**, 770-778 (1984).

- 
16. Zude, F., Fan, W., Trautmann, N., Herrmann, G. & Eichler, B. Thermochemistry of platinum elements in oxygen: Radiochemical studies of the behavior of rhodium, palladium, osmium and platinum. *Radiochim. Acta* **62**, 61-63 (1993).
17. Zhuikov, B.L., Kruz, H. & Zvara, I. Possibilities of chemical identification of short-lived isotopes of element 108. Report P7-86-322, Joint Institut for Nuclear Research, JINR, Dubna, Soviet Union, 1986, p.26 (in Russian).
18. Dougan, R.J., Moody, K.J., Hulet, E.K. & Bethune, G.R. OSCAR: An apparatus for on-line gas-phase separations. FY87 Annual Report UCAR 10062/87, Lawrence Livermore National Laboratory LLNL, Nuclear Chemistry Division, Livermore, USA, 1987, p. 4-17.
19. Pershina, V., Bastug, T., Fricke, B. & Varga, S. The electronic structure and properties of group 8 oxides  $MO_4$ , where  $M=Ru, Os$ , and element 108, Hs. *J. Chem. Phys.* **115**, 792-799 (2001)
20. Düllmann, Ch.E., Eichler, B., Eichler, R., Gäggeler, H.W. & Türler, A. On the stability and volatility of group 8 tetroxides,  $MO_4$  ( $M=ruthenium, osmium, and hassium (Z=108)$ ). *J. Phys. Chem. B* **106**, 6679-6684 (2002).
21. Düllmann, Ch.E. *et al.* IVO, a device for in situ volatilization and on-line detection of products from heavy ion reactions. *Nucl. Instrum. Meth.* **A479**, 631-639 (2002).
22. Kirbach, U.W. *et al.* The Cryo-Thermochemical Separator (CTS): A new rapid separation and  $\alpha$ -detection system for on-line chemical studies of highly volatile osmium and hassium ( $Z=108$ ) tetroxides. *Nucl. Instrum. Meth.* **A484**, 587-594 (2002).
23. Malmbeck, R. *et al.* Separation of  $^{248}Cm$  from a  $^{252}Cf$  neutron source for production of Cm targets. *Radiochim. Acta* **89**, 543-549 (2001).
24. Zvara I. Thermochemical method of separation of chemical elements in nuclear and radiochemistry. *Isotopenpraxis* **26**, 251-258 (1990).

- 
25. Zvara, I. Simulation of thermochromatographic processes by the Monte Carlo method. *Radiochim. Acta* **38**, 95-101 (1985).

---

**References of Chapter 3**

- [Buc91] Buck, B. *et al.* Ground state to ground state alpha decays of heavy even-even nuclei. *J. Phys. G.* **17**, 1223 (1991).
- [Dom84] Domanov, V.P. *et al.* Continuous-flow thermochromatographic separation of unsupported radioisotopes of platinum elements in a stream of air from nuclear reaction products in an accelerator heavy-ion beam. Translated from *Radiokhimiya* **26**, 770 (1984).
- [EiB82] Eichler, B. *et al.* Evaluation of the enthalpy of adsorption from thermochromatographical data. *Radiochim. Acta* **30**, 233 (1982).
- [EiB00] Eichler, B. *et al.* Electrochemical deposition of carrier-free radionuclides. *Radiochim. Acta* **88**, 475 (2000).
- [Fre24] Frenkel, J. Theorie der Adsorption und verwandter Erscheinungen. *Z. Phys.* **26**, 117 (1924).
- [Hof96] Hofmann, S. *et al.* The new element 112. *Z. Phys. A* **354**, 229 (1996).
- [Hof00] Hofmann, S. *et al.* The discovery of the heaviest elements. *Rev. Mod. Phys.* **72**, 733 (2000).
- [Kir02] Kirbach, U.W. *et al.* The Cryo-Thermochromatographic Separator (CTS): A new rapid separation and  $\alpha$ -detection system for on-line chemical studies of highly volatile osmium and hassium ( $Z=108$ ) tetroxides. *Nucl. Instrum. Meth.* **A484**, 587 (2002).
- [Schl89] Schlepütz, F.W. TANDEM, the new data acquisition system at the Paul Scherrer Institute (PSI). *IEEE Trans. Nucl. Sci.* **36**, 1630 (1989).
- [Schm84] Schmidt, K.H. *et al.* Some remarks on the error analysis in the case of poor statistics. *Z. Phys. A* **316**, 19 (1984).
- [Tür96] Türler, A. Gas phase chemistry experiments with transactinide elements. *Radiochim. Acta* **72**, 7 (1996).
- [Zva85] Zvara, I. Simulation of thermochromatographic processes by the Monte Carlo method. *Radiochim. Acta* **38**, 95 (1985).

---

#### 4. On the stability and volatility of group 8 tetroxides, $\text{MO}_4$ (M=ruthenium, osmium, and hassium (Z=108))

Christoph E. Düllmann<sup>1,2</sup>, Bernd Eichler<sup>1</sup>, Robert Eichler<sup>2</sup>, Heinz W. Gäggeler<sup>1,2,\*</sup>, Andreas Türler<sup>2,\*\*</sup>

<sup>1</sup>Department for Chemistry and Biochemistry, Berne University, CH-3012 Berne, Switzerland

<sup>2</sup>Paul Scherrer Institute, CH-5232 Villigen, Switzerland

\*\*Present address: Institut für Radiochemie, Technische Universität München, D-85748 Garching, Germany

Published in:

*The Journal of Physical Chemistry B* **106**, 6679-6684 (2002).

Reproduced with permission from *The Journal of Physical Chemistry B* 106 (2002) 6679. Copyright 2002, American Chemical Society

---

**ABSTRACT**

Recently, an experiment to chemically characterize for the first time a compound of the transactinide element hassium (Hs, Z=108) has been performed. Based on the assumption that Hs will belong to group 8 of the periodic table and will thus be homologous to ruthenium (Ru) and osmium (Os), the presumably very volatile  $\text{HsO}_4$  was isolated by gas adsorption chromatography. The experiment allowed the determination of the enthalpy of adsorption ( $-\Delta H_a^{0(T)}$ ) of  $\text{HsO}_4$  on a silicon nitride surface.

In this work, the trend in standard enthalpies of sublimation ( $\Delta H_S^{0(298)}$ ) of group 8 element tetroxides established by Ru tetroxide and Os tetroxide was extrapolated to Hs tetroxide.  $\Delta H_S^{0(298)}(\text{HsO}_4)$  was found to be very similar to  $\Delta H_S^{0(298)}(\text{OsO}_4)$ . Based on an empirical correlation between the sublimation enthalpies and the enthalpies of adsorption of oxide (and oxyhydroxide) molecules on quartz surfaces  $-\Delta H_a^{0(T)}(\text{HsO}_4)$  was predicted to be  $(46 \pm 15)$   $\text{kJ}\cdot\text{mol}^{-1}$ . A trend for the values of the adsorption enthalpies of  $\text{RuO}_4 \approx \text{OsO}_4 \approx \text{HsO}_4$  was found.

A different theoretical approach makes use of the relation between the interaction distance of a physisorbed, non-polar molecule on a dielectric surface and the interaction energy. From literature values of the adsorption of noble gases on metal surfaces it was found that this distance is independent of the adsorbed species as well as of the adsorbent material. Using this universal interaction distance,  $-\Delta H_a^{0(T)}(\text{OsO}_4)$  was calculated only from molecular geometries of  $\text{OsO}_4$ , the polarizability and the first ionization potential and was found to agree with experimental results found in gas adsorption chromatography experiments.  $-\Delta H_a^{0(T)}$  of  $\text{RuO}_4$  and  $\text{HsO}_4$  were calculated using the same procedure; where no experimental values of molecular properties were available, these were extrapolated or published values obtained from density functional calculations were used.  $-\Delta H_a^{0(T)}(\text{HsO}_4) = (47 \pm 11)$   $\text{kJ}\cdot\text{mol}^{-1}$  is predicted, in agreement with the extrapolated value.

---

KEYWORDS: ruthenium tetroxide / osmium tetroxide / hassium tetroxide / gas chromatography / adsorption / thermochemical properties

## 4.1 Introduction

The experimental chemical characterization of transactinide elements ( $Z \geq 104$ ) is an extremely challenging task since these elements can only be produced at accelerators on a “one-atom-at-a-time” scale.<sup>1</sup> In addition, even the longest-lived known isotopes of these elements have half-lives of only a few minutes or seconds. Due to the minute production rates, experiments to investigate their chemical properties are very time consuming. To date, the heaviest chemically characterized element is bohrium (Bh,  $Z=107$ ).<sup>2</sup> In order to proceed to the next heavier element hassium (Hs,  $Z=108$ ) it is necessary to carefully evaluate the expected chemical stability of Hs containing molecules.

The first successful identification of three atoms of Hs after physical separation was reported in 1984 when the nuclide  $^{265}\text{Hs}$  ( $T_{1/2} = 1.55$  ms) was produced in the heavy ion induced fusion reaction of  $^{58}\text{Fe}$  and  $^{208}\text{Pb}$  at the Gesellschaft für Schwerionenforschung mbH in Darmstadt.<sup>3</sup> A much more long-lived isotope with mass number 269 was identified<sup>4</sup> in the  $\alpha$  decay chain of  $^{277}\text{112}$  in 1996. A half-life of about 10 s was measured<sup>4,5</sup> making this nuclide feasible for chemical investigations.

The elements in each group of the periodic table have a similar electronic structure and therefore exhibit similar chemical properties. Hs is expected to be a member of group 8 of the periodic table and should thus behave homologous to Os and partly also like Ru. Well-known volatile compounds of Ru and Os are their tetroxides. Hence, also for Hs the formation of a volatile tetroxide may be expected. Indeed, recently it was possible to show that in an oxygen containing gas a very volatile molecule of Hs, most likely  $\text{HsO}_4$ , could be produced.<sup>6</sup> The experiment yielded an adsorption enthalpy of  $-\Delta H_a^{0(\text{T})}(\text{HsO}_4) = (46 \pm 2) \text{ kJ} \cdot \text{mol}^{-1}$  on silicon nitride surfaces based on only 7 detected atoms. It was concluded that the interaction of  $\text{HsO}_4$  with a dielectric surface is significantly stronger than the one of  $\text{OsO}_4$ .<sup>6</sup> The influence of the surface material appeared to be negligible for physisorption processes on dielectric surfaces such as silicon oxides or nitrides as was concluded from

comparable adsorption enthalpies of OsO<sub>4</sub> on these two surfaces.<sup>6</sup> In order to interpret thermochemical data of transactinides it is instrumental to make predictions based on the knowledge of homologous compounds. One approach is to perform relativistic density functional calculations of molecular properties as was recently reported for group 8 tetroxides.<sup>7</sup> Application of semiempirical models for the interaction of HsO<sub>4</sub> with a quartz surface<sup>7</sup> predicted a sequence RuO<sub>4</sub>>OsO<sub>4</sub>≥HsO<sub>4</sub> for  $-\Delta H_a^{0(T)}$ .

In this work predictions on the stability and volatility, i.e. the sublimation enthalpy of oxide compounds of group 8 elements are made based on thermodynamical extrapolations. In a second part the adsorption behavior of tetroxide molecules of group 8 elements on quartz surface is predicted assuming physisorption on a dielectric surface. Finally, the predicted adsorption enthalpies are compared with experimental data.

## 4.2 Extrapolation of chemical properties from RuO<sub>4</sub> and OsO<sub>4</sub> to HsO<sub>4</sub>

Within the groups there exist trends in chemical properties that usually are followed when going from one period to the next one. As an example, the standard enthalpies of sublimation ( $\Delta H_S^{0(298)}$ ) of mononuclear oxides of d elements with the highest possible oxidation states of the metals exhibit trends for the elements of groups 4 through 8 (see Figure 4-1). The data depicted in Figure 4-1 are differences of the standard formation enthalpies of the solid and the gaseous species. The reason for the observed increasing sublimation enthalpies with atomic number is that the stability of the solid state increases more strongly than the stability of the gaseous state. However, this trend holds only for group 4, 5 and 6 oxides. For group 7 and 8 oxides  $\Delta H_S^{0(298)}$  seems to be independent of the atomic number. Based on this simple picture it is expected that  $\Delta H_S^{0(298)}$  of HsO<sub>4</sub> should be very similar to that of OsO<sub>4</sub> and RuO<sub>4</sub>.

The standard enthalpy of sublimation  $\Delta H_S^{0(298)}$  is a measure for the volatility of a compound. Gas phase experiments with carrier free amounts have clearly proven that excellent linear empirical correlations exist between  $\Delta H_S^{0(298)}$

values for a given class of compounds (e.g. oxides) and measured retention temperatures.<sup>8</sup> From the latter, adsorption enthalpies ( $-\Delta H_a^{0(T)}$ ) may be calculated and hence,  $\Delta H_s^{0(298)}$  and  $-\Delta H_a^{0(T)}$  can be directly linked.<sup>9</sup>

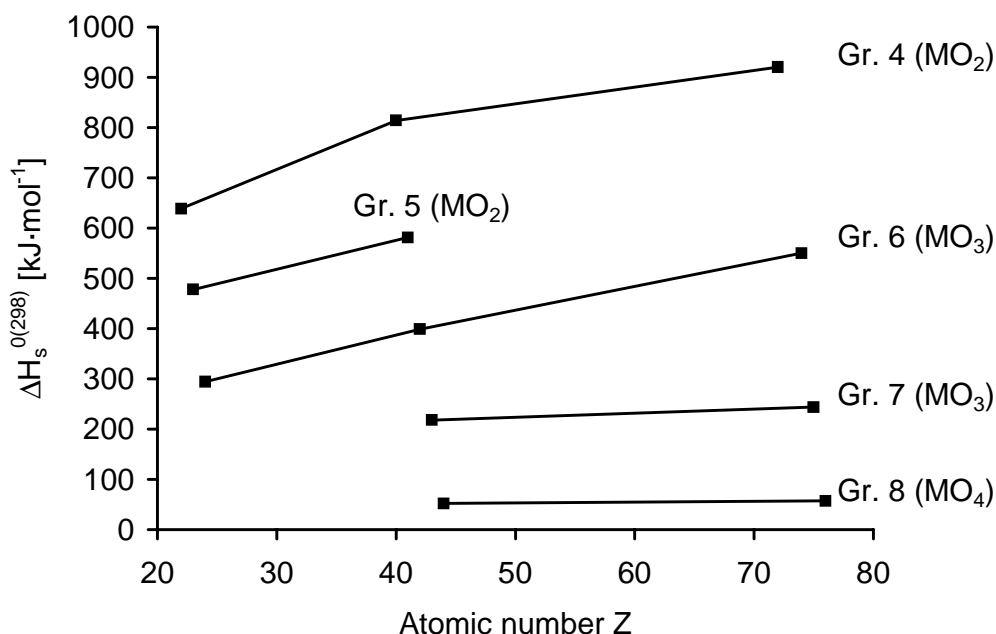


Fig. 4-1 Standard sublimation enthalpies calculated from standard formation enthalpies as a function of the atomic number of mononuclear d element oxides of groups 4 through 8 where the metal is in the highest possible oxidation state. Data from refs 30-36.

#### 4.2.1 Stability and volatility of oxides

Standard formation enthalpies and standard entropies of O, O<sub>2</sub>, Ru and Os and their oxides and some other physico-chemical data used in this work are summarized in Tables 4-1 and 4-2.

Empirical linear correlations were found between different thermochemical properties and molecular characteristics (e.g. molar volumes or radii) of compounds in several groups of the periodic table, e.g. groups 6 (including seaborgium (Sg, Z=106))<sup>10</sup> and 7 (including Bh).<sup>11</sup>

As a reference for the extrapolation of formation enthalpies, the standard enthalpies of the gaseous monatomic elements  $\Delta H^{0(298)}(M)_{(g)}$  were used.

Tab. 4-1 Standard formation enthalpies and standard entropies of oxygen, ruthenium, osmium, ruthenium oxides and osmium oxides used in this work.

Compound	$\Delta H_f^0$ [kJ·mol <sup>-1</sup> ]	ref	$\Delta S_f^0$ [J·mol <sup>-1</sup> ·K <sup>-1</sup> ]	ref
O (g)	249.2 ± 0.1	37	160.95 ± 0.02	37
O <sub>2</sub> (g)	0		205.0	37
Ru (s)	0		26.86	37
Ru (g)	+648.5 ± 5.4	38	186.5	38
RuO (s)	-		-	
RuO (g)	+372 ± 42	31	242	31
RuO <sub>2</sub> (s)	-313.52 ± 0.08	39	46.15 ± 0.05	40
RuO <sub>2</sub> (g)	+119 ± 10	31,41	265 ± 5	31
RuO <sub>3</sub> (s)	-251	38	79.5 ± 6	38
RuO <sub>3</sub> (g)	-70.8 ± 6.6	31	285.8 ± 8.4	31
RuO <sub>4</sub> (s)	-244.4 ± 4.4	31	154.0 ± 1.1	31
RuO <sub>4</sub> (g)	-192.7 ± 4.0	31	290.6 ± 0.6	31
Os (s)	0		32.7	35,40
Os (g)	784.6 ± 3.8	38	191.8 ± 2.5	38
OsO (s)	-		-	
OsO (g)	>+448	42	-	
OsO <sub>2</sub> (s)	-295.96 ± 0.08	39	49.8 ± 0.2	39
OsO <sub>2</sub> (g)	+193	42	-	
OsO <sub>3</sub> (s)	-190.5	42	-	
OsO <sub>3</sub> (g)	-167.5 ± 12.6	35	276	35
OsO <sub>4</sub> (s)	-394 ± 8	35	137 ± 8	35
OsO <sub>4</sub> (g)	-337 ± 8	35	293.9 ± 0.3	35

Because an accurate prediction of  $\Delta H^{0(298)}(\text{Hs})_{(g)}$  is difficult, a realistic range limited by two values for  $\Delta H^{0(298)}(\text{Hs})_{(g)}$ , denoted by Hs I and Hs II, was chosen.  $\Delta H^{0(298)}(\text{Hs I})_{(g)} = 790 \text{ kJ}\cdot\text{mol}^{-1}$  was predicted by Eichler<sup>12</sup> based on a linear extrapolation. Another calculation performed by Fricke<sup>13</sup> yielded  $\Delta H^{0(298)}(\text{Hs II})_{(g)} = 842 \text{ kJ}\cdot\text{mol}^{-1}$ . A value nearly identical to  $\Delta H^{0(298)}(\text{Hs I})_{(g)}$  of  $791 \text{ kJ}\cdot\text{mol}^{-1}$  has been calculated by Ionova et al.<sup>14</sup> based on a semi-empirical model which is primarily based on the estimation of trends in  $\Delta H_s^{0(298)}$  in the transactinide series. The trends were shown to be governed by the ground

Tab. 4-2 Compilation of relevant physico-chemical data used in this work.

Compound	RuO <sub>4</sub>	ref	OsO <sub>4</sub>	ref	HsO <sub>4</sub>	ref
Polarizability $\alpha$ [cm <sup>3</sup> ]	(7.92±0.15)·10 <sup>-24</sup>	<sup>a</sup>	8.17·10 <sup>-24</sup>	43	8.46·10 <sup>-24</sup>	7 <sup>b</sup>
1 <sup>st</sup> ionization potential IP <sub>1</sub> [eV]	12.33±0.23	44	12.97±0.12	44	12.27	7
Molar weight M [g·mol <sup>-1</sup> ]	165.1	30	254.2	30		
Density $\rho$ [g·cm <sup>-3</sup> ]	3.29	30	5.1	30		
Critical volume V <sub>c</sub> [cm <sup>3</sup> ·mol <sup>-1</sup> ]			156.93	45		
Critical density $\rho_c$ [g·cm <sup>-3</sup> ]			1.62	45		
Subl. enthalpy $\Delta H_S^{0(298)}$ [kJ·mol <sup>-1</sup> ]	51.7±5.9	31 <sup>c</sup>	57±11 59.95±0.25	35 <sup>c</sup> 35 <sup>d</sup>		
Symmetry group	T <sub>d</sub>	37	T <sub>d</sub>	37		
Distance M-O [nm]	0.171±0.0003	37	0.171±0.0003	37		
Angle O-M-O [deg]	109.5	37	109.5	37		
SiO <sub>2</sub>						
Dielectric constant $\epsilon$	3.81	46				
1 <sup>st</sup> ionization potential IP <sub>1</sub> [eV]	11.7±0.5	42				

<sup>a</sup> this work

<sup>b</sup> adjusted value, see text

<sup>c</sup> calculated from formation enthalpies cited therein

<sup>d</sup> experimental

state electronic configuration of the atom in the free and the metallic state. (In ref 15 a value of 628 kJ·mol<sup>-1</sup> is erroneously cited from ref 16 as  $\Delta H^{0(298)}(\text{Hs})_{(g)}$  instead of correctly  $\Delta G^{0(298)}(\text{Hs})_{(g)}$ ).

In the next step the atomic formation enthalpies of the gaseous and solid oxides  $\Delta H^*(\text{MO}_x)_{(g,s)}$  were determined with

$$\Delta H^*(\text{MO}_x)_{(g)} = \Delta H^{0(298)}(\text{MO}_x)_{(g)} - \Delta H^{0(298)}(\text{M})_{(g)} - x \cdot \Delta H^{0(298)}(\text{O})_{(g)} \quad (4-1)$$

$$\Delta H^*(\text{MO}_x)_{(s)} = \Delta H^{0(298)}(\text{MO}_x)_{(s)} - \Delta H^{0(298)}(\text{M})_{(g)} - x \cdot \Delta H^{0(298)}(\text{O})_{(g)} \quad (4-2)$$

and are shown in Figure 4-2 as a function of the standard enthalpy of the gaseous metals ( $\Delta H^{0(298)}(\text{M})_{(g)}$ ). Also included are linear extrapolations for Hs I

and Hs II. The slopes and intercepts of the extrapolations are listed in Table 4-3.

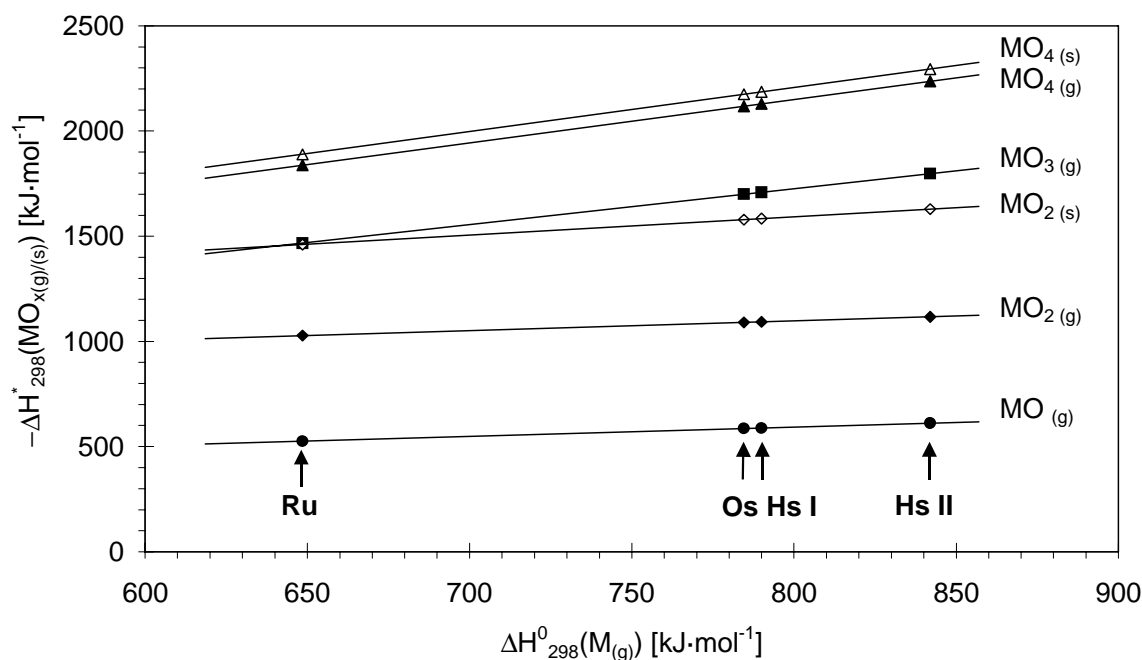


Fig. 4-2 Atomic formation enthalpies of the gaseous and solid oxides of group 8 elements as a function of the standard enthalpy of the gaseous metals (slopes and intercepts are summarized in Table 4-3).  $\text{MO}_{(s)}$  and  $\text{MO}_{3(s)}$  are unknown.

Tab. 4-3 Constants of the linear regression analysis between atomic formation enthalpies of oxides (s, g) and the atomic formation enthalpy of the gaseous metal.

	$\text{MO}_{(g)}$	$\text{MO}_{2(g)}$	$\text{MO}_{3(g)}$	$\text{MO}_{4(g)}$	$\text{MO}_{2(s)}$	$\text{MO}_{4(s)}$
Slope	0.44	0.46	1.71	2.06	0.87	2.10
Intercept [ $\text{kJ}\cdot\text{mol}^{-1}$ ]	239.30	731.05	357.64	501.93	895.59	530.28

Since the  $\Delta H^{0(298)}(\text{M})_{(g)}$  values are already included in the quantities of  $\Delta H^*(\text{MO}_x)_{(g,s)}$ , the stability of the compound  $\text{MO}_x$  increases with increasing atomic number if the slope of the correlation of  $\Delta H^*(\text{MO}_x)_{(g,s)}$  against  $\Delta H^{0(298)}(\text{M})_{(g)}$  for elements of a given group is larger than one. It therefore follows for the gaseous and solid tetroxides that the stability increases from  $\text{RuO}_4$  to  $\text{OsO}_4$ . Consequently,  $\text{HsO}_4$  is expected to be thermodynamically even more stable as has also been predicted in ref 7.

$\Delta H_S^{0(298)}$  can be deduced from the atomic formation enthalpies as

$$\Delta H_S^{0(298)}(MO_x) = \Delta H^*(MO_x)_{(g)} - \Delta H^*(MO_x)_{(s)} \quad (4-3)$$

which yields  $\Delta H_S^{0(298)}(HsO_4) = (57 \pm 11) \text{ kJ} \cdot \text{mol}^{-1}$  and  $(58 \pm 13) \text{ kJ} \cdot \text{mol}^{-1}$  for Hs I and Hs II. These values agree within the error limits with the  $\Delta H_S^{0(298)}$  values for  $OsO_4$  of  $57 \text{ kJ} \cdot \text{mol}^{-1}$  and  $60 \text{ kJ} \cdot \text{mol}^{-1}$  (see Table 4-2).

#### 4.2.2 Relation between sublimation enthalpy and adsorption enthalpy

A good empirical linear correlation was found between the standard sublimation enthalpy ( $\Delta H_S^{0(298)}$ ) of macroscopic amounts of a number of oxides and oxyhydroxides and their respective adsorption enthalpy on quartz surfaces ( $-\Delta H_a^{0(T)}$ ), measured for carrier free amounts.<sup>8</sup> An updated correlation that takes into account also more recent experiments resulted in<sup>9</sup>

$$-\Delta H_a^{0(T)} = (6.3 \pm 7.8) + (0.680 \pm 0.028) \cdot \Delta H_S^{0(298)} \quad (4-4)$$

Applying eq (4-4) to the values for  $\Delta H_S^{0(298)}$  listed in Table 4-2 for  $OsO_4$  and  $RuO_4$  yields  $-\Delta H_a^{0(T)}$  values of  $(45 \pm 15) \text{ kJ} \cdot \text{mol}^{-1}$  and  $(41 \pm 12) \text{ kJ} \cdot \text{mol}^{-1}$ . These values agree reasonably well with literature values from gas adsorption chromatography experiments (Table 4-4).

Using the average value for Hs I and Hs II for  $\Delta H_S^{0(298)}(HsO_4)$  and applying eq (4-4),  $-\Delta H_a^{0(T)}(HsO_4) = (46 \pm 15) \text{ kJ} \cdot \text{mol}^{-1}$  is derived. The following trend for the volatility of the group 8 tetroxides is therefore expected:  $RuO_4 \approx OsO_4 \approx HsO_4$ .

### 4.3 A model for the physisorption of volatile molecules on dielectric surfaces

In the following, an independent approach is made to describe the adsorption of a group 8 tetroxide molecule with a physisorption model and an assumed equivalence of the sorption process to that of noble gases.

Tab. 4-4 Enthalpies and entropies of adsorption of RuO<sub>4</sub> and OsO<sub>4</sub> evaluated in gas adsorption chromatography experiments with carrier-free amounts described in literature. The surface material was SiO<sub>2</sub> in refs 8,26-29,47 and Si<sub>3</sub>N<sub>4</sub> in ref 6. The standard states were the same in all refs except in ref 29.

Compound	$-\Delta H_a^{0(T)}$ [kJ·mol <sup>-1</sup> ]	$\Delta S_a^{0(T)}$ [J·mol <sup>-1</sup> ·K <sup>-1</sup> ]	Experimental Method	ref
RuO <sub>4</sub>	55.0±4.2	-168.7±0.5 <sup>a</sup>	Off-line TC	47
	10.7±1.7	-139.9±3.1	IC	29
OsO <sub>4</sub>	39±1	-170.5 <sup>a</sup>	On-line TC	6
	50±5	-180 <sup>b</sup>	Off-line TC	8
	41±2	-180 <sup>b</sup>	On-line TC	26
	57±4	-180 <sup>b</sup>	Off-line TC	26
	9.8±2.0	-157.5±6.8	IC	29
	38.0±1.5	-170.5 <sup>a</sup>	IC	27
	40.2±1.5		On-line TC	28

<sup>a</sup> calculated according to the model of mobile adsorption (ref 20)

<sup>b</sup> assumed as -180 J·mol<sup>-1</sup>·K<sup>-1</sup> for the evaluation of  $-\Delta H_a^{0(T)}$

### 4.3.1 Adsorption of polarizable molecules

The interaction energy of molecules without a permanent dipole moment with a dielectric solid involves mainly dispersion forces. Attraction due to physisorption forces can be written in the form<sup>17</sup>

$$E_B = -\frac{C_1}{r^6} \quad (4-5)$$

where  $E_B$ : interaction energy [eV]

$C_1$ : VAN DER WAALS constant between two systems (1) and (2)

$r$ : interaction distance [cm]

The total interaction energy between a molecule and a two-dimensional surface of infinite extent can be obtained by a summation over all molecule-molecule interactions.<sup>17</sup> This summation can be replaced by a triple integration.<sup>17</sup> Eq (4-5) then has the form<sup>17</sup>

$$E_B = -\left(\frac{\pi}{6}\right) \cdot N \cdot C_1 \cdot \frac{1}{r^3} \quad (4-6)$$

where  $N$ : number of atoms per  $\text{cm}^3$ .

Generally for two different types of interacting molecules (1) and (2),  $C_1$  is<sup>18</sup>

$$C_1 = \frac{3}{2} \cdot \alpha_1 \cdot \alpha_2 \cdot \frac{E_{DT(1)} \cdot E_{DT(2)}}{E_{DT(1)} + E_{DT(2)}} \quad (4-7)$$

where  $\alpha$ : polarizabilities of the molecules (1) and (2) [ $\text{cm}^3$ ]

$E_{DT}$ : average dipole transition energy of the molecules [eV].

The polarizability of quartz can be calculated from the well-known equation for solids<sup>7</sup>

$$\alpha_2 = \frac{3}{4 \cdot \pi \cdot N} \cdot \frac{(\epsilon - 1)}{(\epsilon + 2)} \quad (4-8)$$

where  $\epsilon$ : dielectric constant of the solid.

Introducing eqs (4-7) and (4-8) into eq (4-6) yields

$$E_B = \frac{3 \cdot \alpha}{16 \cdot r^3} \cdot \frac{(\epsilon - 1)}{(\epsilon + 2)} \cdot \frac{E_{DT(1)} \cdot E_{DT(2)}}{E_{DT(1)} + E_{DT(2)}} \quad (4-9)$$

Pauling empirically found the average dipole transition energy  $E_{DT}$  to be a function of the first ionization potential  $IP_1$ :<sup>19</sup>

$$E_{DT} = 1.57 \cdot IP_1 \quad (4-10)$$

where  $IP_1$ : first ionization potential [eV]

$E_B$  cannot be measured directly, but in gas adsorption chromatographic measurements  $-\Delta H_a^{0(T)}$  of the species on the surface material is usually evaluated (Table 4-4). The relation between  $\Delta H_a^{0(T)}$  and  $E_B$  can be understood as follows (Figure 4-3): in order to remove a molecule with zero degree of freedom (no translatory or vibrational degrees of freedom, i.e. "frozen state

approximation") from the surface to an infinite distance, the energy  $E_B$  is needed. If the molecule then is released from its frozen state into the gaseous phase three translatory degrees of freedom have to be added, requiring an energy of  $1.5 \cdot R \cdot T$ . In the model of mobile adsorption<sup>20</sup> (right-hand side of Figure 4-3), an energy of  $\Delta H_a^{0(T)}$  is gained when a molecule from the gaseous phase is adsorbed to the surface. This adsorbed state differs from the frozen state approximation by having one vibrational and two translatory degrees of freedom. The energy of the vibrational degree of freedom amounts to  $R \cdot T$  and the energy of each translatory degree of freedom amounts to  $0.5 \cdot R \cdot T$ .

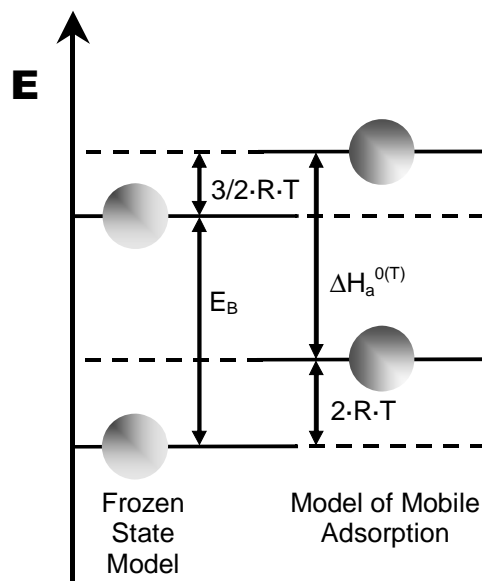


Fig. 4-3 Relation between  $E_B$  and  $\Delta H_a^{0(T)}$ . For explanations see text.

Therefore,

$$E_B = -\Delta H_a^{0(T)} + 0.5 \cdot R \cdot T \quad (4-11)$$

### 4.3.2 Calculation of the adsorption distances of noble gases

The distances of noble gases adsorbed on metal surfaces were calculated<sup>18</sup> using experimental adsorption data<sup>21,22</sup> of the noble gases Ne, Ar, Kr, Xe and Rn on 15 different metal surfaces. The results are summarized in Table 4-5 and show that  $r$  is independent of the noble gas and the adsorbent metal. Thus, the assumption of a mean value of  $r = (0.247 \pm 0.020)$  nm seems to be

justified and we therefore assume this universal adsorption distance for symmetrical molecules and noble gas atoms.

Tab. 4-5 Adsorption distances of noble gas atoms on metal surfaces using data from refs 21,22.

Noble Gas	Mean r [nm]	Std. dev. [nm]	Number of values
Ne	0.2342	0.0036	3
Ar	0.2533	0.0198	5
Kr	0.2636	0.0197	14
Xe	0.2393	0.0188	29
Rn	0.2452	-	1
Mean	0.247	0.020	52

### 4.3.3 Application of the model to OsO<sub>4</sub>

Due to the coordinative saturation of the metal ions in symmetrical molecular geometries such as the tetrahedral group 8 tetroxides, the interaction of these compounds with surfaces is dominated by physisorptive forces. We therefore assume that this process can be treated similar to the sorption process of noble gases to surfaces. The universal distance  $r$  given above is slightly larger than the "size" of the OsO<sub>4</sub> molecule characterized by the VAN DER WAALS radius  $r_{\text{vdW}}$  (ref 23)

$$r_{\text{vdW}} = \left( \frac{3 \cdot b}{16 \cdot \pi \cdot N_0} \right)^{\frac{1}{3}} \quad (4-12)$$

with  $r_{\text{vdW}}$ : VAN DER WAALS radius [cm]

$b$ : VAN DER WAALS constant  $b$  [cm<sup>3</sup>]

$N_0$ : Avogadro's number ( $6.022 \cdot 10^{23}$ )

The value of the VAN DER WAALS constant  $b$  can be derived from:<sup>23</sup>

$$b = \frac{V_c}{3} \quad (4-13)$$

with  $V_c$ : critical molar volume [cm<sup>3</sup>·mol<sup>-1</sup>]

For OsO<sub>4</sub> with a VAN DER WAALS constant  $b$  of 52.31 cm<sup>3</sup>·mol<sup>-1</sup>,  $r_{\text{vdW}}(\text{OsO}_4) = 0.1731$  nm is obtained. Comparison with data of the noble gases<sup>24,25</sup> shows that  $r_{\text{vdW}}(\text{Xe}) < r_{\text{vdW}}(\text{OsO}_4) < r_{\text{vdW}}(\text{Rn})$ .

Using  $r = (0.247 \pm 0.020)$  nm,  $E_{\text{B}}(\text{OsO}_4)$  can be evaluated with eq (4-9) using data from Table 4-2 as  $E_{\text{B}}(\text{OsO}_4)_{\text{calc}} = (0.47 \pm 0.11)$  eV. Subsequently  $-\Delta H_{\text{a}}^{0(\text{T})}(\text{OsO}_4)_{\text{calc}} = (47 \pm 11)$  kJ·mol<sup>-1</sup> is calculated using eq (4-11). This value agrees within the error limits with experimental values<sup>6,26-28</sup> obtained in on-line gas-chromatography experiments on silicon oxide and silicon nitride summarized in Table 4-4 which yielded an average value of  $-\Delta H_{\text{a}}^{0(\text{T})}(\text{OsO}_4)_{\text{exp}} = (39.6 \pm 1.3)$  kJ·mol<sup>-1</sup> and also with the value  $(45 \pm 15)$  kJ·mol<sup>-1</sup> deduced in Section 4.2.2.

#### 4.3.4 Extrapolation of the adsorption enthalpies for RuO<sub>4</sub> and HsO<sub>4</sub>

There exists no experimental information on the polarizability of RuO<sub>4</sub>. Comparison of the bond lengths, the molar volumes and the volatilities shows that RuO<sub>4</sub> closely resembles OsO<sub>4</sub>. The polarizability of RuO<sub>4</sub> can therefore be estimated under the assumption that it is proportional to the molar volume, the bond length, and the sublimation enthalpy normalized to those of OsO<sub>4</sub>. Averaging the three values followed by multiplication with the polarizability of OsO<sub>4</sub> yields  $\alpha(\text{RuO}_4) = (7.92 \pm 0.15) \cdot 10^{-24}$  cm<sup>3</sup>. In ref 7,  $\alpha(\text{RuO}_4)$  has been calculated by different methods as  $6.48 \cdot 10^{-24}$  cm<sup>3</sup> and  $6.77 \cdot 10^{-24}$  cm<sup>3</sup>.

With  $\alpha = (7.92 \pm 0.15) \cdot 10^{-24}$  cm<sup>3</sup>  $-\Delta H_{\text{a}}^{0(\text{T})}(\text{RuO}_4) = (44 \pm 11)$  kJ·mol<sup>-1</sup> is obtained with eqs (4-9) and (4-11) using the values given in Table 4-2 and assuming an "universal"  $r$  of  $(0.247 \pm 0.020)$  nm and subsequently  $\Delta H_{\text{S}}^{0(298)}(\text{RuO}_4) = (55 \pm 28)$ .

Pershina et al.<sup>7</sup> calculated  $\text{IP}_1(\text{HsO}_4) = 12.27$  eV and  $\alpha(\text{HsO}_4) = 6.26 \cdot 10^{-24}$  cm<sup>3</sup>. Since the agreement of  $\alpha(\text{OsO}_4)$  calculated by the same procedure with experimental data was rather poor, the obtained values have been adjusted by the authors by using the experimental value of  $\alpha(\text{OsO}_4)$  as a reference.  $\alpha(\text{HsO}_4) = 8.46 \cdot 10^{-24}$  cm<sup>3</sup> is therefore recommended in ref 7. Using this value and  $r(\text{HsO}_4) = (0.247 \pm 0.020)$  nm,  $-\Delta H_{\text{a}}^{0(\text{T})}(\text{HsO}_4) = (47 \pm 11)$  kJ·mol<sup>-1</sup> is calculated. From this value  $\Delta H_{\text{S}}^{0(298)}(\text{HsO}_4) = (60 \pm 28)$  kJ·mol<sup>-1</sup> follows with eq

(4-4). These values agree within the error limits with the ones obtained by the linear extrapolation method in Section 4.2.2.

#### 4.4 Conclusions

Two independent methods were applied to predict the adsorption behavior of  $\text{HsO}_4$  on quartz surfaces. The first bases on a thermodynamic extrapolation of sublimation enthalpies of group 8 tetroxides from which adsorption enthalpies are deduced based on an empirical correlation. The second approach describes the sorption process with a physisorption model of polarizable molecules, assuming an “universal” adsorption distance. Table 4-6 summarizes the adsorption enthalpies for  $\text{OsO}_4$  and  $\text{HsO}_4$  from this work in comparison with literature values based on a fully relativistic calculation as well as with a recent experiment.

Tab. 4-6 Summary of theoretical and experimental values for  $-\Delta H_a^{0(T)}$  of  $\text{OsO}_4$  and  $\text{HsO}_4$ .

Method	$-\Delta H_a^{0(T)}(\text{OsO}_4)$ [kJ·mol <sup>-1</sup> ]	$-\Delta H_a^{0(T)}(\text{HsO}_4)$ [kJ·mol <sup>-1</sup> ]	ref
Linear extrapolation	45±15	46±15	this work
Physisorption model	47±11	47±11	this work
Relativistic DFT+Interaction Model	38.0±1.5 <sup>a</sup>	35.9±1.5	7
Experiment	39.6±1.3 <sup>b</sup>	46±2	6

<sup>a</sup> value (experimental result from ref 27) used as reference point

<sup>b</sup> average value of on-line experiments (refs 6,26-28)

As can be seen, the values derived in this work agree with each other within the error limits as well as with those found in ref 7 and experimental results. However, there seems to be a systematic difference of the experimental values depending on the technique used. While all experimental  $-\Delta H_a^{0(T)}(\text{OsO}_4)$  values obtained in the on-line regime lie around 40 kJ·mol<sup>-1</sup> (refs 6,26-28), the ones obtained in off-line experiments<sup>8,26</sup> are higher by about 10-15 kJ·mol<sup>-1</sup> (except the ones of ref. 29 where a different standard state was used). Probably, the sticking coefficient (probability of a species hitting the surface to adsorb) is smaller than one. This influence is more pronounced in experiments with high gas-flow rates (on-line experiments). It is

---

therefore important to compare only  $-\Delta H_a^{0(T)}$ -values obtained under similar experimental conditions.

### Acknowledgment

Fruitful discussions with V. Pershina are gratefully acknowledged.

### References

- (1) Hoffman, D.C.; Lee, D.M. *J. Chem. Educ.* **1999**, *76*, 331.
- (2) Eichler, R.; Bröchle, W.; Dressler, R.; Düllmann, Ch.E.; Eichler, B.; Gäggeler, H.W.; Gregorich, K.E.; Hoffman, D.C.; Hübener, S.; Jost, D.T.; Kirbach, U.W.; Laue, C.A.; Lavanchy, V.M.; Nitsche, H.; Patin, J.B.; Piguet, D.; Schädel, M.; Shaughnessy, D.A.; Strellis, D.A.; Taut, S.; Tobler, L.; Tsyganov, Y.S.; Türlér, A.; Vahle, A.; Wilk, P.A.; Yakushev, A.B. *Nature* **2000**, *407*, 63.
- (3) Münzenberg, G.; Armbruster, P.; Folger, H.; Hessberger, F.P.; Hofmann, S.; Keller, J.; Poppensieker, W.; Reisdorf, W.; Schmidt, K.-H.; Schött, H.-J.; Leino, M.E.; Hingmann, R. *Z. Phys. A* **1984**, *317*, 235.
- (4) Hofmann, S.; Ninov, V.; Hessberger, F.P.; Armbruster, P.; Folger, H.; Münzenberg, G.; Schött, H.J.; Popeko, A.G.; Yeremin, A.V.; Saro, S.; Janik, R.; Leino, M. *Z. Phys. A* **1996**, *354*, 229.
- (5) Hofmann, S.; Münzenberg, G. *Rev. Mod. Phys.* **2000**, *72*, 733.
- (6) Düllmann, Ch.E.; Bröchle, W.; Dressler, R.; Eberhardt, K.; Eichler, B.; Eichler, R.; Gäggeler, H.W.; Ginter, T.N.; Glaus, F.; Gregorich, K.E.; Hoffman, D.C.; Jäger, E.; Jost, D.T.; Kirbach, U.W.; Lee, D.M.; Nitsche, H.; Patin, J.P.; Pershina, V.; Piguet, D.; Qin, Z.; Schädel, M.; Schausten, B.; Schimpf, E.; Schött, H.-J.; Soverna, S.; Sudowe, R.; Thörle, P.; Timokhin, S.N.; Trautmann, N.; Türlér, A.; Vahle, A.; Wirth, G.; Yakushev, A.B.; Zielinski, P.M. *Nature* (submitted).
- (7) Pershina, V.; Bastug, T.; Fricke, B.; Varga, S. *J. Chem. Phys.* **2001**, *115*, 792.

- 
- (8) Eichler, B.; Domanov, V.P. *J. Radioanal. Chem.* **1975**, *28*, 143.
- (9) Eichler, R.; Eichler, B.; Gäggeler, H.W.; Jost, D.T.; Dressler, R.; Türler, A. *Radiochim. Acta* **1999**, *87*, 151.
- (10) Eichler, B.; Türler, A.; Gäggeler, H.W. *J. Phys. Chem. A* **1999**, *103*(46), 9296.
- (11) Eichler, R. PSI Technical Report, Paul Scherrer Institut, Villigen, 2000, PSI-TM-18-00-04.
- (12) Eichler, B. *Kernenergie* **1976**, *19*(10), 307.
- (13) Fricke, B. *Structure and Bonding*, Springer-Verlag: Berlin, Heidelberg, New York, 1975, Vol. 21, p. 92ff.
- (14) Ionova, G.V.; Pershina, V.P.; Zuraeva, I.T.; Suraeva, N.I. *Radiokhimiya* **1995**, *37*, 307.
- (15) Keller Jr, O.L.; Seaborg, G.T. *Annu. Rev. Nucl. Sci.* **1977**, *27*, 139.
- (16) David, F. *Inst. Phys. Nucl. Orsay Rep.* **1971**, *RC-71-06*.
- (17) Adamson, A.W. *Physical Chemistry of Surfaces*, 4th ed.; John Wiley & Sons: New York, 1982.
- (18) Lide, D.R. Ed. *CRC Handbook of Chemistry and Physics*, 82th ed.; CRC Press: Boca Raton, 2001; 10-161.
- (19) Pauling, L.; Simonetta, M. *J. Chem. Phys.* **1952**, *20*, 29.
- (20) Eichler, B.; Zvara, I. *Radiochim. Acta* **1982**, *30*, 233.
- (21) Miedema, A.R.; Nieuwenhuys, B.E. *Surface Sci.* **1981**, *104*, 491.
- (22) Eichler, B.; Kim Son Chu *Isotopenpraxis* **1985**, *21*, 180.
- (23) Schwabe, K. *Physikalische Chemie*, Akademie-Verlag GmbH: Berlin, 1973; Band 1, Chapters 4, 5.

- 
- (24) Lide, D.R. Ed. *CRC Handbook of Chemistry and Physics*, 82th ed.; CRC Press: Boca Raton, 2001; 6-45.
- (25) Eichler, B.; Zimmermann, H.P.; Gäggeler, H.W. *J. Phys. Chem. A* **2000**, *104*, 3126.
- (26) Domanov, V.P.; Zvara, I. *Radiokhimiya* **1984**, *26*, 770.
- (27) Düllmann, Ch.E.; Eichler, B.; Eichler, R.; Gäggeler, H.W.; Jost, D.T.; Piguet, D.; Türlér, A. *Nucl. Instrum. Meth.* **2002**, *A479*, 631.
- (28) Kirbach, U.W., Folden III, C.M., Ginter, T.N., Gregorich, K.E., Lee, D.M., Ninov, V., Omtvedt, J.P., Patin, J.B., Seward, N.K., Strellis, D.A., Sudowe, R., Türlér, A., Wilk, P.A., Zielinski, P.M., Hoffman, D.C., Nitsche, H. *Nucl. Instrum. Meth.* **2002**, *A484*, 587.
- (29) Steffen, A.; Bächmann, K. *Talanta* **1978**, *25*, 551.
- (30) Lide, D.R. Ed. *CRC Handbook of Chemistry and Physics*, 82th ed.; CRC Press: Boca Raton, 2001; Chapters 4,5.
- (31) Rard, J.A. *Chem. Rev.* **1985**, *85*, 1.
- (32) Knacke, O.; Kubaschewski, O.; Hesselmann, K. *Thermochemical Properties of Inorganic Substances*, 2nd ed.; Springer-Verlag: Berlin, 1991; Vols. I&II.
- (33) Samsonov, G.V. Ed. *The Oxide Handbook*, 2nd ed.; IFI/Plenum: New York, 1982.
- (34) Wagman, D.D.; Evans, W.H.; Parker, B.P.; Schumm, R.H.; Halow, I.; Bailey, S.M.; Churney, K.L.; Nuttall, R.L. *J. Phys. Chem. Ref. Data* **1982**, *11*, 1.
- (35) Oppermann, H.; Marklein, B. *Z. Naturforsch.* **1998**, *53 b*, 1352.
- (36) Häfeli, T. Diploma thesis, Universität Bern, Bern, 1999.

- 
- (37) Efimov, A.J. *Svoistva Neorganiceskikh Soedinenij*; Izd. Khimija: Leningrad, 1983.
- (38) Nikol'skii, A.B.; Ryabov, A.N. *Russ. J. Inorg. Chem.* **1965**, *10*, 1.
- (39) Jacob, K.T.; Mishra, S. *J. Am. Ceram. Soc.* **2000**, *83*, 1745.
- (40) Cordfunke, E.H.P.; Konings, R.J.M.; Westrum Jr, E.F.; Shaviv, R. *J. Phys. Chem. Solids* **1989**, *50*, 429.
- (41) Eichler, B.; Zude, F.; Fan, W.; Trautmann, N.; Herrmann, G. *Radiochim. Acta* **1992**, *56*, 133.
- (42) Gurvic, L.C. *Energija razriva khimiceskikh svjazei*; Izd. Nauka: Moskva, 1974.
- (43) Lide, D.R. Ed. *CRC Handbook of Chemistry and Physics*, 82th ed.; CRC Press: Boca Raton, 2001; 10-165.
- (44) Dillard, J.G.; Kiser, R.W. *J. Phys. Chem.* **1965**, *65*, 3893.
- (45) Borchers, H.; Hausen, H.; Hellwege, K.-H.; Schäfer, Kl.; Schmidt, E. Hrsg. *Landolt-Börnstein, Zahlenwerte und Funktionen aus Physik, Chemie, Astronomie, Geophysik und Technik*, 6. Aufl., Springer-Verlag: Berlin, Heidelberg, New York, 1971; II. Band, 1. Teil.
- (46) Lide, D.R. Ed. *CRC Handbook of Chemistry and Physics*, 82th ed.; CRC Press: Boca Raton, 2001; 12-63.
- (47) Düllmann, Ch.E.; Eichler, B.; Gäggeler, H.W.; Türler, A. PSI Scientific Report 1998, Paul Scherrer Institut, Villigen, 1999, Vol. I, 122.



## 5. Outlook and closing remarks

The present experiment yielded the first chemical information on hassium, even though the isotopes  $^{269,270}\text{Hs}$  produced in this study were formed in the  $^{26}\text{Mg}+^{248}\text{Cm}$  reaction at a cross section level of only a few picobarn.

Hs was shown to form a highly volatile oxide, presumably  $\text{HsO}_4$ . It therefore behaves similarly to Os and is a member of group 8 of the periodic table.

Via direct comparison to  $\text{OsO}_4$  it was shown that the interaction of  $\text{HsO}_4$  with a silicon nitride surface is significantly stronger than that of  $\text{OsO}_4$ . However, the interpretation of this result is not trivial. So far, the properties of  $\text{HsO}_4$  have been investigated theoretically in only two papers [Jon02, Per02a]. A volatility similar to that of  $\text{OsO}_4$  was predicted by Pershina [Per02a] who performed fully relativistic density functional theory (DFT) calculations of the electronic structure of the group 8 tetroxides and calculated the enthalpy of adsorption applying physisorption models similar to the ones used in the "noble gas" model described in this work in Chapter 4.3. The decision whether relativistic effects are expressed dominantly is not easy. Both the DFT calculations (which fully include relativistic effects) as well as the extrapolation of the trend within group 8 (which naturally includes relativistic effects already manifested in the lighter homologues, but not nonlinear effects due to the strong increase of the Coulomb forces in heaviest elements which are proportional to  $Z^2$  [EiB99]) pointed to the formation of  $\text{HsO}_4$ . In both approaches, its stability was estimated to be higher than that of  $\text{OsO}_4$ , and its interaction with a dielectric surface was also predicted to be similar for both these compounds. Different consequences of relativistic effects are e.g. (i) smaller ionic radii, (ii) smaller polarizability, and (iii) higher ionization potential (always compared to non-relativistic calculations) [Per02b]. In a measured interaction energy with a surface these partly cancel each other. Hence measurement of the volatility of  $\text{HsO}_4$  is not adequate to judge the influence of relativistic effects in the chemistry of Hs. It is also difficult to conclude which property is mainly responsible for the higher adsorption enthalpy of  $\text{HsO}_4$  compared to  $\text{OsO}_4$ . Since relativistic effects are more pronounced in neutral atoms (i.e. elemental

---

Hs) than compounds containing charged Hs cations (even if the effective metal charge of Hs in  $\text{HsO}_4$  is only +1.39 [Per02a]) it would be advantageous to investigate Hs in lower valent (or even elemental) state.

Comparison of the experimental result with the prediction based on the trend in group 8 established by  $\text{RuO}_4$  and  $\text{OsO}_4$  does not reveal any unexpected behavior of Hs. Like its two lighter homologues it forms a highly volatile compound with oxygen, presumably  $\text{HsO}_4$  and can therefore be oxidized to the (formal) 8+ state. However, small deviations from the trend cannot be detected since the accuracy of the extrapolation is rather low. This is due to two reasons: (i) the thermodynamic data of the homologous tetroxides are not known accurately enough, and (ii) the correlation linking microscopic quantities with macroscopic ones (e.g.  $\Delta H_{\text{ads}}$  and  $\Delta H_{\text{s}}$ , eq 4-4) established by a great number of less volatile oxides and oxyhydroxides which interact with a surface via chemisorption is not accurate for highly volatile species. It seems therefore desirable to search for a correlation linking microscopic and macroscopic quantities of species whose interaction with surfaces is dominantly governed by physisorptive processes.

With the discovery of relatively long-lived isotopes of elements 112 [Oga99a] and 114 [Oga99b, Oga99c] which are produced on a cross section level of approximately one picobarn, chemical investigation of these elements appears possible (and will probably be performed before elements 109-111 are characterized). Thus the question of the atomic number at which relativistic effects severely change chemical properties (i.e. lead to a behavior of the element totally different from that of the lighter "homologues") seems answerable. First attempts to investigate element 112 have been reported [Yak01, Yak02a]. Different groups are performing preparatory studies to the chemical characterization of element 112 [EiR02a, Sov02, Yak02a] and experiments with element 114 are planned [EiR02b, Yak02b]. The decay chains of these nuclei end in an unknown region of the chart of nuclides and hence unambiguous proof that nuclei of new elements have actually been observed is not possible from observation of decay chains alone. Thus, independent confirmation of the atomic number is valuable to fulfill the criteria

---

established by the IUPAC to recognize the discovery of a new chemical element [TWG91]. Nuclear chemistry investigations of relatively long-lived members of these decay chains are vital tools to identify their atomic number. Besides  $^{283}_{112}$ , which was already used in chemical studies on element 112 [Yak01, Yak02a], the nuclide  $^{277}_{112}\text{Hs}$  which was the last member of the decay chain starting at  $^{289}_{114}$  [Oga99c] is a possible candidate. It was produced in the reaction  $^{244}_{94}\text{Pu}(^{48}_{20}\text{Ca}, 3n)$  with a cross section of 1 pb. So far, only one event was observed which decayed after a lifetime of 16.5 min by SF with a total deposited energy of about 190 MeV. [Oga99c]. As shown in the present work, the separation of Hs nuclides from other spontaneously fissioning nuclides is excellent in the oxygen system. All fission fragments observed in this experiment were registered in detectors 2 through 4. Observation of fission fragments in the relevant temperature range in an IVO-COLD experiment using the reaction  $^{48}_{20}\text{Ca}+^{244}_{94}\text{Pu}$  would give strong evidence that a Hs isotope was indeed present and would support the claim by the Dubna group that the long-sought "superheavies" were detected in their experiments.

Another possible application of the IVO-COLD system is the search for  $^{268}_{112}\text{Hs}$ , which is yet unknown and predicted to decay mainly by emission of  $\alpha$ -particles. In the literature, the estimated half-life ranges from a few tens of ms [Pat91, Roy02] to almost 20 s [Iwa96, Möl97]. From trends in the chart of nuclides, a value of a few hundred ms seems reasonable and would probably be sufficient to detect this nuclide applying the technique used in this work. Suitable production reactions would be  $^{248}_{98}\text{Cm}(^{24}_{12}\text{Mg}, 4n)$  or  $^{248}_{98}\text{Cm}(^{25}_{12}\text{Mg}, 5n)$  with cross sections of about 1 pb and 3 pb according to HIVAP calculations.

In our experiment, presumably both nuclides,  $^{269}_{112}\text{Hs}$  and  $^{270}_{112}\text{Hs}$  were produced, but an unambiguous assignment of the observed decay chains to either of these was not possible in all cases due to similar decay properties of the daughters as well as of the grand-daughters of both isotopes. An experiment with the IVO-COLD system at a lower beam energy of about 135 MeV (where the maximum cross section of the 4n evaporation channel is predicted by the HIVAP code, see Figure 1-7) would probably indicate whether  $^{270}_{112}\text{Hs}$  was really discovered in the present experiment. The production of  $^{269}_{112}\text{Hs}$  is very

---

unlikely at such a low beam energy and the decay chains detected in such an experiment could be assigned to  $^{270}\text{Hs}$  with much higher probability.

Another recent development which opens up new possibilities in the field of experimental investigations of transactinides is the application of physical preseparators which deliver isolated EVR to a chemistry apparatus and separate transfer products and the intense heavy-ion beam. A first separator of this kind is the Berkeley Gas-filled Separator (BGS) [Gre00]. The power of such a device for heavy element chemistry was recently demonstrated for the first time [Omt02] in studies of Rf with the SISAK system [Omt98], a liquid-liquid extraction system where the detection of the nuclear decay is accomplished by liquid-scintillation counting. This method is sensitive to the high  $\beta$ -background usually present in transactinide experiments not using a preseparator. The development of a new physical preseparator dedicated to chemistry experiments was proposed in a workshop at GSI in April 2002. Such a device is considered mandatory for the chemical identification of element 112 [EiR02a] by correlated decay chains in gas phase experiments. Without a preseparator, these will probably be masked by short-lived  $\alpha$ -decaying Rn isotopes and their daughters that are produced in nuclear transfer reactions with rather large cross sections. Another application of such a separator will be gas chemical investigations of the lighter transactinides. Only few inorganic molecules of the latter (e.g. halides, oxyhalides, hydroxides or oxides) have so far been investigated. The limiting factor with respect to more "complicated" molecules was the plasma in the recoil chamber caused by the intense beam. For example, any organic ligand would immediately be destroyed. With the beam separated, the synthesis of organometallic compounds and their investigation in gas phase experiments becomes feasible and opens up a new field in transactinide chemistry. Let us chose the group 8 elements as an example. Several classes of organometallic compounds are volatile at moderate temperatures. The metallocenes  $M(\text{cp})_2$  (cp=cyclopentadienyl) look especially suitable. The sublimation enthalpy of  $\text{Os}(\text{cp})_2$  is only 75 kJ/mol [Fis59]. All group 8 metallocenes have 18 electrons and are relatively stable compounds. Decomposition only occurs above 470 °C for all group 8 metallocenes, and  $\text{Ru}(\text{cp})_2$  is the most thermostable of all

---

known metallocenes [Fis59]. Baumgärtner et al. observed the formation of carrier-free  $\text{Ru}(\text{cp})_2$  after irradiation of a mixture of  $\text{Fe}(\text{cp})_2$  and  $\text{U}_3\text{O}_8$  with neutrons. Ru isotopes produced in the fission of U were found to have replaced Fe in ferrocene molecules, and a pure  $\text{Ru}(\text{cp})_2$  fraction was obtained [Bau61]. Another promising system is that of the pentacarbonyles  $\text{M}(\text{CO})_5$ . Recently, Ono et al. reported on the separation of Ru isotopes produced in the spontaneous fission of  $^{252}\text{Cf}$  from other fission products in the form of dpm complexes (dpm=dipivaloylmethane) produced at 350 °C which were volatile below 300 °C [Ono02].

The availability of radioactive ion beams of high intensity [vEg99, Gue02, Nol02] allows the hope of extending the chart of nuclides to heavier elements and more neutron rich (and probably longer-lived) nuclei as the next spherical neutron shell at  $N=184$  is approached. Chemical investigations of a multitude of compounds would then seem possible.

In the next decades, many experiments including heavier elements and more complex compounds will hopefully become feasible. The thrilling work at the upper ends of the periodic table and the chart of nuclides will continue.

---

**References of Chapter 5**

- [Bau61] Baumgärtner, F. *et al.* Zur Chemie bei Kernprozessen - II. Anwendung der Uranspaltung zur Synthese trägerfreien  $^{103}\text{Ru}(\text{cp})_2$ . *Z. Naturforsch.* **16a**, 374 (1961).
- [EiB99] Eichler, B. *et al.* Thermochemical characterization of seaborgium compounds in gas adsorption chromatography. *J. Phys. Chem. A* **103**, 9296 (1999).
- [EiR02] a) Eichler, R. *et al.* Adsorption of radon on metal surfaces: a model study for chemical investigations of elements 112 and 114. *J. Phys. Chem. B* **106**, 5413 (2002).  
b) Eichler, R. *et al.* Vacuum thermochromatography - Revival of a gas phase adsorption separation method to be coupled to a future "ChemSep". Contribution to the Workshop on Recoil Separator for Superheavy Element Chemistry, GSI Darmstadt, Germany, March 20-21, 2002.
- [Fis59] Fischer, E.O. *et al.* Di-cyclopentadienyl-osmium. *Chem. Ber.* **92**, 2302 (1959) (in german).
- [Gre00] Gregorich, K.E. *et al.* Superheavy elements with the Berkeley Gas-filled Separator. *J. Nucl. Radiochem. Sci.* **1**, 1 (2000).
- [Gue02] Guerreau, D. Radioactive beam facilities: european perspectives. *Eur. J. Phys. A* **13**, 263 (2002).
- [Iwa96] Iwamoto, A. *et al.* Collisions of deformed nuclei: a path to the far side of the superheavy island. *Nucl. Phys.* **A596**, 329 (1996).
- [Jon02] Johnson, E. *et al.* Ionization potentials and radii of neutral and ionized species of elements 107 (bohrium) and 108 (hassium) from extended multiconfiguration Dirac-Fock calculations. *J. Chem. Phys.* **116**, 1862 (2002).
- [Möl97] Möller, P. *et al.* Nuclear properties for astrophysical and radioactive-ion-beam applications. *At. Data Nucl. Data Tab.* **66**, 131 (1997).
- [Nol02] Nolen, J.A. Prospects for exotic beam facilities in North America. *Eur. J. Phys. A* **13**, 255 (2002).
- [Oga99] a) Oganessian, Yu.Ts. *et al.* Search for new isotopes of element 112 by irradiation of  $^{238}\text{U}$  with  $^{48}\text{Ca}$ . *Eur. Phys. J. A* **5**, 63 (1999).  
b) Oganessian, Yu.Ts. *et al.* Synthesis of nuclei of the superheavy element 114 in reactions induced by  $^{48}\text{Ca}$ . *Nature* **400**, 242 (1999).  
c) Oganessian, Yu.Ts. *et al.* Synthesis of superheavy nuclei in the  $^{48}\text{Ca} + ^{244}\text{Pu}$  reaction. *Phys. Rev. Lett.* **83**, 3154 (1999).
- [Omt98] Omtvedt, J.P. *et al.* Review of the SISAK system in transactinide research recent developments and future prospects. *J. Alloy. Comp.* **271-273**, 303 (1998).
- [Omt02] Omtvedt, J.P. *et al.* SISAK liquid-liquid extraction experiments with preprepared  $^{257}\text{Rf}$ . *J. Nucl. Radiochem. Sci.* **3**, 121 (2002).

- 
- [Ono02] Ono, S. *et al.* Thermo chromatographic behavior of fission products combined with dipivaloylmethane. *J. Nucl. Radiochem. Sci.* (submitted).
- [Pat91] Patyk, Z. *et al.* Ground-state properties of the heaviest nuclei analyzed in a multidimensional deformation space. *Nucl. Phys.* **A533**, 132 (1991).
- [Per02] a) Pershina, V. *et al.* The electronic structure and properties of group 8 oxides MO<sub>4</sub>, where M=Ru, Os, and element 108, Hs. *J. Chem. Phys.* **115**, 792 (2001).  
b) Pershina, V., private communication, 2002.
- [Roy02] Royer, G. *et al.* On the formation and alpha decay of superheavy elements. *Nucl. Phys.* **A699**, 479 (2002).
- [Sov02] Soverna, S. *et al.* Model studies of mercury for a future experiment with element 112. Booklet of Abstracts of the 14<sup>th</sup> Radiochemical Conference, Mariánské Lázně, Czech Republic, April 14-19, 2002, p.175.
- [TWG91] IUPAC & IUPAP Transfermium Working Group. Criteria that must be satisfied for the discovery of a new chemical element to be recognized. *Pure Appl. Chem.* **63**, 879 (1991).
- [vEg99] von Egidy, T. *et al.* The Munich Accelerator for Fission Fragments (MAFF) at the new reactor FRM II. *Act. Phys. Slov.* **49**, 107 (1999).
- [Yak01] Yakushev, A.B. *et al.* First attempt to chemically identify element 112. *Radiochim. Acta* **89**, 743 (2001).
- [Yak02] a) Yakushev, A.B. *et al.* First chemistry experiments with element 112. Contribution to the Workshop on Recoil Separator for Superheavy Element Chemistry, GSI Darmstadt, Germany, March 20-21, 2002.  
b) Yakushev, A.B. *et al.* Approaches to element 114 chemistry with and without physical pre-separation. Contribution to the same workshop.



---

## Acknowledgements

I am indebted to many people without whose help this work would not have been possible.

First of all I would like to thank Prof. Heinz Gaggeler, head of the Laboratory for Radio- and Environmental Chemistry at the University of Berne and Paul Scherrer Institute for offering me the possibility to follow extraordinary and interesting PhD work in his group, for his support and confidence. He enabled me to work in an exotic and thrilling field of today's nuclear chemistry and offered me possibilities of performing experiments at different laboratories and participating in international conferences and in a Summer School at ITU in Karlsruhe. On all these occasions, I had many interesting experiences and got to know people from all over the world.

My sincere thanks go as well to Prof. Bernd Eichler, head of the Heavy Element Group at PSI and Prof. Andi Türler from the TU München, who was a senior scientist in our group before leaving Switzerland. Prof. Eichler was always willing to discuss any chemical problem and allowed me to profit from his lifelong experience. Prof. Andi Türler was a great help in evaluating the experimental data and was always ready to discuss physical aspects behind it all.

Dr. Dieter Jost, Dr. Rugard Dressler, Dr. Robert Eichler, scientific members of the Heavy Element Group at PSI, as well as Dave Piguet, our invaluable technician, were always willing to put in extra effort if necessary (usually during beamtimes around 3 o'clock on Sunday morning...). A special "thank you" goes to Dr. Robert Eichler and Sandra Soverna, fellow PhD students in the "Heavies" group, with whom I shared many good experiences.

I am indebted to all the members of the Hassium Collaboration who made tremendous efforts in the experiment at GSI to get every single piece of the whole system working on time. Thank you all for your assistance! We could not have achieved our goal without working as a team. Special thanks to the on-site leaders, Dr. Matthias Schädel from GSI and Prof. Andi Türler.

---

Essential to our success was the rotating  $^{248}\text{Cm}$  target which was produced by Dr. Klaus Eberhardt and Dr. Petra Thörle from the University of Mainz.

Dr. Alexander Yakushev became a good friend and was a great help with his experience in gas phase chemistry not only in the Hs experiment but also in many test experiments at PSI. I also gladly remember his family's warm hospitality during my weeks in Dubna, as well as that of Dr. Vyacheslav Lebedev and Dr. Sergeij Timokhin.

Ueli Kindler and his team from the mechanical workshop at the University of Berne who built the COLD housing, and René Schraner and Kurt v. Escher from the electronical workshop were always at hand to get things running and to make everything easier than I had first supposed - and usually in a very short time. The people from the hardware shop at the University of Berne, too, were always helpful when something was needed urgently.

F. Glaus from the Laboratory for Micro- and Nanotechnology manufactured the tiny spacers of the COLD and the PIN-diode sandwiches, an admirable feat!

The team of Dr. P. Schmelzbach at the PHILIPS cyclotron at PSI always succeeded in persuading the machine to deliver O and Ne beams beyond the ideas of the original manufacturer. The operators of the UNILAC at GSI, and the ECR ion source team provided stable and highly intense Mg beams which allowed a chemistry experiment on a level of a few picobarns.

Dr. Siegfried Hübener, Dr. Annett Vahle and Dr. Steffen Taut from the Forschungszentrum Rossendorf were always willing to fill in during beam times at PSI if we were short (which was usually the case).

The members of the Laboratory for Radio- and Environmental Chemistry at the University of Berne and at the Paul Scherrer Institute were helpful and supportive in this work. The lanthanide targets used in the Os experiments were produced by Elfie Rössler at PSI. Dr. Vincent Lavanchy and Sandra Soverna gave crucial PC-support. A lot of organizing was done by our two secretaries, Ruth Lorenzen at PSI and Madeleine Gertsch at Bern University.

---

During the course of my PhD work I experienced many office-mates in Berne and at PSI. Special thanks for a good working climate go to Prof. Andi Türlér, Dr. Dieter Jost, Dr. Rugard Dressler, Dr. Robert Eichler, Dr. Sönke Szidat and to Sandra Soverna.

With Dr. Valeria Pershina from GSI I had many interesting discussions on theoretical calculations and the expected properties of the transactinides.

PD Dr. Urs Baltensperger and Dr. Markus Ammann from PSI introduced me to the field of aerosol science and Dr. Ernest Weingartner, also from PSI, introduced me to the DMA-CNC system.

The Swiss National Science Foundation as well as the Paul Scherrer Institute provided financial support for the present work which I gratefully acknowledge.

I would like to thank Irene Bächler for the careful proof-reading of the manuscript.

The success of this work should also be considered as a reward to my parents for their continuous support. They always believed in me and supported me whenever possible. Thank you for everything!

My wife Salomé deserves a big hug and many thanks for her continuous support. She always had an open ear, kept me steadfast and was equally willing to share the successes and the hard times. She showed me that home is with her, not at the University or at PSI. I am very grateful for your love!



## Appendix

### Pictures of the experiment

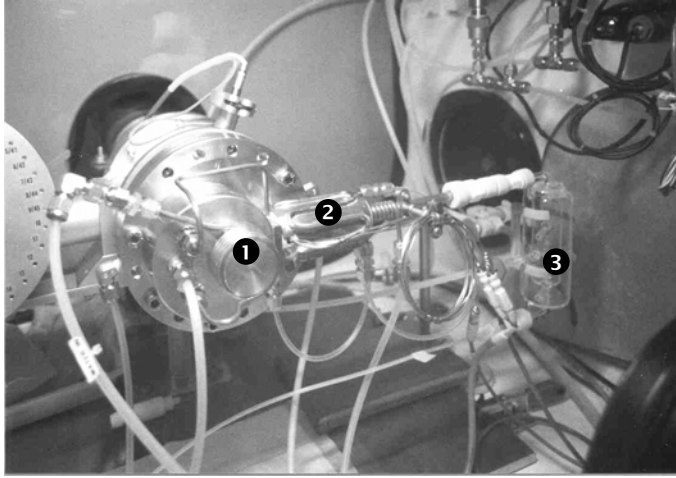


Fig. A-1 IVO installed at the beamline at PSI

- (1) Beam-stop
- (2) Oven
- (3) Cluster chamber

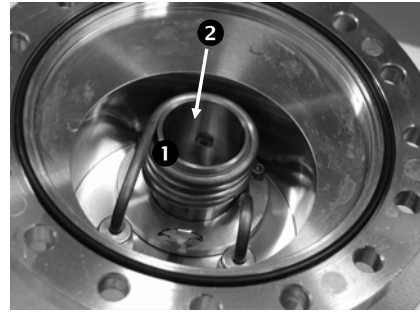


Fig. A-2 The water-cooled target chamber

- (1) Target chamber
- (2) Exit to the quartz column

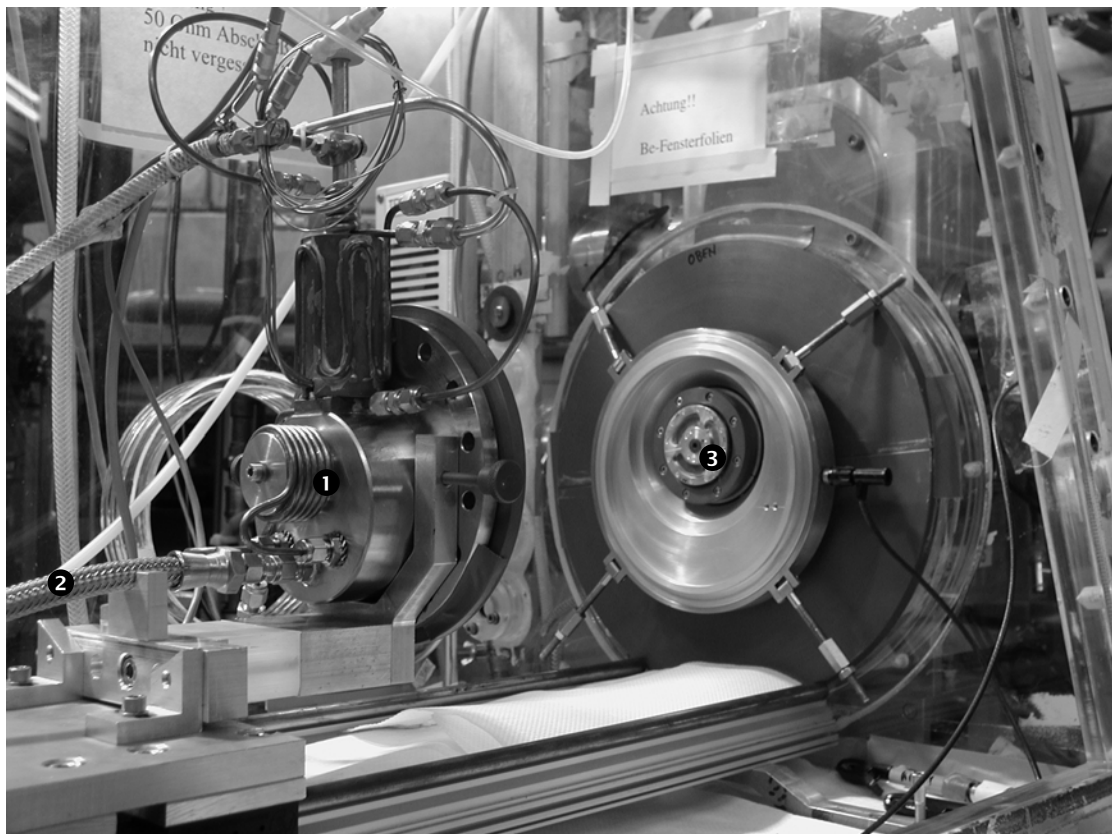


Fig. A-2 IVO installed at the beamline at GSI (open position to have access to the target)

- (1) IVO
- (2) Carrier gas inlet
- (3) Rotating window-target system

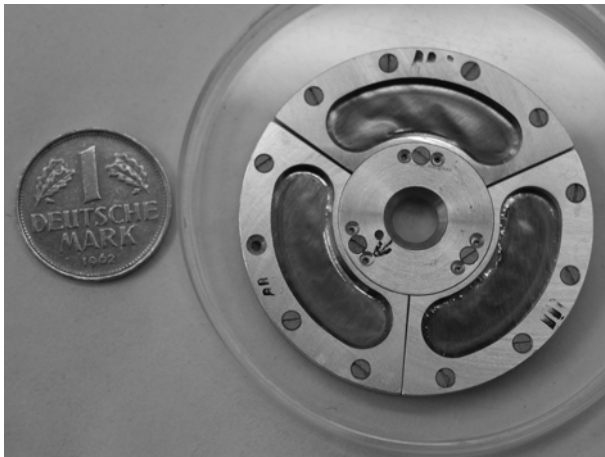


Fig. A-4 The rotating 3-segment target

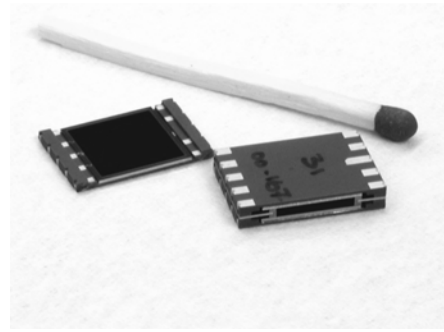


Fig. A-5 A single PIN diode and a sandwich pair as installed in COLD

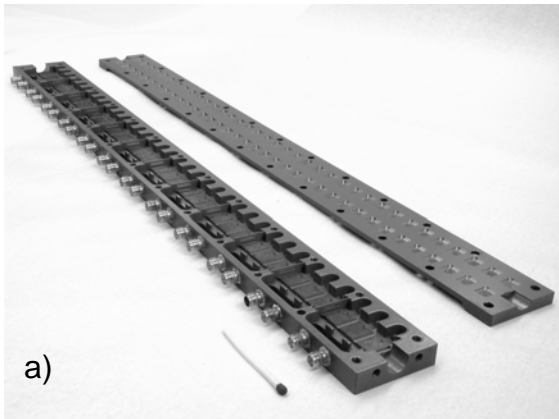
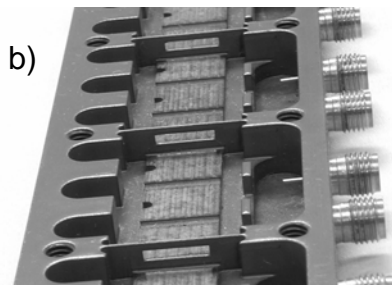


Fig. A-6 (a) The PTFE Teflon<sup>®</sup> coated Cu bar that served as holder for the PIN diode pairs



(b) Enlarged cut-out

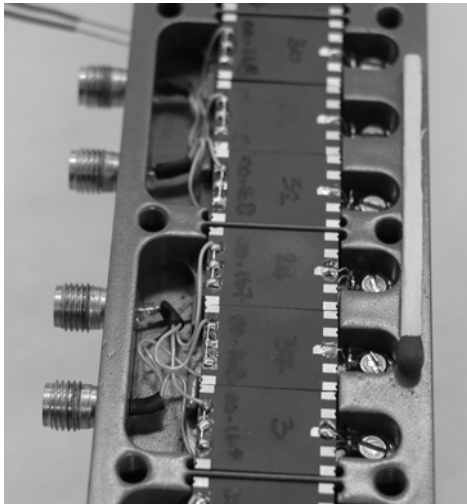


Fig. A-7 PIN-Diodes installed inside the copper bar

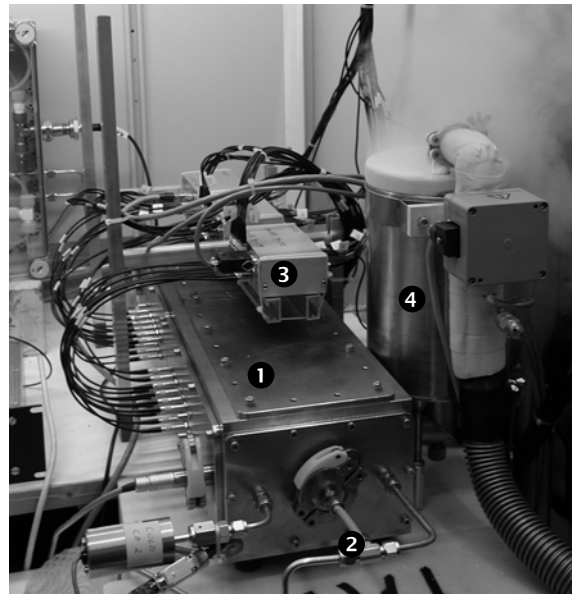


Fig. A-8 The COLD housing  
 (1) Housing  
 (2) Gas outlet  
 (3) Pre-amplifiers  
 (4) LN<sub>2</sub>-container

---

## Curriculum vitae

Christoph Emanuel Düllmann

Born on 15 January 1972

Citizen of Ferenbalm BE

- 1979-1988 Schools in Mühleberg (BE) and Allenlütten (BE)
- 1988-1993 College in Berne (BE)
- 1992 Course "Strahlenschutz-Betriebsassistent" at the Mühleberg Nuclear Power Plant
- 1993 Maturity Type C (Mathematics and Natural Sciences)
- 1993-1998 Chemistry studies at the University of Berne  
Summer job as health physicist at the Mühleberg Nuclear Power Plant
- 1998 Diploma in Chemistry at the University of Berne  
"Thermochromatographische Untersuchung von radioaktivem Ruthenium ( $^{106}\text{Ru}$ ) mit Sauerstoff als Trägergas"
- 1998-2002 PhD student at the University of Berne and the Paul Scherrer Institute  
Participation in experiments to synthesize and classify the heaviest elements:  
1997-2002 PSI Villigen (Db, Sg, Bh)  
2000 JINR Dubna (Hs)  
2001 GSI Darmstadt (Hs)  
Assistant at the Department for Chemistry and Biochemistry at the University of Berne
- 2002 PhD thesis "Chemical Investigation of Hassium (Hs, Z=108)"

Burgdorf, June 24, 2002.

---

**Notes**

